
Doctoral

Science

1989-01-01

Reactions of Hydroxyl Radicals and Chlorine Atoms with Compounds of Group IV Elements.

Denis J. O'Farrell
Technological University Dublin

Follow this and additional works at: <https://arrow.tudublin.ie/sciendoc>

 Part of the [Chemistry Commons](#)

Recommended Citation

O'Farrell, D. (1989). *Reactions of hydroxyl radicals and chlorine atoms with compounds of group iv elements*. Doctoral thesis. Technological University Dublin. doi:10.21427/D7559W

This Theses, Ph.D is brought to you for free and open access by the Science at ARROW@TU Dublin. It has been accepted for inclusion in Doctoral by an authorized administrator of ARROW@TU Dublin. For more information, please contact arrow.admin@tudublin.ie, aisling.coyne@tudublin.ie, vera.kilshaw@tudublin.ie.

REACTIONS OF HYDROXYL RADICALS AND CHLORINE
ATOMS WITH COMPOUNDS OF GROUP IV ELEMENTS

A thesis submitted to

THE NATIONAL UNIVERSITY OF IRELAND

for the degree of

DOCTOR OF PHILOSOPHY

by

DENIS J. O'FARRELL

Based on research carried out in the Chemistry Departments of University College, Dublin, the Dublin Institute of Technology, Dublin, and Risø National Laboratory, Roskilde, Denmark, under the direction of Professor David Feakins and the supervision of Dr. Howard Sidebottom and Dr. Jack Treacy.

University College,

Dublin.

May, 1989

Dublin Institute of Technology,

Kevin Street,

Dublin.

ACKNOWLEDGEMENTS

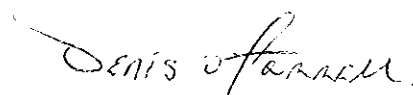
I wish to express my gratitude to Dr. Howard Sidebottom of University College, Dublin, for his expertise and assistance given to me during this work, and to Professor David Feakins under whose direction this work was carried out. I also wish to thank Dr. Ole John Nielsen of Risø National Laboratory, Roskilde, Denmark, for the advice and encouragement he gave me during my visits to Denmark.

I would like to thank, especially, Dr. Jack Treacy of the Dublin Institute of Technology, without whose expertise, encouragement and companionship this work would not have been completed.

To my friends and colleagues in the Physical Chemistry Department, University College, Dublin, and the Chemistry Department of The Dublin Institute of Technology, I wish to express my thanks for their friendship and helpfulness at all times.

Finally, I would like to thank the staff at the institutes where this work was carried out for the assistance so readily offered to me.

Denis O'Farrell

A handwritten signature in cursive script that reads "DENIS O'FARRELL".

CONTENTS

	SUMMARY	(i)
1.0	INTRODUCTION	1
2.0	REACTIONS OF HYDROXYL RADICALS AND CHLORINE ATOMS WITH A SERIES OF SUBSTITUTED SILANES	
	2.1 Introduction	15
	2.2 Experimental	20
	2.3 Results	49
	2.4 Discussion	78
3.0	REACTIONS OF HYDROXYL RADICALS AND CHLORINE ATOMS WITH COMPOUNDS OF GROUP IV ELEMENTS	
	3.1 Introduction	101
	3.2 Experimental	106
	3.3 Results	114
	3.4 Discussion	128
4.0	LITERATURE CITED	151

TABLES

- (i) Rate constants for the reaction of OH radicals with a series of substituted silanes (ii)
- (ii) Rate constants for the reaction of Cl atoms with a series of substituted silanes (iv)
- (iii) Rate constants for the reaction of OH radicals with tetraalkyl compounds of Group IV elements (vi)
- (iv) Rate constants for the reaction of Cl atoms with tetraalkyl compounds of Group IV elements (vii)
- 1 Bond dissociation energies in organo-silicon compounds and their carbon analogues 10

2	Arrhenius parameters for hydrogen atom abstraction from trimethylsilane and trichlorosilane by CH_3 , CF_3 and CCl_3 radicals	11
3	Rate constants for the reaction of OH radicals, $\text{O}(^3\text{P})$, H and Cl atoms with silane and methyl substituted silanes	16
4	Analytical conditions for OH radical reactions	36
5	Analytical conditions for Cl atom reactions	38
6	OH reference rate constants used in chapter 2.0	51
7	Reactant concentrations and slope for the reaction of OH radicals with substituted silanes using CH_3ONO as the radical source	52

8	Reactant concentrations and slope for the reaction of OH radicals with substituted silanes using H_2O_2 as the radical source	55
9	Cl reference rate constants used in chapter 2.0	62
10	Reactant concentrations and slope for the reaction of Cl atoms with substituted silanes	63
11	Reactant concentrations and slope for the reaction of OH radicals with substituted silanes using H_2O_2 as the radical source	74
12	Rate constant data for OH radical and Cl atom reactions with silane and a series of methyl and ethyl silanes	80
13	Rate constants per Si-H bond	87

14	Rate constants for H-atom abstraction from methyl- and chloro- substituted silanes	94
15	Polar effects for OH radical and Cl atom reactions	95
16	Rate data for H atom abstraction from fluoro- substituted methylsilanes	99
17	Analytical conditions for OH radical reactions with tetramethyl compounds of Group IV elements	109
18	Analytical conditions for OH radical reactions with tetraethyl compounds of Group IV elements	110
19	Analytical conditions for Cl atom reactions with tetramethyl compounds of Group IV elements	111

20	Analytical conditions for Cl atom reactions with tetraethyl compounds of Group IV elements	112
21	OH reference rate constants used in chapter 3.0	115
22	Reactant concentrations for OH radical reactions with tetramethyl compounds of Group IV elements using CH_3ONO as the radical source	116
23	Reactant concentrations for OH radical reactions with tetraethyl compounds of Group IV elements using CH_3ONO as the radical source	118
24	Cl atom reference rate constants used in chapter 3.0	120
25	Reactant concentrations for Cl atom reactions with tetramethyl compounds of Group IV elements	121

26	Reactant concentrations for Cl atom reactions with tetraethyl compounds of Group IV elements	123
27	Reactant concentrations for OH radical reactions with tetraalkyl compounds of Group IV elements using H ₂ O ₂ as the radical source	125
28	Rate constant data for the reaction of OH radicals with tetraalkyl compounds of Group IV elements	129
29	Rate constant data for the reaction of Cl atoms with tetraalkyl compounds of Group IV elements	134
30	Arrhenius parameters for the reactions of CH ₃ , CD ₃ and CF ₃ with a series of tetraalkyl compounds of Group IV elements	148

FIGURES

1	Infrared spectrum of SiH_4	24
2	Infrared spectrum of $(\text{CH}_3)\text{SiH}_3$	24
3	Infrared spectrum of $(\text{C}_2\text{H}_5)\text{SiH}_3$	25
4	Infrared spectrum of $(\text{CH}_3)_2\text{SiH}_2$	26
5	Infrared spectrum of SiD_4	26
6	Infrared spectrum of $(\text{CH}_3)_3\text{SiD}$	27
7	Infrared spectrum of SiCl_3H	28
8	Infrared spectrum of CH_3ONO	29
9	Diagrammatic representation of the vacuum system used in the relative rate study	32

10	Diagrammatic representation of the reaction bag - lamp assembly - analytical layout used in the relative rate study	33
11	Diagrammatic representation of the vacuum system used in the absolute rate study	43
12	Diagrammatic representation of the experimental apparatus used in the absolute rate study	44
13	OH decay plots for the absolute rate study	48
14	Relative rate constant plots of OH + methyl-substituted silanes	56
15	Relative rate constant plots of OH + silanes showing isotope effects	57
16	Relative rate constant plots of OH + ethyl substituted silanes	58

17	Relative rate constant plots of OH + chloro-substituted silanes	59
18	Relative rate constant plots of OH + fluoro-substituted silanes	60
19	Relative rate constant plots of Cl + methyl-substituted silanes	66
20	Relative rate constant plots of Cl + silanes showing isotope effects	67
21	Relative rate constant plots of Cl + ethyl-substituted silanes	68
22	Relative rate constant plots of Cl + chloro-substituted silanes	69
23	Relative rate constant plots of Cl + fluoro-substituted silanes	70
24	Absolute rate constant plots of OH + methyl-substituted silanes	75

25	Absolute rate constant plots of OH + ethyl-substituted silanes	76
26	Absolute rate constant plots of OH + fluoro-substituted silanes	77
27	Plot of OH per Si-H bond vs the number substituent alkyl groups for a series of alkyl silanes	90
28	Relative rate constant plots of OH + silanes showing polar effects	97
29	Relative rate constant plots of OH + tetramethyl compounds of Group IV elements	117
30	Relative rate constant plots of OH + tetraethyl compounds of Group IV elements	119

31	Relative rate constant plots of Cl + tetramethyl compounds of Group IV elements	122
32	Relative rate constant plots of Cl + tetraethyl compounds of Group IV elements	124
33	Absolute rate constant plots of OH + tetramethyl compounds of Group IV elements	126
34	Absolute rate constant plots of OH + tetraethyl compounds of Group IV elements	127
35	Plot of Cl atoms + $(\text{CH}_3)_4\text{Pb}$ showing the decay of $(\text{CH}_3)_4\text{Pb}$ and the formation of CH_3Cl	142
36	Plot of $\log_{10} k_{\text{OH}}$ vs D(M-C)	146
37	Plot of $\log_{10} k_{\text{Cl}}$ vs D(M-C)	147

SUMMARY

Rate data are reported for the reaction of hydroxyl radicals with a series of substituted silanes. The data presented suggest the presence of polar effects in the transition state. Good agreement is reported between a relative rate study and an absolute rate study, Table (i). The corresponding reaction of chlorine atoms with the series of substituted silanes support the suggestion of polar effects in the transition state, Table (ii).

Rate data are also reported for the reaction of hydroxyl radicals with a series of tetramethyl and tetraethyl compounds of the Group IV elements. The data presented show an enhanced reactivity along the series from tetraalkylcarbon to tetraalkyllead. Good agreement is reported between a relative rate study and an absolute rate study, Table (iii). The corresponding reactions of chlorine atoms also demonstrate enhanced reactivity along the series from tetraalkylcarbon to tetraalkyllead, Table (iv).

Table (i)

Rate constants for the reaction of OH radicals with a series of substituted silanes.

$k \times 10^{12} \text{ cm}^3 \text{ molecule}^{-1} \text{ s}^{-1}$, (298±2K). Errors are twice the standard deviation of the slope.

SUBSTRATE	RELATIVE RATE CONSTANT	ABSOLUTE RATE CONSTANT
SiH ₄	15.6 ±2.1	
SiD ₄	4.52±2.56	
(C ₂ H ₅) ₂ SiH ₂	44.8 ±1.4	
(C ₂ H ₅) ₃ SiH	41.6 ±3.9	39.8 ±8.5
(CH ₃)SiH ₃	33.8 ±2.7	
(CH ₃) ₂ SiH ₂	40.9 ±1.9	
(CH ₃) ₃ SiH	36.4 ±1.2	37.2 ±5.6
(CH ₃) ₃ SiD	26.6 ±1.9	

Table (i)/contd.

$(\text{CH}_3)_2\text{SiClH}$	15.9 ± 1.4	
$(\text{CH}_3)\text{SiCl}_2\text{H}$	5.16 ± 0.24	
SiCl_3H	2.39 ± 0.26	
$(\text{C}_2\text{H}_5)_4\text{Si}$	8.24 ± 1.17	7.92 ± 0.54
$(\text{CH}_3)_4\text{Si}$	1.05 ± 0.08	1.12 ± 0.18
$(\text{CH}_3)_3\text{SiF}$	0.28 ± 0.03	0.35 ± 0.05
$(\text{CH}_3)_2\text{SiF}_2$	< 0.10	0.09 ± 0.04

Table (ii).

Rate constants for the reaction of Cl atoms with a series of substituted silanes.

$k \times 10^{11} \text{ cm}^3 \text{ molecule}^{-1} \text{ s}^{-1}$, (298±2K). Errors are twice the standard deviation of the slope.

SUBSTRATE	RELATIVE RATE CONSTANT
SiH ₄	40.9 ±4.7
SiD ₄	41.6 ±2.0
(C ₂ H ₅)SiH ₃	51.2 ±3.2
(C ₂ H ₅) ₂ SiH ₂	40.1 ±1.2
(C ₂ H ₅) ₃ SiH	45.6 ±2.9
(CH ₃)SiH ₃	38.0 ±0.5
(CH ₃) ₂ SiH ₂	33.1 ±0.8
(CH ₃) ₃ SiH	22.6 ±0.5
(CH ₃) ₃ SiD	23.5 ±1.8

Table (ii)/contd.

$(\text{CH}_3)_2\text{SiClH}$	12.5 ± 1.3
$(\text{CH}_3)\text{SiCl}_2\text{H}$	8.34 ± 0.24
SiCl_3H	2.71 ± 0.16
$(\text{C}_2\text{H}_5)_4\text{Si}$	39.3 ± 1.6
$(\text{CH}_3)_4\text{Si}$	13.7 ± 0.8
$(\text{CH}_3)_3\text{SiF}$	1.53 ± 0.60
$(\text{CH}_3)_2\text{SiF}_2$	< 0.47

Table (iii).

Rate constants for the reaction of OH radicals with Group IV compounds.

$k \times 10^{12} \text{ cm}^3 \text{ molecule}^{-1} \text{ s}^{-1}$, (298±2K). Errors are twice the standard deviation of the slope.

SUBSTRATE	RELATIVE RATE CONSTANT	ABSOLUTE RATE CONSTANT
$(\text{CH}_3)_4\text{C}$	0.84±0.11	0.79± 0.10
$(\text{CH}_3)_4\text{Si}$	1.05±0.08	1.12± 0.18
$(\text{CH}_3)_4\text{Ge}$	1.22±0.08	1.36± 0.17
$(\text{CH}_3)_4\text{Sn}$	1.52±0.03	
$(\text{CH}_3)_4\text{Pb}$	4.10±0.22	
$(\text{C}_2\text{H}_5)_4\text{C}$	4.69±0.28	5.11± 0.75
$(\text{C}_2\text{H}_5)_4\text{Si}$	8.24±1.17	7.92± 0.54
$(\text{C}_2\text{H}_5)_4\text{Ge}$	15.9 ±0.7	15.0 ± 2.1
$(\text{C}_2\text{H}_5)_4\text{Sn}$	28.1 ±3.1	40.8 ± 8.1
$(\text{C}_2\text{H}_5)_4\text{Pb}$	65.1 ±3.6	66.6 ±24.1

Table (iv).

Rate constants for the reaction of Cl atoms with
Group IV compounds.

$k \times 10^{11} \text{ cm}^3 \text{ molecule}^{-1} \text{ s}^{-1}$, (298±2K). Errors are
twice the standard deviation of the slope.

SUBSTRATE	RELATIVE RATE CONSTANT
$(\text{CH}_3)_4\text{C}$	10.0 ± 0.3
$(\text{CH}_3)_4\text{Si}$	13.7 ± 0.8
$(\text{CH}_3)_4\text{Ge}$	15.4 ± 1.1
$(\text{CH}_3)_4\text{Sn}$	21.6 ± 1.0
$(\text{CH}_3)_4\text{Pb}$	29.6 ± 0.3
$(\text{C}_2\text{H}_5)_4\text{C}$	30.4 ± 2.8
$(\text{C}_2\text{H}_5)_4\text{Si}$	39.3 ± 1.6
$(\text{C}_2\text{H}_5)_4\text{Ge}$	53.3 ± 2.4
$(\text{C}_2\text{H}_5)_4\text{Sn}$	61.1 ± 1.2
$(\text{C}_2\text{H}_5)_4\text{Pb}$	80.5 ± 10.3

REACTIONS OF HYDROXYL RADICALS AND CHLORINE
ATOMS WITH COMPOUNDS OF GROUP IV ELEMENTS

1.0 INTRODUCTION

It is now well established that the hydroxyl radical, OH, plays an important role in the chemistry of the atmosphere, where it dominates the chemistry of the troposphere in the same way that oxygen atoms and ozone dominate the chemistry of the stratosphere.¹ It is the main reaction sink for both natural and anthropogenic compounds emitted into the troposphere. For example, the gas-phase oxidation of SO₂ and the homogeneous oxidation of NO₂ compounds are principally photochemical oxidation reactions, with attack by OH being the main reaction pathway.^{2,3} The relative reactivity of organic species with OH determine not only their level in the troposphere but also the amounts which are transported into the stratosphere, and is a directly measurable index of their potential importance in the production of secondary pollutants.^{4,5} Hydroxyl radicals also play an important role in the oxidation and combustion of hydrogen containing compounds, the principal mechanism of fuel consumption being the abstraction of hydrogen atoms from alkanes by OH radicals. The rates of such a reaction are reflected in the C-H bond energies which vary with the degree of alkyl group substitution on the

involved carbon atom.⁶

The existence of the hydroxyl radical was first recognised in 1924 by Watson,⁷ who proposed that the water bands emitted by flames and electric discharges in moist air were due to the OH radical. By 1928 Bonhoffer and Reichardt⁸ had obtained the absorption spectrum of the OH radical in partially dissociated water vapour, and in 1935 Oldenberg⁹ was able to follow the decay of the radical in the products resulting from an electrical discharge through water vapour. Bates and Witherspoon,¹⁰ 1952, first indicated the importance of the hydroxyl radical in atmospheric chemistry, by proposing reactions involving OH and HO₂ as likely sinks for carbon monoxide and methane.² Leighton,¹¹ 1961, suggested that the OH radical could be an intermediate species playing an important role in photochemical air pollution. Because free radicals have an unpaired electron in their outer shell, and thus an affinity for adding a second electron, they can act as strong oxidizers of atmospheric trace gases.¹²

The important sources of OH radicals in the troposphere are from the reaction of O(¹D) atoms, formed from the photodissociation of O₃ ($\lambda \leq 319$ nm) with water

vapour⁴



from the photodissociation of HONO ($\lambda \leq 400 \text{ nm}$)



and from the reaction of HO₂ radicals with NO



Kinetic data are now available for the gas-phase reactions of the OH radical with a wide variety of organics, such as alkanes, haloalkanes, alkenes, haloalkenes, alkynes, oxygen-, nitrogen-, sulphur- and phosphorus-containing organics. Aromatic and organometallic compounds have also been studied. The great majority of this work has been carried out since 1970. Computer modelling studies have aided in the elucidation of the reaction sequences but although numerous mechanistic and product studies have been carried out in the past few years there are still significant areas of uncertainty concerning the mechanisms and products of OH radical reactions with organic compounds.⁴

In practice, two experimental methods have been used to study the kinetics of OH radical reactions with organics, namely absolute and relative rate constant

techniques. The absolute methods have involved mainly the discharge flow and flash photolysis techniques with techniques such as pulse radiolysis being used in only a limited number of studies.

Recent discharge flow investigations have utilized the reaction of the H atom with NO₂ as a source of OH



with detection of the OH radical being accomplished by techniques such as resonance absorption or resonance fluorescence for example. In the flash photolysis technique OH radicals are typically produced from the pulsed photodissociation of H₂O or HNO₃, although other methods may be used. The detection systems most commonly employed for the OH radical are kinetic spectroscopy or resonance fluorescence techniques.

The technique of pulse radiolysis is analogous to the older and more widely used flash photolysis technique. It was first applied to liquid systems by Matheson and Dorfman¹³ and extended to gases by Sauer and Dorfman.¹⁴ Early studies on gases were limited because the concentration of radical species is much lower than in a liquid system, since due to the lower densities less energy can be absorbed. However, the use of multiple reflection cells and the development of

fast sensitive detection equipment such as kinetic spectroscopy has made it possible to make observations comparable with those in liquid systems.¹⁵

To-day, precise relative rate constant data for a wide variety of organics can be provided, the lower limit for the OH radical rate constants attainable being set by the reproducibility of the analytical monitoring techniques used.⁴ In general, the technique monitors the relative rates of disappearance of two or more organic compounds in chemical systems containing OH radicals. It is clearly important that the loss process measured should be solely due to reaction with the OH radical and any other loss processes must be taken into account. Experimentally this is not, in general, a difficult task.

The use of a collapsible Teflon bag reaction chamber, as developed by Atkinson,¹⁶ avoids dilution problems due to sampling and minimizes errors due to wall effects. Analytical monitoring by gas chromatography or infrared spectroscopy allows the change in concentration of the compounds of interest to be monitored during the course of an experiment. Only relative measurements of the reactant substrate and reference organic are necessary, so that a constant

radical concentration is not required.

In certain cases kinetic data from gas-phase reactions of the OH radical allow possible rate constant trends and correlations to be examined.⁴ For example, correlations have been made with other electrophilic species such as O(³P), NO₃, O₃ and Cl atoms.^{4,17} Such correlations are valid provided the reaction mechanisms are the same. Correlation between O(³P) atoms and the OH radical are excellent as are correlations between Cl atoms and OH radicals for reactions with the alkanes.^{4,17} However, there are no apparent correlations between the reactivities of Cl atoms and OH radicals towards the oxygenated organics studied by Wallington et al.¹⁷ suggesting that one or other of the reactions may proceed via an alternative mechanism. Similarly, the effects of ring strain energy on the ozone reaction rate constants make correlations with OH radical rate constants much more complex.⁴

For OH radical reactions which proceed via H-atom abstraction, the most used correlation to date has been that between the OH radical rate constant and the C-H bond dissociation energy or the related quantity, the C-H bond stretching frequencies.^{18,19} Other forms of correlation based on a structure-reactivity relationship

have led to accurate rate constant data predictions. For example, Atkinson²⁰ has derived "group rate" data for H-atom abstraction from a 1⁰, 2⁰ or 3⁰ carbon atom as well as from a number of functional groups.

Kinetic isotope effects are often used in mechanistic studies. For example, a C-H bond may be substituted by a C-D bond. In such a case the absence of an isotope effect shows that the zero point energies associated with the bending and stretching of the C-H bond are not changed significantly in going from the reactants to the transition state. Such an observation is usually transformed into the categorical conclusion that the bond to hydrogen is not being broken in the rate controlling step of the reaction. This is not necessarily the correct conclusion in all cases. In some reactions, such as a highly exothermic reaction, the isotope effect might be undetectably small merely because only a slight weakening of the C-H bond would bring the intermediate to the second transition state.

Chlorine atoms play an important role in the chemistry of the stratosphere. The destruction of the ozone layer by Cl atoms has received much media attention lately. However, Cl atom reactions are also important loss processes for organics such as

hydrocarbons, chloroalkanes, aromatic species and oxygenated species in the stratosphere.^{17,21} Therefore rate data for the reaction of Cl atoms with these species has been obtained.^{17,21,22} The mechanisms include simple two-step free radical chains which substitute chlorine for hydrogen in the original starting material²³



Both steps are exothermic and proceed virtually at collisional rates with close to zero activation energy.^{22,23}

Little kinetic data is available for OH radical and Cl atom reactions with other members of the Group IV series,²⁴ although the reactions of many other atoms and radicals with organometallic and inorganic compounds have generated much interest. In particular, attack on silanes by radical species has been extensively studied. A considerable amount of kinetic data on hydrogen abstraction from organosilicon compounds by atoms and free radicals, particularly alkyl and fluoroalkyl radicals, has been collected.²⁵

Silicon is a larger atom than carbon ($R_{\text{Si}} = 1.17$ Å, $R_{\text{C}} = 0.77$ Å), it forms weaker bonds to itself, to

carbon and to hydrogen than does carbon; but because of its greater electropositivity, or because of its accessible 3d orbitals, it forms stronger bonds than does carbon to electronegative atoms with lone pairs, such as halogens, nitrogen and oxygen. Also silicon does not form stable p π -p π double bonds to itself or to other elements.²⁶

Silicon - hydrogen bonds are approximately 10, to 50 kJ mol⁻¹ weaker than their carbon - hydrogen analogs. A major feature of silane and the methylsilanes is the almost constant Si-H bond strength.²⁷ This is in contrast to the weakening effect of substituent methyl groups in the simple alkanes, Table 1. The difference can be rationalized in terms of the lower electronegativity of silicon compared to carbon (1.8 and 2.6 respectively on the Pauling scale). Hence, silicon will be a poorer acceptor of electron density from the substituent alkyl groups than will carbon.²⁷ Such differences between silicon and carbon make kinetic studies on the reactions of silicon compounds of interest in their own right as well as in relation to the analogous reactions of carbon compounds.

TABLE 1

Bond dissociation energies (kJ mol^{-1}) in organo-silicon compounds and their carbon analogues.

BOND	D	BOND	D
$\text{H}_3\text{Si-H}$	377.5 ^a	$\text{H}_3\text{C-H}$	439.3 ^b
$\text{CH}_3\text{SiH}_2\text{-H}$	374.5 ^c	$\text{CH}_3\text{CH}_2\text{-H}$	410.5 ^d
$(\text{CH}_3)_2\text{SiH-H}$	373.7 ^c	$(\text{CH}_3)_2\text{CH-H}$	397.5 ^d
$(\text{CH}_3)_3\text{Si-H}$	377.5 ^e	$(\text{CH}_3)_3\text{C-H}$	389.6 ^d
$\text{Cl}_3\text{Si-H}$	381.6 ^f	$\text{Cl}_3\text{C-H}$	401.3 ^c
$(\text{CH}_3)_3\text{SiCH}_2\text{-H}$	414.7 ^g	$(\text{CH}_3)_3\text{CCH}_2\text{-H}$	416.8 ^g
$(\text{CH}_3)_3\text{Si-Cl}$	472.3 ^c	$(\text{CH}_3)_3\text{C-Cl}$	334.4 ^h
$(\text{CH}_3)_3\text{Si-Br}$	401.3 ^c	$(\text{CH}_3)_3\text{C-Br}$	267.5 ^h
$(\text{CH}_3)_3\text{Si-I}$	321.9 ^c	$(\text{CH}_3)_3\text{C-I}$	213.2 ^h

a, Doncaster et al.²⁸

b, Baghal-Vayjooee et al.²⁹

c, Walsh²⁷

d, Golden et al.³⁰

e, Doncaster et al.³¹

f, Walsh et al.³²

g, Doncaster et al.³³

h, Kerr et al.³⁴

Reliable bond dissociation energies for silicon-containing compounds have enabled the factors influencing reactivity to be closely studied. Table 2 contrasts the

Arrhenius parameters determined for the reaction of CCl_3 , CF_3 and CH_3 radicals with $(\text{CH}_3)_3\text{SiH}$ and SiHCl_3 .

TABLE 2

Arrhenius parameters^a for hydrogen atom abstraction from trimethylsilane and trichlorosilane by CH_3 , CF_3 and CCl_3 radicals.

RH	D(R-H) ^b	CH_3		CF_3		CCl_3	
		$\log_{10}A$	E	$\log_{10}A$	E	$\log_{10}A$	E
$(\text{CH}_3)_3\text{SiH}$	377.5 ^c	8.7 ^d	34.7 ^d	8.7 ^e	33.0 ^e	9.3 ^f	23.4 ^f
SiHCl_3	381.6 ^c	7.8 ^g	18.0 ^g	8.6 ^g	40.6 ^g	8.8 ^f	25.1 ^f

a, E in kJ mol^{-1} ; A in $\text{l mol}^{-1} \text{s}^{-1}$

b, D(R-H) in kJ mol^{-1}

c, Walsh²⁷

d, Berkley et al.³⁵

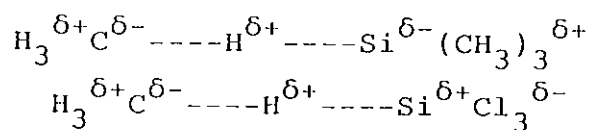
e, Morris et al.³⁶

f, Rice et al.³⁷

g, Kerr et al.³⁸

The decrease of 17 kJmol^{-1} in the activation energy for H-atom abstraction in going from $(\text{CH}_3)_3\text{SiH}$ to SiHCl_3 for the nucleophilic methyl radical can be rationalized in terms of a change from repulsive to

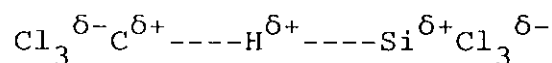
attractive polar forces in the transition states of the two reactions,



The change in the nature of the polar forces for the electrophilic species CF_3 and CCl_3 are in the opposite direction compared to the methyl radical and leads to an increase in the activation energy for the above reaction.³⁷ The polar attraction between the abstracted hydrogen atom and the electrophilic CCl_3 or CF_3 radical decreases as the electron density on the hydrogen atom is reduced by the increasing inductive effect of chlorine substitution on the silicon atom.

Rice et al.³⁷ have shown that the variation in the reaction rates of H-atom abstraction by the CCl_3 radical for a series of tri-substituted silanes arises mainly from differences in the activation energies. These authors have shown that an increase in substitution of alkyl groups by chlorine atoms increases the activation energy for hydrogen abstraction. Similar silicon-hydrogen bond strengths in these compounds, Table 1, indicate that the activation energy increase is probably polar rather than enthalpy related. This is ascribed to the inductive effect of the chlorine atoms reducing the electron density on the hydrogen atom which is

abstracted. This results in repulsion in the transition state for the reaction of the electrophilic CCl_3 radical with chlorosilanes



Polar effects have also been used to explain the marked increase in activation energy with increasing fluorination for hydrogen atom abstraction from the methyl group in methylfluorosilanes by CF_3 and C_2F_5 radicals.^{39,40} Similar effects, although less pronounced, have been reported for the reaction of CF_3 radicals with chlorosubstituted methylsilanes.^{41,42} Analogous reactions of CCl_3 radicals with chlorinated methylsilanes show only a relatively small activation energy increase with increasing chlorination.³⁷ The Arrhenius parameters for $(\text{CH}_3)_3\text{SiBr}$ are within experimental error of those determined for $(\text{CH}_3)_4\text{Si}$.³⁷ This suggests that the inductive electron withdrawing effects of chlorine or bromine atoms bonded to silicon do not significantly influence the rate of CCl_3 radical attack on a methyl group hydrogen in methylsilanes. However, fluorine atom substitution in these compounds does increase the activation energy for H-atom abstraction from the methyl group.³⁷ Presumably the inductive effect of fluorine atoms is sufficient to decrease the electron density on the abstracted hydrogen

atom, and hence to cause polar repulsion between the substrate and the attacking CCl_3 radical. The inductive effects of chlorine and bromine atoms are progressively weaker and hence so are the polar effects in the transition state.

REACTIONS OF HYDROXYL RADICALS AND CHLORINE ATOMS
WITH A SERIES OF SUBSTITUTED SILANES

2.1 INTRODUCTION

Little kinetic data is available for the abstraction of hydrogen atoms from silane and the methylsilanes. The most complete data set is for abstraction by hydrogen atoms and has been reviewed by Arthur et al.,⁴⁴ Table 3. The data presented are "best value" data representing a wide number of different techniques. The authors suggest that within the large error limits associated with the available rate constants, the reactivities of SiH_4 and the methylsilanes towards hydrogen atom attack on a H-atom bonded to silicon are approximately the same. The data available for the analogous reactions of OH radicals, Cl and $\text{O}(^3\text{P})$ atoms with silane and the methyl substituted silanes, Table 3, suggests a much wider variation in the reactivities of SiH_4 and the methylsilanes. However, the data is not sufficient to enable any clear trend or mechanistic route to be proposed.

TABLE 3

Rate constants^a for the reaction of OH radicals and O(³P), H and Cl atoms with silane and a series of methyl substituted silanes, at 298 ± 2 K.

Substrate	$k_{\text{OH}} \times 10^{12}$	$k_{\text{O}} \times 10^{13}$	$k_{\text{H}} \times 10^{13}$	$k_{\text{Cl}} \times 10^{11}$	D(Si-H) ^b
SiH ₄	12.4 ± 1.9 ^c 2.1 ± 0.4 ^g	4.8 ^c	3.6 ^d	41.7 ± 4.8 ^e 9.2 ± 2 ^h	377.5 ^f
SiD ₄		0.74 ^g	2.5 ^g		
CH ₃ SiH ₃			5.3 ^g		374.5 ⁱ
(CH ₃) ₂ SiH ₂			4.4 ^g		373.7 ⁱ
(CH ₃) ₃ SiH	40.0 ± 20 ^j	26.0 ± 3.0 ^j	3.8 ^g		377.5 ^k
(CH ₃) ₄ Si			<0.1 ^g		414.7 ^k

a, units of cm³ molecule⁻¹ s⁻¹

b, D(Si-H) in kJ mol⁻¹.

c, Atkinson et al.⁴³

d, Arthur et al.⁴⁴

e, Niki et al.⁴⁵

f, Doncaster et al.²⁸

g, Hoffmeyer et al.⁴⁶

h, Schlyer et al.⁴⁷

i, Walsh²⁷

j, Hoffmeyer et al.⁴⁸

k, Doncaster et al.³³

Atkinson et al.⁴³ reported an absolute rate constant for the reaction of the OH radical with silane, $k(\text{OH} + \text{SiH}_4) = (12.4 \pm 1.9) \times 10^{-12} \text{ cm}^3 \text{ molecule}^{-1} \text{ s}^{-1}$,

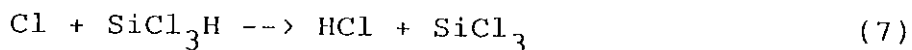
at 300 K, and a rate constant for the analogous reaction of $O(^3P)$, $k(O(^3P) + SiH_4) = 4.8 \times 10^{-13} \text{ cm}^3 \text{ molecule}^{-1} \text{ s}^{-1}$, at 297 K. Both rate constants were determined using a flash photolysis technique. Hoffmeyer et al.,⁴⁸ using a discharge flow method, determined a value for the reaction of $O(^3P)$ with $(CH_3)_3SiH$ of $k(O(^3P) + (CH_3)_3SiH) = (26.0 \pm 3.0) \times 10^{-12} \text{ cm}^3 \text{ molecule}^{-1} \text{ s}^{-1}$ at 298 K. They argued that as the bond dissociation energies in SiH_4 and $(CH_3)_3SiH$ are almost equal, Table 3, and assuming H-atom abstraction is the major reaction process in both cases, it would be expected that the rate constant for SiH_4 should be about four times higher than that found for $(CH_3)_3SiH$ on statistical grounds. On this basis Hoffmeyer et al.⁴⁸ suggested that Atkinson's value of the rate constant for $O(^3P) + SiH_4$ was anomalous. However, further discharge flow measurements at room temperature reported by Hoffmeyer et al.⁴⁶ for the reaction of $O(^3P)$ with SiH_4 and SiD_4 gave the rate constants $k(O(^3P) + SiH_4) = (2.1 \pm 0.4) \times 10^{-13} \text{ cm}^3 \text{ molecule}^{-1} \text{ s}^{-1}$ and $k(O(^3P) + SiD_4) = 0.74 \times 10^{-13} \text{ cm}^3 \text{ molecule}^{-1} \text{ s}^{-1}$ respectively, providing support for Atkinson's original work. It was concluded that the strong isotope effect found for the $O(^3P) + \text{silane}$ reaction indicates a H-atom abstraction pathway and that the significant increase in reactivity of $(CH_3)_3SiH$ probably arises from a change in mechanism. It was

tentatively suggested that the accessible 3d orbitals could lead to an addition process. A similar reactivity pattern for the reaction of OH radicals with SiH_4 and $(\text{CH}_3)_3\text{SiH}$ has also been observed although the error limits for the reported rate constant for the $\text{OH} + (\text{CH}_3)_3\text{SiH}$ reaction are extremely high.⁴⁸

The rate constant for the reaction of chlorine atoms with SiH_4 at room temperature has been determined by Schlyer et al.⁴⁷ and Niki et al.⁴⁵ Schlyer reported a value of $k(\text{Cl} + \text{SiH}_4) = (9.2 \pm 2.0) \times 10^{-11} \text{ cm}^3 \text{ molecule}^{-1} \text{ s}^{-1}$, using a discharge flow resonance fluorescence method. However, Niki et al. obtained a value of $k = (41.7 \pm 4.8) \times 10^{-11} \text{ cm}^3 \text{ molecule}^{-1} \text{ s}^{-1}$, using a relative rate technique. Niki suggested that the value measured by Schlyer could be in error, as in the absence of O_2 the initially formed radical SiH_3 might have reacted to a significant extent with the Cl_2 to regenerate Cl atoms. These authors pointed out that SiH_4 is highly susceptible to chain chlorination yielding all the $\text{SiH}_x\text{Cl}_{4-x}$ ($x = 0-3$) compounds, even in the dark. Evidence for hydrogen abstraction was given by Niki based on the stoichiometry of the reaction.

In a later study, Niki et al.⁴⁹ reported a room temperature rate constant for H-atom abstraction from

SiCl₃H by Cl atoms, $k(\text{Cl} + \text{SiCl}_3\text{H}) = (2.9 \pm 0.3) \times 10^{-11}$ cm³ molecule⁻¹ s⁻¹, again using a relative rate technique. They suggested that the reaction



predominates, followed by O₂ reaction with the primary radical SiCl₃. Interestingly, they remark on the value of the rate constant for the reaction being an order of magnitude smaller than that determined for the analogous reaction with SiH₄,⁴⁵ although the Si-H bond energies for SiH₄ and SiCl₃H are similar (377.5 and 381.6 kJ mol⁻¹, respectively.)⁵⁰ However, no explanation for the reduced reactivity of SiCl₃H compared to SiH₄ was provided.

In this work a comprehensive kinetic investigation of the reactions of OH radicals and Cl atoms with methyl, ethyl and halogenated silanes has been undertaken to establish the likelihood or otherwise of polar effects playing a part in the mechanisms of such reactions. Rate constant data is reported for OH radical reactions with the silanes and is compared with the data obtained, and reported, for the analogous reactions of Cl atoms. An explanation for the observed reactivity trends in these reactions is provided.

2.2 EXPERIMENTAL

2.2a Materials:

The materials used and their manufacturers are listed below:

Triethylsilane (>99%), diethylsilane (>98%), tetrachlorosilane (>99%), dimethyldichlorosilane (99.5%), ethyltrichlorosilane (>98%), trimethylsilane (>99%), dimethylchlorosilane (>97%), methylchlorosilane (>98%), trichlorosilane (>99%), trimethylchlorosilane (>99%), trimethylbromosilane (>97%), trimethyliodosilane (98%), and n-hexane (>99.96%) were all obtained from Fluka AG.

Trimethylfluorosilane (>99%) and dimethyldifluorosilane (>99%) were obtained from Fluorochem Ltd.

Tetraethylsilane (99%), tetramethylsilane (99.9%), n-heptane (99%), n-nonane (99%), 2-iodo-2-methylpropane (>98%), 2-bromo-2-methylpropane (>98%) and 2-chloro-2-methylpropane (>98%) were all obtained from the Aldrich Chemical Company Ltd.

i-Butane (>99%), neopentane (2,2-dimethylpropane) (>99%), 1-butene (>99%), c-hexene (>98%), toluene (98%), sodium nitrate (96%), methanol (99%), sulphuric acid (98%), nitric oxide (99.6%), hydrogen peroxide (60% w/v) and chlorine (99.9%) were all obtained from BDH Chemicals Ltd.

Ethane (>99%), ethene (>99%) and propene (>99%) were obtained from Messer Griesheim GmbH.

c-Hexane (99.95%) was obtained from May and Baker Ltd.

Diethylether (99%) was obtained from Riedel-de Haen AG.

Artificial air (high purity), zero nitrogen (OFN grade) and gas chromatographic gases; air, hydrogen and nitrogen were obtained from BOC Ltd.

Argon (99.9%) was obtained from AGA Denmark.

Water was triply distilled.

All investigated materials were degassed and trap to trap distilled, discarding the upper and lower fractions and retaining the middle fifth before use.

2.2b Preparation of materials.

(i). Silicon hydrides:⁵¹

Silane: A solution of LiAlH_4 in diethylether (pre-dried with Drierite and sodium wire) was placed in a 500 cm^3 3-necked round bottomed flask (cooled in a ice-salt bath). Tetrachlorosilane was added dropwise from a dropping funnel flushed with zero nitrogen. The product, SiH_4 , was carried by a zero nitrogen stream and collected in a liquid nitrogen trap. Silane was analysed by infrared spectroscopy and compared with literature spectra,⁴⁹ Figure 1.

Methylsilane,⁵² Figure 2, ethylsilane,^{52,53} Figure 3, and dimethylsilane,^{53,54} Figure 4, were prepared in an analogous manner from ethyltrichlorosilane, methyltrichlorosilane and dimethyldichlorosilane respectively. The products were analysed by infrared spectroscopy and compared with literature spectra.

Deuterosilane,⁵⁵ Figure 5, and trimethyl deutrosilane, Figure 6, were prepared from tetrachlorosilane and trimethylchlorosilane respectively, in an analogous manner to silane, with the exception that LiAlD_4 was used as the

hydrogenating agent. Each was analysed by infrared spectroscopy and compared with literature spectra.

(ii). Methyl nitrite:⁵⁶

A solution of 50% sulphuric acid in distilled water was added dropwise to a saturated solution of sodium nitrite in methanol. The products were carried by a stream of zero nitrogen through, firstly, a solution of sodium hydroxide (to remove excess acid) and secondly, Drierite (to remove water). Methyl nitrite was collected at -96°C using an acetone / liquid nitrogen slush bath, and purified on a vacuum line by trap to trap distillation. The yellow product was analysed by infra-red spectroscopy and compared with literature spectra,⁵⁷ Figure 8.

FIGURE 1

Infrared spectrum of SiH_4 showing
Si-H stretching vibration at 2190 cm^{-1}
Si-H bending vibration at 910 cm^{-1}

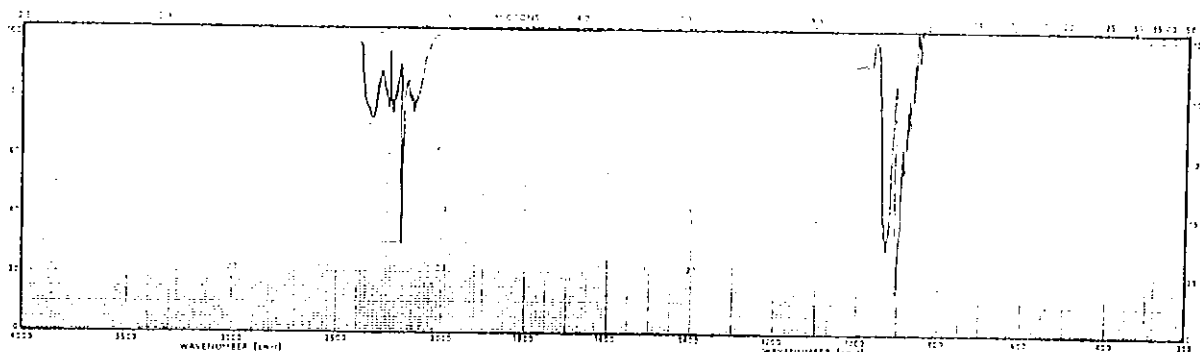


FIGURE 2

Infrared spectrum of $(\text{CH}_3)_3\text{SiH}_3$ showing
Si-H stretching vibration at 2160 cm^{-1}

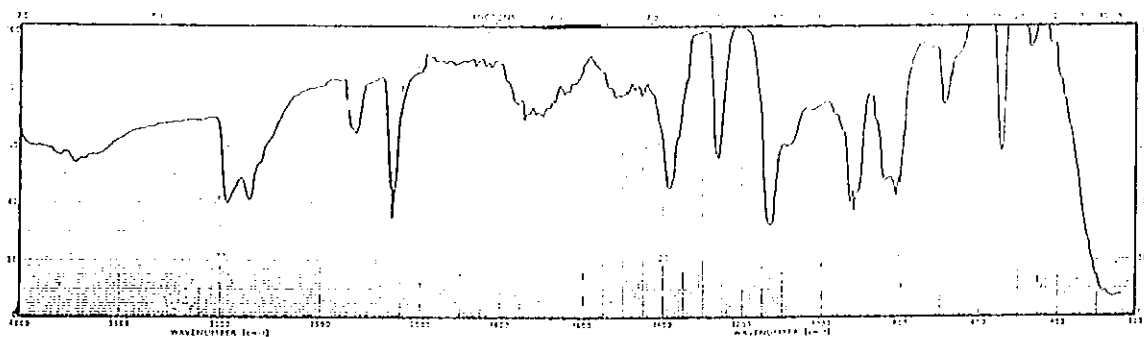


FIGURE 3

Infrared spectrum of $(C_2H_5)_3SiH_3$ showing
Si-H stretching vibration at 2160 cm^{-1}

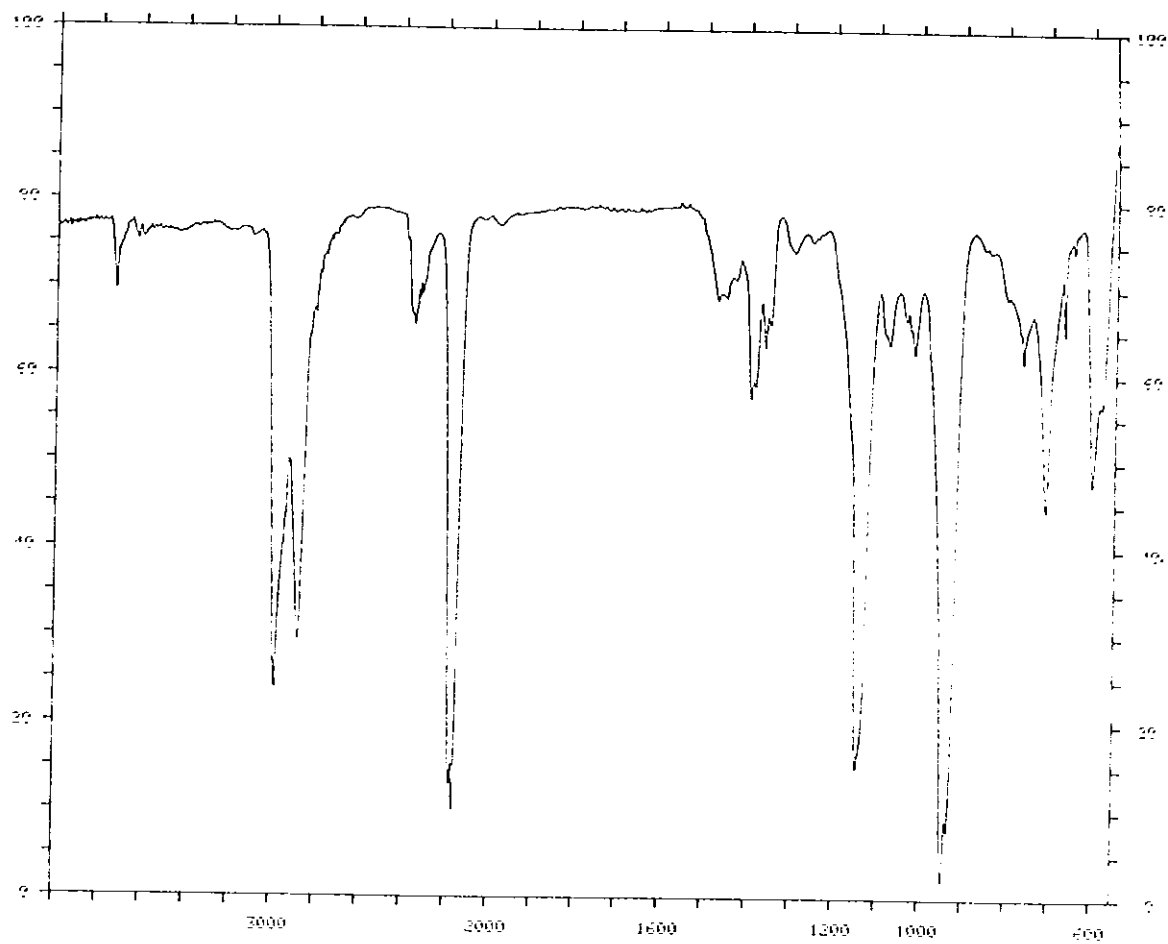


FIGURE 4

Infrared spectrum of $(\text{CH}_3)_2\text{SiH}_2$ showing
Si-H stretching vibration at 2120 cm^{-1}

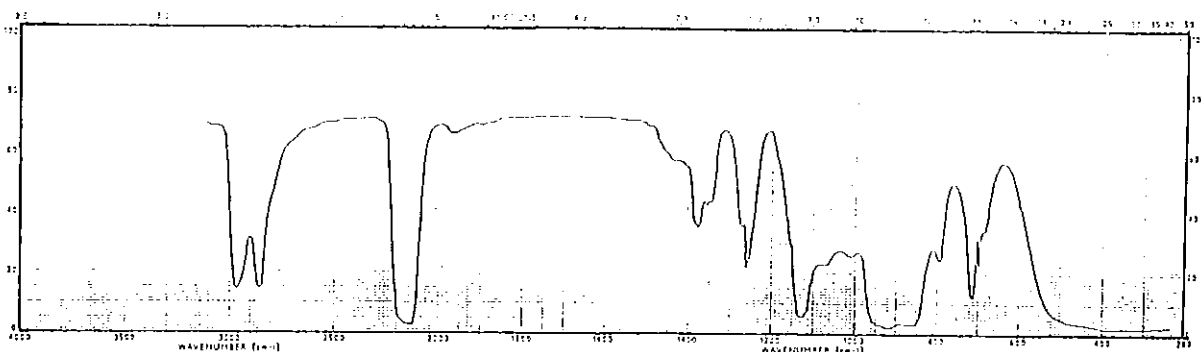


FIGURE 5

Infrared spectrum of SiD_4 showing
Si-D stretching vibration at 1589 cm^{-1}

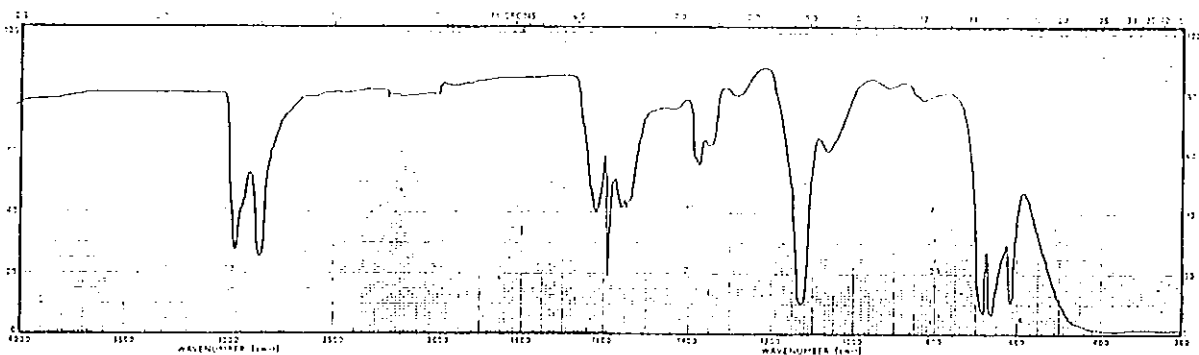


FIGURE 6

Infrared spectrum of $(\text{CH}_3)_3\text{SiD}$ showing
Si-D stretching vibration at 1550 cm^{-1}

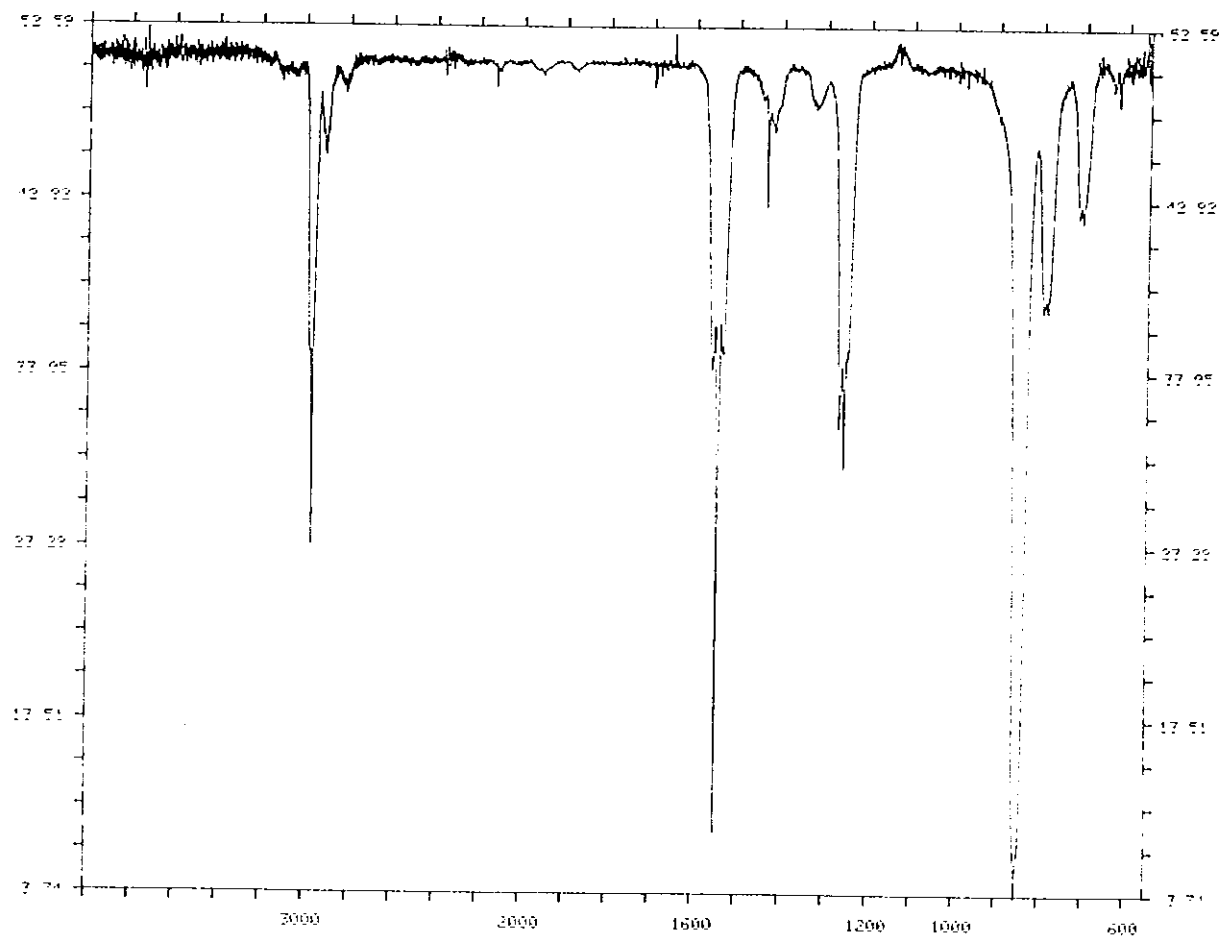


FIGURE 7

Infrared spectrum of SiCl_3H showing
Si-H bending vibration at 817 cm^{-1}

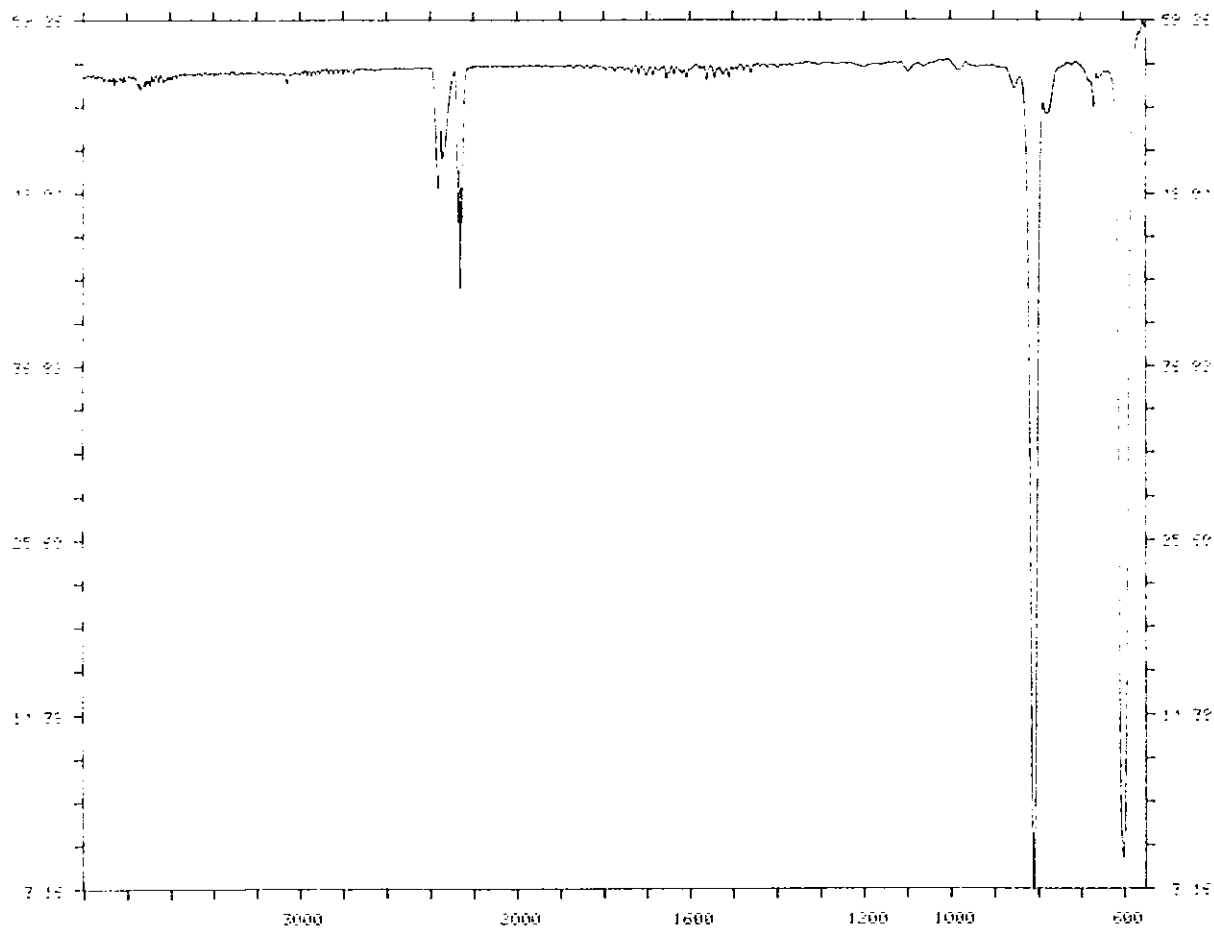
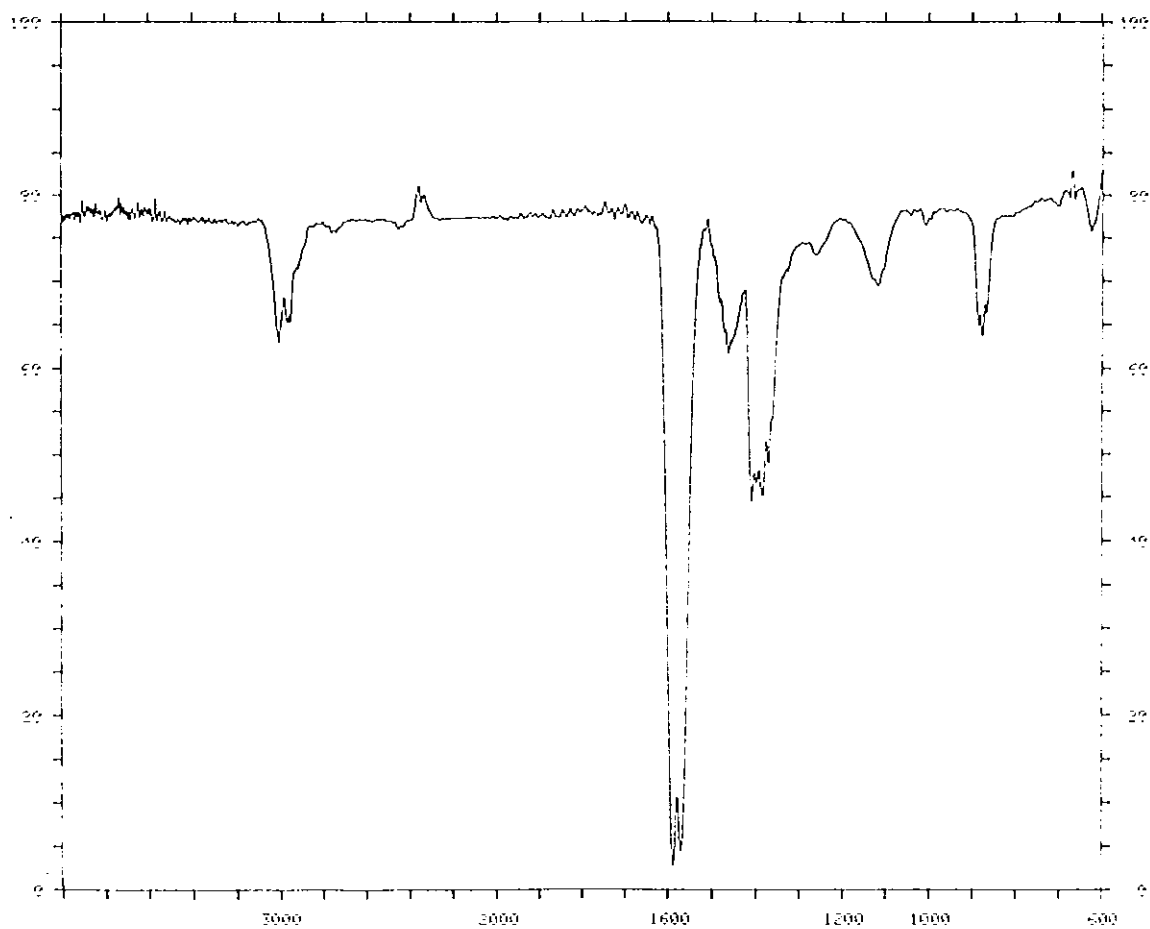


FIGURE 8

Infrared spectrum of methyl nitrite, CH_3ONO



(iii). Hydrogen peroxide.

Hydrogen peroxide (60% w/v) was pumped by rotary pump to approximately one-fifth of its original volume, giving an approximate concentration of 90% H_2O_2 at a vapour pressure of 1.5 torr.

A: The relative rate study

2.2c Apparatus:

The apparatus shown in Figure 9 consisted of a conventional mercury-free, high vacuum line, made of Pyrex glass. The vacuum was maintained by means of an Edwards silicon oil diffusion pump, model D202, backed by an Edwards double stage rotary pump, model E2M2. Taps were of the greaseless variety with Teflon o-rings, obtained from J. Young Ltd. Acton. The vacuum was monitored using an Edwards Pirani gauge head, model G6A, in conjunction with an Edwards speedivac-gauge, model B5. Reactant pressures were measured using an MKS Baratron type 222BA (0-760 torr), and an MKS Baratron type 222CA (0-10 torr), in conjunction with a readout unit. A pressure of 1 torr of reactant in the 565 cm^3 mixing bulb corresponded to a concentration of about 10 ppm of reactant when blown into

the reaction chamber. Figure 10, shows the reaction chamber, lamp assembly and analytical layout. Irradiations were carried out in an approximately 60 litre FEP Teflon cylindrical reaction chamber surrounded by 10 TL 20W/08 "black" lamps (Philips) and 10 TL 20W/09 "sun" lamps (Philips). Both emit radiation between 300 and 450 nm with a maximum intensity at approximately 352 nm. Photolysis of H_2O_2 was achieved by 10-20 TUV15W germicidal lamps (Philips) with the major output at 254 nm. The lamp assembly was arranged on four electrical circuits (two front, two rear) with every second lamp being on a different circuit. Thus variations in light intensity could be achieved. Prior to irradiation, the reaction chamber and lamp assembly were covered with an opaque cover to prevent photolysis of the reactants.

FIGURE 9

Diagrammatic representation of the vacuum system used in the relative rate study.

- | | |
|---------------------------------------|---------------------|
| a,b. Expansion bulbs | l. Vacuum gauge |
| c,d. Storage bulbs | n. Male connections |
| e-h. Storage traps | o-p. Traps |
| i. 565cm ³ mixing bulb | q. Diffusion pump |
| j. MKS Baratron capacitance manometer | r. Air inlet |
| k,m. Readout units | s. To rotary pump |

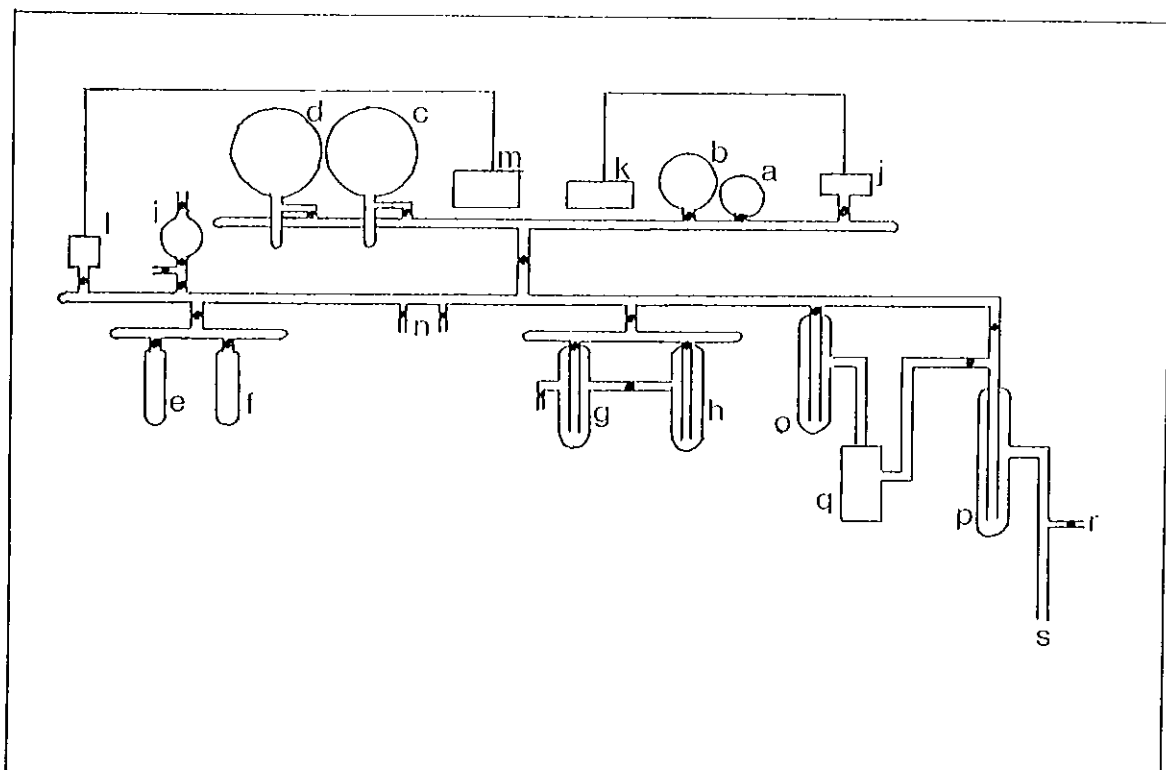
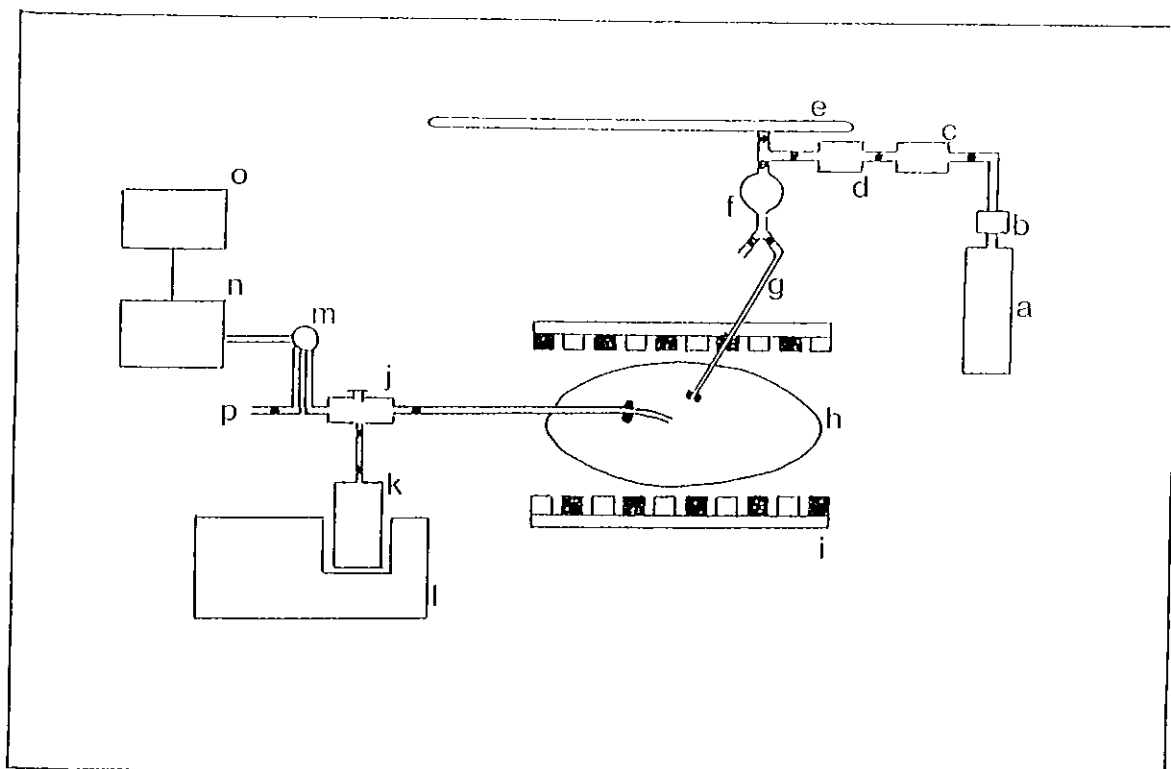


FIGURE 10

Diagrammatic representation of the reaction chamber - lamp assembly - analytical layout used in the relative rate study.

- | | |
|---|--------------------------------|
| a. Air /N ₂ cylinder | i. Lamp assembly |
| b. Cylinder head | j. Sample bulb with septum |
| c. Molecular sieve | k. Long path IR cell |
| d. Flowmeter | l. IR spectrometer |
| e. Vacuum line | m. Injection loop |
| f. 565 cm ³ mixing bulb | n. Gas chromatograph |
| g. Teflon tubing | o. Chart recorder / integrator |
| h. 60 dm ³ Teflon reaction chamber | |



2.2d Procedure:

The method of filling the reaction chamber was often varied to check that it did not effect the results. However, the following method was typically used. The reaction chamber was approximately half-filled with diluent gas (zero nitrogen or artificial air). The vacuum line was then evacuated to about 10^{-5} torr pressure. A reactant was released into the vacuum line and mixing bulb until a desired pressure was achieved, typically 0.300 - 3.00 torr (3 - 30 ppm in the reaction vessel). The 565 cm³ mixing bulb was sealed off from the remainder of the line and the reactant was mixed with diluent gas immediately prior to being blown into the reaction chamber. The reactant remaining in the vacuum line was frozen back into its storage trap. The process was repeated for each reactant, and the reaction chamber was then filled to capacity with diluent gas. The Teflon reaction chamber was connected to the vacuum line and analytical instruments by means of 1/8" O.D. Teflon tubing. The reaction mixture was left in the dark for a period of about half an hour to allow for mixing of the reactants. Complete mixing was confirmed by gas chromatographic analysis, or in special cases by infrared analysis. The reaction mixture was kept in the dark for up to three hours to determine the extent of any dark reaction. It was also irradiated for a period

of time, in the absence of the radical source, to ensure that photolysis of the substrate or reference compound was unimportant.

2.2e Analysis:

Two methods of analysis were used. For most reactant compounds gas chromatography sufficed, but for some, long path infrared spectroscopy was employed.

Gas chromatographic analysis.

A Perkin-Elmer F11 gas chromatograph incorporating a flame ionization detector was used for all gas chromatographic analyses. The carrier gas was nitrogen. Carrier flow was regulated with needle valve flow controls. Sample injection was by a 2 cm³ (or occasionally 4 cm³ or 10 cm³) "on line" Teflon coated - stainless steel injection loop, attached to a Valco 6-port gas sampling valve. Hamilton gas-tight syringes were also used. The chromatograms were recorded on a 2 mV f.s.d. Servogor potentiometric chart recorder (Gelman instrument company) with disk integrator. Relative concentrations of a compound were determined during an analysis by measuring peak heights and peak areas.

Tables 4 and 5 list the reference compound and

analytical conditions used with each substrate for the OH radical and Cl atom reactions respectively.

TABLE 4

Analytical conditions for OH radical reactions.

Substrate	Reference	Column Type	Support	Mesh Size	Length and O.D.	Oven Temperature (°C)	Flow Rate (cm ³ min ⁻¹)
SiH ₄ [*]	n-C ₆ H ₁₄	20% DC200	Chromosorb-WHP	80/100	4'x1/8"	30	35
SiD ₄ [*]	n-C ₆ H ₁₄	20% DC200	Chromosorb-WHP	80/100	4'x1/8"	30	35
(CH ₃) ₃ SiH	n-C ₆ H ₁₄	20% DC200	Chromosorb-WHP	80/100	4'x1/8"	50	25
	C ₃ H ₆	15% Squalane	Chromosorb-P	80/100	12'x1/8"	60	20
(CH ₃) ₃ SiD	n-C ₆ H ₁₄	20% DC200	Chromosorb-WHP	80/100	4'x1/8"	25	30
	C ₃ H ₆	15% Squalane	Chromosorb-P	80/100	12'x1/8"	60	20
(C ₂ H ₅) ₃ SiH	c-C ₆ H ₁₂	20% DC200	Chromosorb-WHP	80/100	4'x1/8"	60	20
	c-C ₆ H ₁₀	20% DC200	Chromosorb-WHP	80/100	4'x1/8"	60	20
	(CH ₃) ₃ SiH	15% Squalane	Chromosorb-P	80/100	6'x1/4"	25	15
(C ₂ H ₅) ₂ SiH ₂	1-C ₄ H ₈	15% Squalane	Chromosorb-P	80/100	6'x1/4"	65	30
	c-C ₆ H ₁₀	15% Squalane	Chromosorb-P	80/100	6'x1/4"	65	30
	(C ₂ H ₅) ₃ SiH	20% DC200	Chromosorb-WHP	80/100	4'x1/8"	30	30

Table 4/contd.

$(\text{CH}_3)_2\text{SiH}_2$	C_3H_6	15% Squalane	Chromosorb-P	80/100	12'x1/8"	25	60
	$(\text{CH}_3)_3\text{SiH}$	15% Squalane	Chromosorb-P	80/100	12'x1/8"	25	60
CH_3SiH_3	1- C_4H_8	15% Squalane	Chromosorb-P	80/100	4'x1/8"	40	20
	$(\text{CH}_3)_3\text{SiH}$	15% Squalane	Chromosorb-P	80/100	4'x1/8"	40	20
$(\text{CH}_3)_2\text{SiHCl}$	n- C_6H_{14}	20% DC200	Chromosorb-WHP	80/100	4'x1/8"	50	25
	i- C_4H_{10}	20% DC200	Chromosorb-WHP	80/100	4'x1/8"	40	20
$\text{CH}_3\text{SiHCl}_2$	C_3H_6	15% Squalane	Chromosorb-P	80/100	6'x1/4"	25	30
	i- C_4H_{10}	15% Squalane	Chromosorb-P	80/100	6'x1/4"	25	30
	n- C_6H_{14}	15% Squalane	Chromosorb-P	80/100	6'x1/4"	80	30
SiHCl_3^*	n- C_6H_{14}	20% DC200	Chromosorb-WHP	80/100	4'x1/8"	30	35
$(\text{C}_2\text{H}_5)_4\text{Si}$	c- C_6H_{12}	20% DC200	Chromosorb-WHP	80/100	4'x1/8"	95	20
$(\text{CH}_3)_4\text{Si}$	n- C_6H_{14}	15% Squalane	Chromosorb-P	80/100	6'x1/4"	25	10
	i- C_4H_{10}	20% DC200	Chromosorb-WHP	80/100	12'x1/8"	40	10
$(\text{CH}_3)_3\text{SiF}$	C_2H_6	20% DC200	Chromosorb-WHP	80/100	12'x1/8"	25	40
	i- C_4H_{10}	20% DC200	Chromosorb-WHP	80/100	12'x1/8"	25	40
$(\text{CH}_3)_2\text{SiF}_2$	$(\text{CH}_3)_3\text{SiF}$	20% DC200	Chromosorb-WHP	80/100	12'x1/8"	25	40

* denotes a substrate also analysed by infrared spectroscopy

TABLE 5

Analytical conditions for Cl atom reactions.

Substrate	Reference	Column Type	Support	Mesh Size	Length and O.D.	Oven Temperature (°C)	Flow Rate (cm ³ min ⁻¹)
SiH ₄ [*]	n-C ₆ H ₁₄	20% DC200	Chromosorb-WHP	80/100	4'x1/8"	25	35
	i-C ₄ H ₁₀	15% Squalane	Chromosorb-P	80/100	12'x1/8"	50	25
SiD ₄ [*]	i-C ₄ H ₁₀	15% Squalane	Chromosorb-P	80/100	12'x1/8"	25	20
	(CH ₃) ₃ SiH	15% Squalane	Chromosorb-P	80/100	12'x1/8"	25	20
(CH ₃) ₃ SiH	i-C ₄ H ₁₀	15% Squalane	Chromosorb-P	80/100	12'x1/8"	50	30
(CH ₃) ₃ SiD	i-C ₄ H ₁₀	15% Squalane	Chromosorb-P	80/100	12'x1/8"	50	30
(C ₂ H ₅) ₃ SiH	c-C ₆ H ₁₂	20% DC200	Chromosorb-WHP	80/100	4'x1/8"	60	20
(C ₂ H ₅) ₂ SiH ₂	n-C ₆ H ₁₄	15% Squalane	Chromosorb-P	80/100	6'x1/4"	75	30
C ₂ H ₅ SiH ₃	(CH ₃) ₄ C	15% Squalane	Chromosorb-P	80/100	12'x1/8"	25	10
(CH ₃) ₂ SiH ₂	n-C ₆ H ₁₄	15% Squalane	Chromosorb-P	80/100	12'x1/8"	25	20
CH ₃ SiH ₃	i-C ₄ H ₁₀	15% Squalane	Chromosorb-P	80/100	12'x1/8"	50	20
(CH ₃) ₂ SiHCl	c-C ₆ H ₁₂	20% DC200	Chromosorb-WHP	80/100	4'x1/8"	25	25
	C ₆ H ₅ CH ₃	20% DC200	Chromosorb-WHP	80/100	4'x1/8"	25	25
CH ₃ SiHCl ₂	i-C ₄ H ₁₀	20% DC200	Chromosorb-WHP	80/100	4'x1/8"	25	15
	i-C ₄ H ₁₀	15% Squalane	Chromosorb-P	80/100	6'x1/4"	25	5

Table 5/contd.

SiHCl_3^*	C_2H_6	15% Squalane	Chromosorb-P	80/100	6'x1/4"	25	5
$(\text{C}_2\text{H}_5)_4\text{Si}$	$\text{c-C}_6\text{H}_{12}$	20% DC200	Chromosorb-WHP	80/100	4'x1/8"	40	35
$(\text{CH}_3)_4\text{Si}$	$\text{i-C}_4\text{H}_{10}$	20% DC200	Chromosorb-WHP	80/100	4'x1/8"	40	5
	$\text{i-C}_4\text{H}_{10}$	15% Squalane	Chromosorb-P	80/100	6'x1/4"	30	15
$(\text{CH}_3)_3\text{SiF}$	C_2H_6	20% DC200	Chromosorb-WHP	80/100	12'x1/8"	25	15
	$\text{i-C}_4\text{H}_{10}$	20% DC200	Chromosorb-WHP	80/100	12'x1/8"	25	15
$(\text{CH}_3)_2\text{SiF}_2$	$(\text{CH}_3)_3\text{SiF}$	20% DC200	Chromosorb-WHP	80/100	12'x1/8"	25	15

* denotes a substrate also analysed by infrared spectroscopy

Infrared analysis:

A Perkin-Elmer model 457 grating infrared spectrophotometer, with ordinate expansion, was used for all infrared analyses. The instrument was fitted with a Wilks 14.5 m variable pathlength gas cell (model 410). The interior of the cell was Teflon coated and housed gold coated Pyrex mirrors and KBr windows. The cell was evacuated and filled directly from the reaction chamber. The relative concentrations of the silane substrate were determined by measuring the absorbance of either the Si-H stretching or bending vibration band using the equation, $A = \log_{10} I_0/I$, where A is the absorbance, I_0 is the intensity of the incident radiation and I is the intensity of the transmitted radiation. Where deviations from the Lambert-Beer law occurred a calibration curve was used.

B: The absolute rate study

2.2f Apparatus

The apparatus shown in Figure 11 consisted of a stainless steel high vacuum line, with Viton o-ring joints. The vacuum was maintained by means of a Leybold rotary pump, model D2, and an Edwards silicon oil diffusion pump, model D203, backed by an Alcatel rotary pump, model 2008A. The taps were either Hoke vacuum taps or Saunders Edwards speedivalves. The vacuum was monitored using a Pirani-cold cathode gauge in conjunction with a Pirani-cold cathode gauge control, model PKG 020. Reactant pressures were measured using a MKS Baratron 170 series absolute electronic manometer, in conjunction with an MKS Baratron range multiplier, type 170M-6C, and a Hewlett Packard 3465A digital voltmeter.

Reactions were carried out in a stainless steel cell (1 dm^3 approximately), fitted with a set of conjugate mirrors allowing a multiple pass (12 traversals) pathlength of 120 cm of analyzing light through the sample, as described by White.⁵⁸ The mirrors were frequently changed to maintain the maximum optical intensity, Figure 12.

Reactions were initiated by a single pulse of electrons of 30 ns duration with a maximum current of about 3000 amperes, provided by a field-emission accelerator (Febetron 705B), Figure 12. In principle, the Febetron consists of a series of capacitor modules in parallel, with their central spark gaps in open circuit charged from a high-voltage power supply. The high-voltage output is discharged via a short pulse adapter into the field-emission tube and passed out of the tube window. The pulse to pulse repeatability is specified as 5%

FIGURE 11

Diagrammatic representation of the vacuum system used in the absolute rate study.

- | | |
|--------------------------------------|-----------------------------------|
| a. 1 dm ³ reaction cell | h. Male connections |
| b. Water trap | i. 60 cm ³ mixing bulb |
| c. Pirani gauge head | j. Flowmeter |
| d. Readout unit | k. Diffusion pump |
| e. MKS Baratron manometer | l-m. Cold traps |
| f. Readout unit | n-o. Rotary pumps |
| g. 60 dm ³ Teflon chamber | |

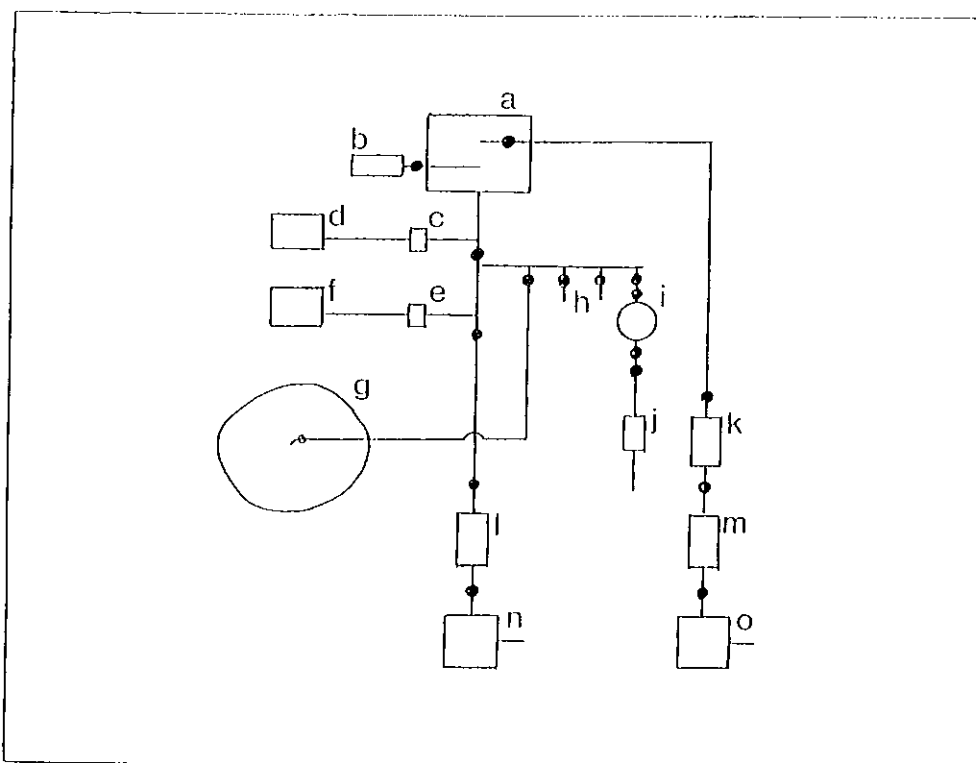
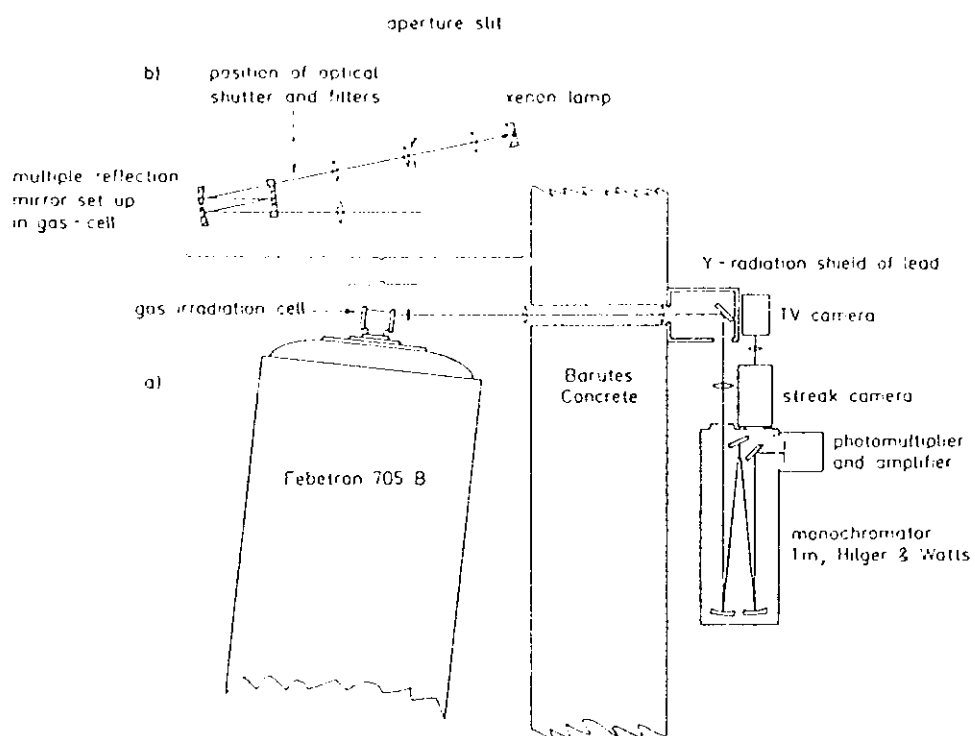


FIGURE 12

Diagrammatic representation of the experimental apparatus. (a) Layout in the horizontal plane. (b) Enlarged vertical cut showing the optics for the analysing light beam from the xenon lamp.



2.2g Procedure:

The normal procedure for filling the reaction cell was to allow a known pressure of substrate to expand directly into the evacuated reaction cell from its cold trap, followed by the addition of 15 torr of triply distilled water. The mixture was then backed up with argon to 1 atmosphere total pressure. However, using this method it was suspected that compounds with a low vapour pressure were adsorbed onto the walls of the reaction cell. To avoid this problem the normal procedure was altered. Where possible, a known pressure of substrate was expanded into an evacuated 60 cm³ mixing bulb, prior to being blown with Ar into an approximately 60 dm³ FEP Teflon chamber (similar to that used in the relative rate study), connected to the line by 1/8" od. Teflon tubing. The chamber was filled with Ar to a known volume through a 0-4 dm³ min⁻¹ flow-meter. The mixture was allowed to mix in the chamber for about thirty minutes. The water (15 torr) was expanded into the reaction cell in the normal way and the substrate / Ar mixture then expanded into the cell to a known pressure and backed up to 1 atm with Ar. In this

way different concentrations of reactant could be obtained from the same reaction mixture in the chamber. As the reactant was mixed in a similar manner to that employed in the relative rate technique, any significant difference in the experimental results between the absolute and relative rate methods could justifiably be attributed to the experimental technique and not to the handling of the chemicals.

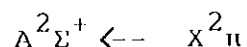
In some cases, the vapour pressure of the reactant was too low to allow for a sufficiently high concentration in the Teflon chamber. In such cases the reactant was shared into the 60 cm³ mixing bulb as before, and then mixed with 1 atm Ar expanded from the Teflon chamber. The bulb was isolated and the reaction cell filled with water in the normal way. The contents of the mixing bulb were then blown into the reaction cell with Ar. The dilution factor was about 22.2. It was expected that this method would prevent the substrate going directly onto the stainless steel cell wall.

2.2h Analysis:

The reaction was analysed by a pulsed Varian 150 watt high-pressure xenon arc lamp. the lamp was coupled to a 1m Hilger and Watts grating spectrograph with a

1200-groove/mm grating blazed at 300 nm to obtain high efficiency down into the uv region (and a reciprocal dispersion of 0.8 nm/mm). The light intensity from the exit-slit of the monochromator was monitored using a Hamamatsu R928 photomultiplier coupled to a current input operational amplifier with adjustable offset. The transient signals were stored in a Biomation 8100 waveform digitizer interfaced to a PDP11 computer that controlled the storage and transfer of raw data for further processing on a mainframe computer.

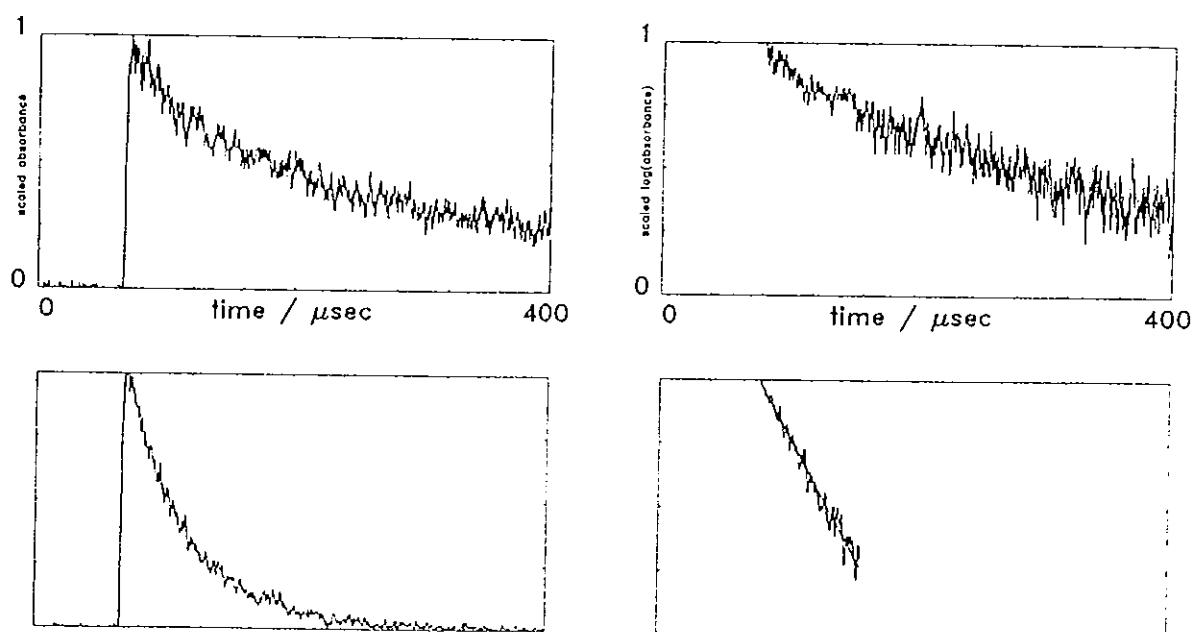
The decay of OH radicals was followed by monitoring the transient absorbance at 309 nm



Several sharp rotational lines are significant in the band used and deviations from the Lambert-Beer law occur. A modified version of the Lambert-Beer law was used to determine the absorbance,^{59,60} $A = (\epsilon cl)^n$, where n is a fractional power between 0 and 1. In this study n was obtained by varying the optical path length in the cell. The observed transient absorbance was a direct measure of the decay of the concentration of hydroxyl radicals.

FIGURE 13

OH decay. Upper left: pure H₂O (15 torr) with Ar to 1 atm. Lower left: with added substrate. The right-hand figures are the corresponding logarithmic plots.

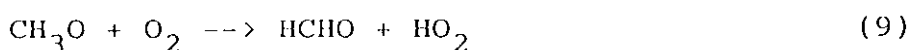
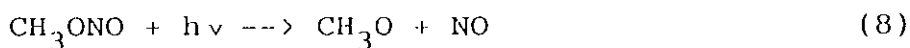


2.3 RESULTS

A: The Relative Rate Method

2.3a Hydroxyl Radical Reactions:

Hydroxyl radicals were generated by the photolysis of methyl nitrite in air at wavelengths ≥ 300 nm



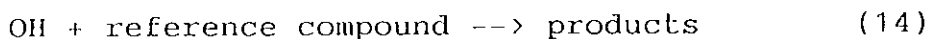
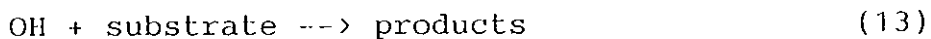
Addition of NO to the reaction mixtures minimized the formation of ozone.¹⁶



Hydroxyl radicals were also generated by the photolysis of hydrogen peroxide at $\lambda = 254$ nm



The OH radicals generated via reactions (8)-(10), or in reaction (12), react with the substrate and reference compound:



Assuming that the substrate and reference compound are consumed only by reaction with OH radicals, and providing dilution is negligible, then

$$-d[\text{substrate}]/dt = k_{13}[\text{OH}][\text{substrate}] \quad (\text{I})$$

$$-d[\text{reference compound}]/dt = k_{14}[\text{OH}][\text{reference compound}] \quad (\text{II})$$

where k_{13} and k_{14} are the OH radical rate constants for reactants (13) and (14) respectively. Hence,

$$-d\ln[\text{substrate}]/dt = k_{13}[\text{OH}] \quad (\text{III})$$

$$-d\ln[\text{reference compound}]/dt = k_{14}[\text{OH}] \quad (\text{IV})$$

thus,

$$d\ln[\text{substrate}]/dt = k_{13}/k_{14} d\ln[\text{reference compound}]/dt \quad (\text{V})$$

and

$$\ln \frac{[\text{substrate}]_0}{[\text{substrate}]_t} = \frac{k_{13}}{k_{14}} \ln \frac{[\text{reference compound}]_0}{[\text{reference compound}]_t} \quad (\text{VI})$$

where $[\text{substrate}]_0$ and $[\text{reference compound}]_0$ are the concentrations of the substrate and reference compounds respectively at time t_0 , and $[\text{substrate}]_t$ and $[\text{reference compound}]_t$ are the corresponding concentrations at time t .

Reactions were carried out at room temperature ($298 \pm 2\text{K}$) and atmospheric pressure (730-750 torr). The relative reactant concentrations were varied as much as the analytical methods permitted. In all cases a plot of $\ln([\text{substrate}]_0/[\text{substrate}]_t)$ against $\ln([\text{reference compound}]_0/[\text{reference compound}]_t)$ gave a straight line with zero intercept and slope k_{13}/k_{14} , Figures 14-18, independent of relative reactant concentrations and

light intensity.

Table 6 lists the OH reference rate constants used in this work.

Table 6

OH reference rate constants used in this work.

k in $\text{cm}^3 \text{ molecule}^{-1} \text{ s}^{-1}$ at 298 K and 1 atm.

Reference Compound	$k_{14} \times 10^{12}$
C_2H_6	0.27 ^a
n- C_4H_{10}	2.53 ^a
i- C_4H_{10}	2.37 ^a
n- C_6H_{14}	5.58 ^a
c- C_6H_{12}	7.38 ^a
$(\text{CH}_3)_4$	0.85 ^a
C_3H_6	26.3 ^a
1- C_4H_8	31.4 ^a
c- C_6H_{10}	67.4 ^a
$(\text{CH}_3)_4\text{Si}$	1.05 ^b
$(\text{CH}_3)_3\text{SiH}$	36.4 ^b
$(\text{C}_2\text{H}_5)_3\text{SiH}$	41.6 ^b

a, Atkinson⁴ b, This work

Table 7 lists the reactant concentrations (ppm) and slope, k_{13}/k_{14} , for the various, Substrate / Reference Compound / CH_3ONO / NO / Air, mixtures, where $1 \text{ ppm} = 2.40 \times 10^{13} \text{ molecules cm}^{-3}$ at 296 K and 735-torr total pressure.

TABLE 7

Reactant concentrations and slope, k_{13}/k_{14} , for the reaction of OH radicals with substituted silanes at room temperature and atmospheric pressure.

Substrate	Concentration (ppm)	Reference	Concentration (ppm)	CH_3ONO Concentration (ppm)	NO Concentration (ppm)	$\frac{k_{13}}{k_{14}}$
SiH_4	30-50	n-C ₆ H ₁₄	5-10	20-30	0-10	2.80±0.40
SiD_4	30-50	n-C ₆ H ₁₄	5	30	10	0.81±0.50
$(\text{CH}_3)_3\text{SiH}$	3	n-C ₆ H ₁₄	5	10	5	6.47±0.57
	6	C ₃ H ₆	5	5	0-10	1.39±0.08
$(\text{CH}_3)_3\text{SiD}$	20-30	C ₆ H ₁₄	5	10-20	0-10	4.89±0.03
	20-30	C ₃ H ₆	5	20	0-10	1.03±0.04
$(\text{C}_2\text{H}_5)_3\text{SiH}$	5-10	c-C ₆ H ₁₂	5	10	0-10	6.20±0.12
	5	c-C ₆ H ₁₀	5	20	0-10	0.62±0.03
	6	$(\text{CH}_3)_3\text{SiH}$	6	10	0-10	1.31±0.09

Table 7/contd.

$(C_2H_5)_2SiH_2$	20	1-C ₄ H ₈	10	10	0-20	1.82±0.11
	10	c-C ₆ H ₁₀	5	10	10	0.66±0.06
	5	$(C_2H_5)_3SiH$	10	30	0-10	1.08±0.02
$(CH_3)_2SiH_2$	10-20	C ₃ H ₆	5-10	20-30	0-10	1.56±0.07
	10-20	$(CH_3)_3SiH$	20-30	20-30	0-10	1.12±0.04
CH ₃ SiH ₃	10-20	1-C ₄ H ₈	5-10	30	15	1.04±0.15
	10-20	$(CH_3)_3SiH$	10	20-30	0-10	0.93±0.06
$(CH_3)_2SiHCl$	5-10	n-C ₆ H ₁₄	2-10	10	0-5	2.86±0.22
	10	i-C ₄ H ₁₀	5	10	0-5	7.26±0.60
CH ₃ SiHCl ₂	30-40	C ₃ H ₆	5	20	0-20	0.21±0.05
	50	i-C ₄ H ₁₀	5	40	0-20	2.29±0.09
	30	n-C ₆ H ₁₄	5	20	0-20	0.86±0.03
$(C_2H_5)_4Si$	5-10	c-C ₆ H ₁₂	5-10	10-15	0-5	1.15±0.16
$(CH_3)_4Si$	7-10	n-C ₆ H ₁₄	5	20	0-5	0.17±0.01
	5-10	i-C ₄ H ₁₀	5	20	0-5	0.44±0.04
$(CH_3)_3SiF$	10	C ₂ H ₆	10	10	10	0.93±0.10
	10	i-C ₄ H ₁₀	2-5	20	0-5	0.13±0.02
$(CH_3)_2SiF_2$	10	$(CH_3)_3SiF$	10	20	0-10	0.36±0.02

Table 8 lists the reactant concentrations (ppm) and slope, k_{13}/k_{14} , for various, Substrate / Reference Compound / H_2O_2 / NO / N_2 , mixtures. Data for $(CH_3)_4Si$ was obtained in both zero N_2 and artificial air, where 1 ppm = 2.40×10^{13} molecule cm^{-3} at 296 k and 735-torr total pressure.

TABLE 8

Reactant concentrations and slope, k_{13}/k_{14} , for the reaction of OH radicals with substituted silanes at room temperature and atmospheric pressure.

Substrate	Reference Concentration (ppm)	Reference Concentration (ppm)	H_2O_2 Concentration (ppm)	NO Concentration (ppm)	$\frac{k_{13}}{k_{14}}$
$(C_2H_5)_2SiH_2$	10	c-C ₆ H ₁₀ 5	15	0	0.82±0.08
SiHCl ₃	10-30	n-C ₆ H ₁₄ 5	15	0	0.20±0.01
$(CH_3)_4Si$	8-10	i-C ₄ H ₁₀ 4-5	15	0-10	0.40±0.01

Figures 14 - 18 show the data plotted in the form of equation VI.

FIGURE 14

Plots in the form of equation VI from which k_{13}/k_{14} was obtained

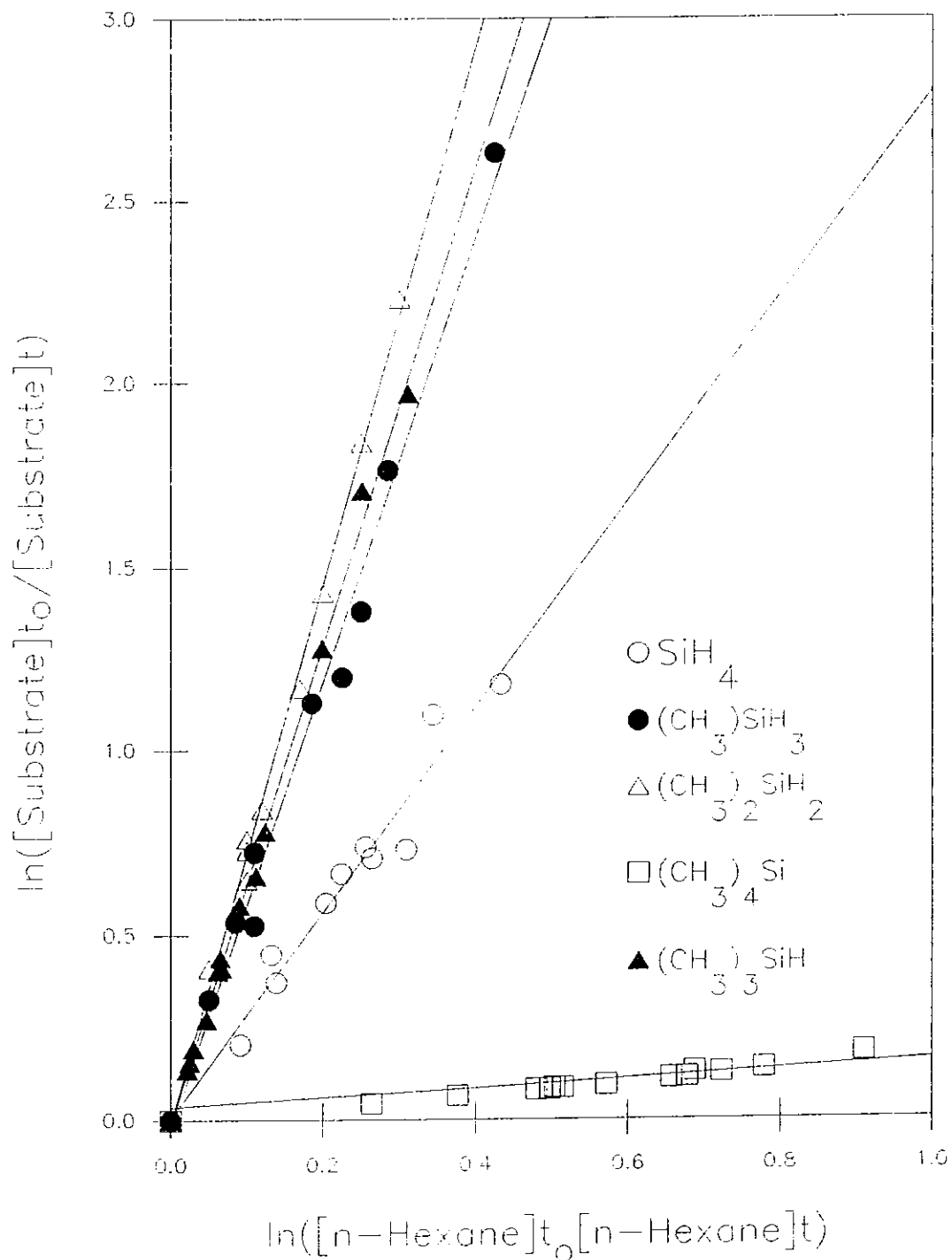
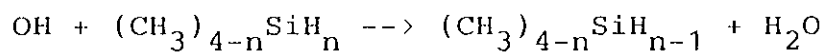
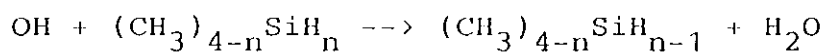


FIGURE 15

Plots in the form of equation VI from which k_{13}/k_{14} was obtained



showing isotope effects.

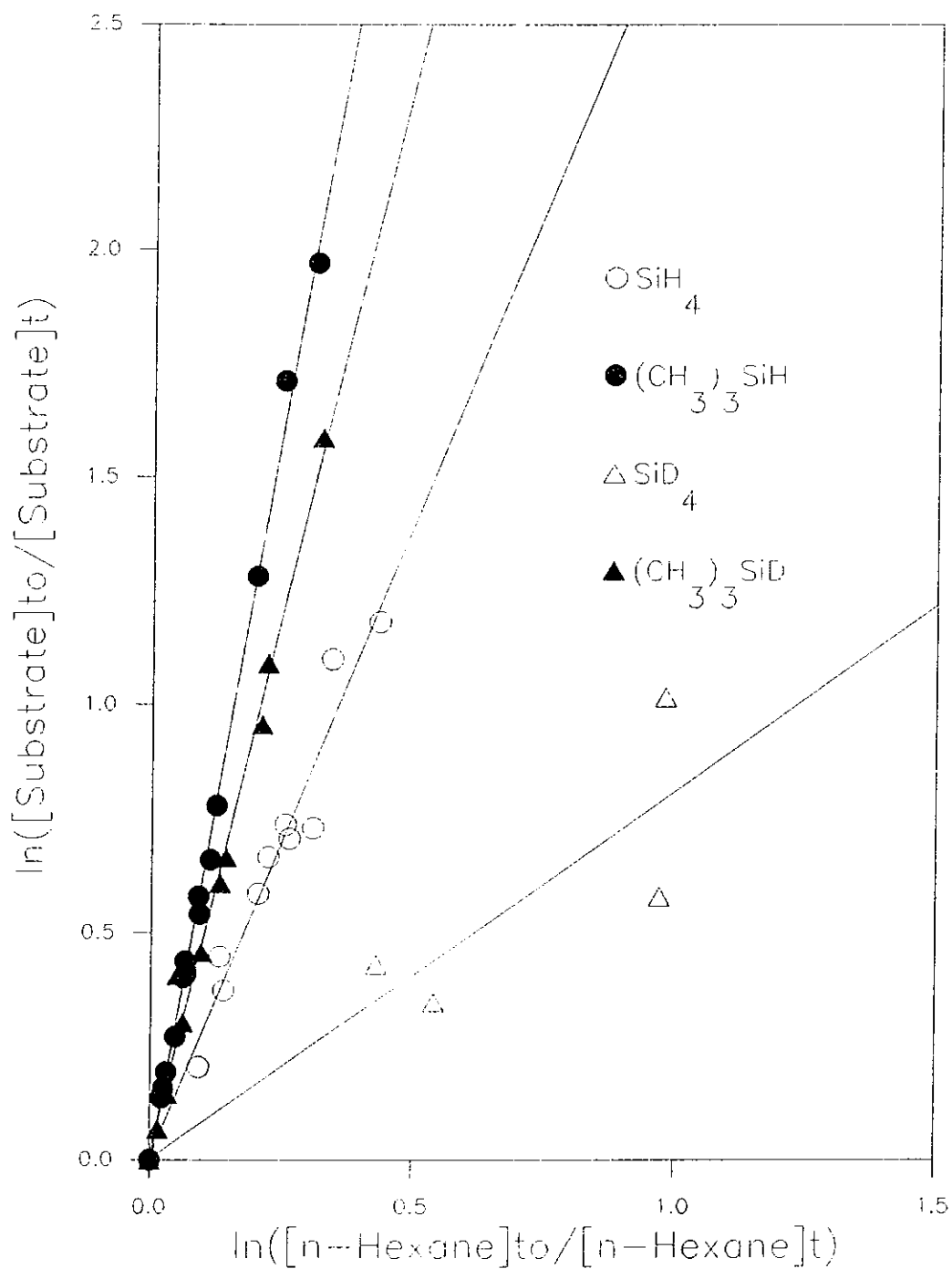


FIGURE 16

Plots in the form of equation VI from which k_{13}/k_{14} was obtained

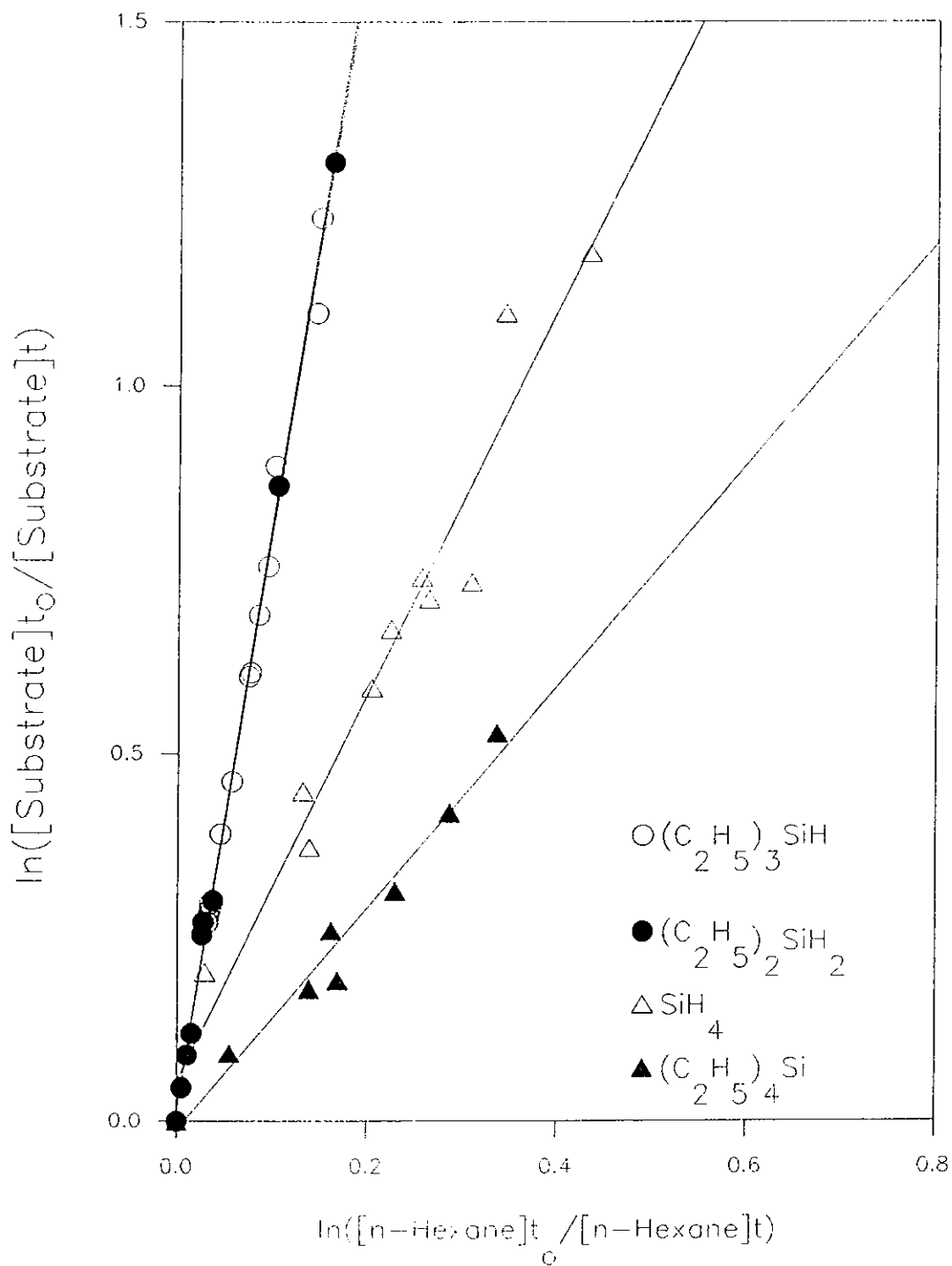
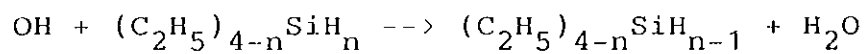


FIGURE 17

Plots in the form of equation VI from which k_{13}/k_{14} was obtained

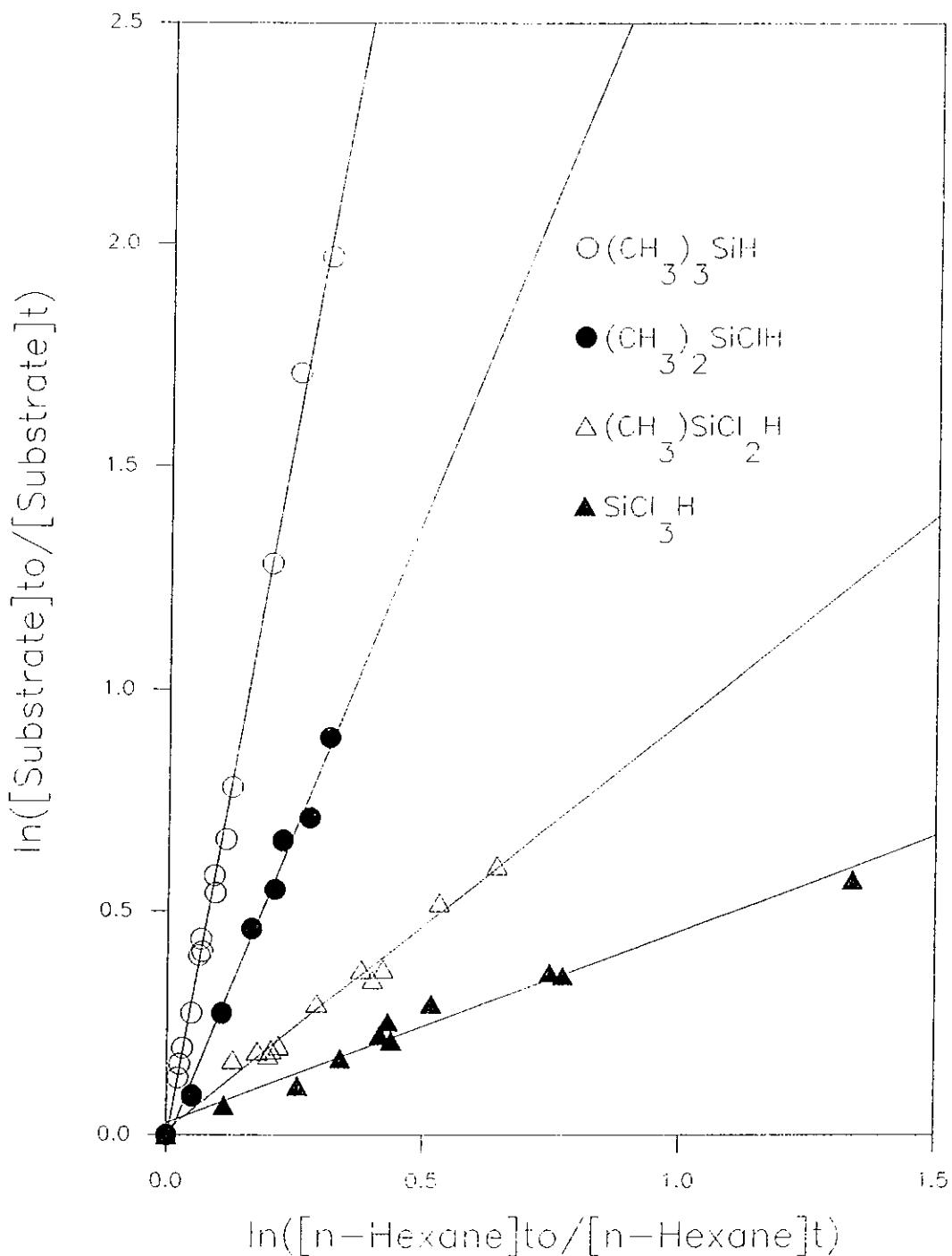
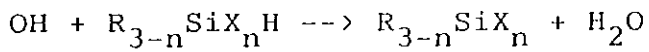
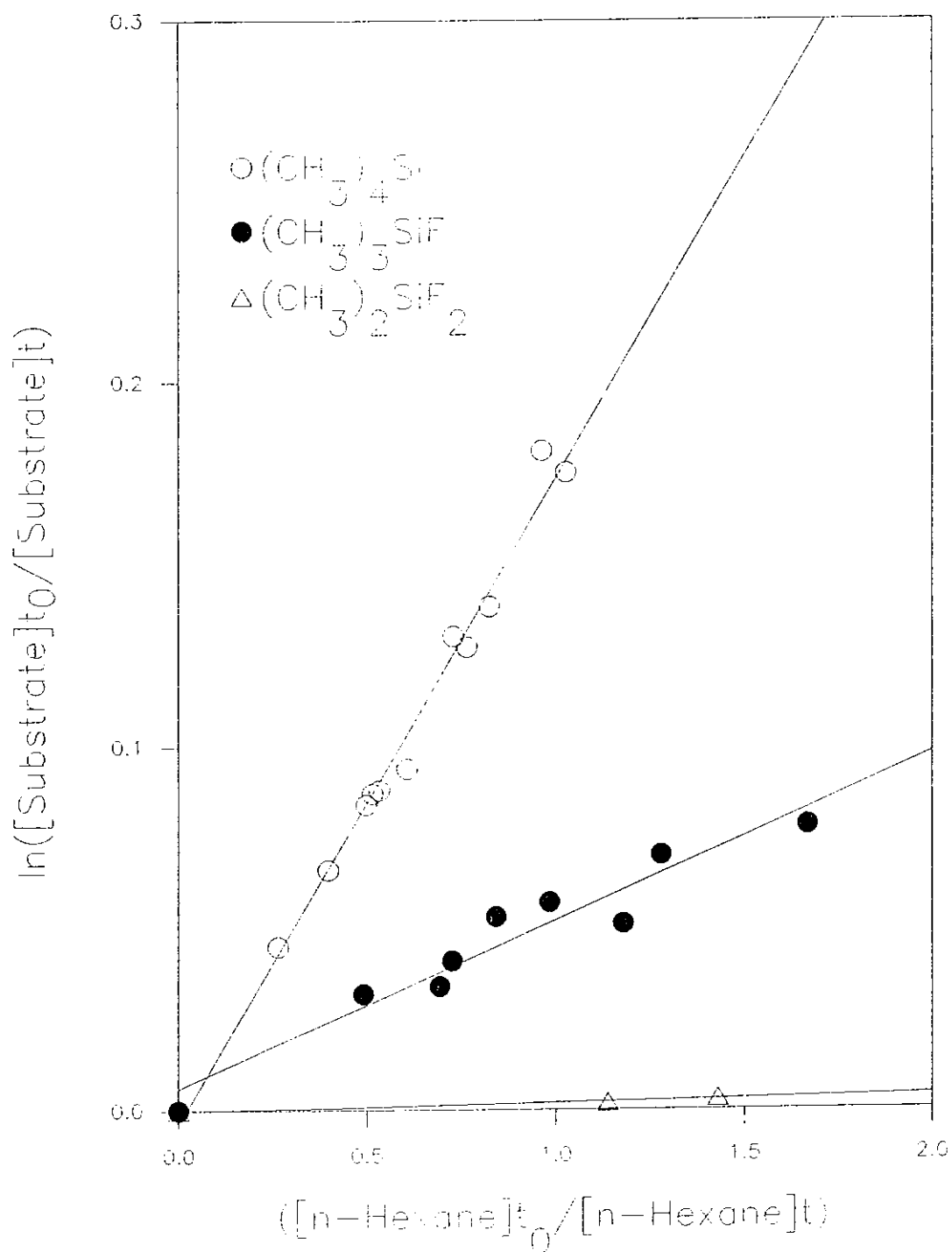
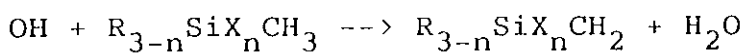


FIGURE 18

Plots in the form of equation VI from which k_{13}/k_{14} was obtained

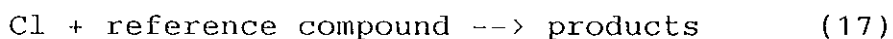
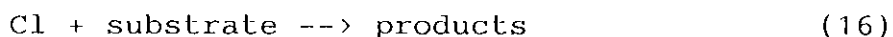


2.3b Chlorine Atom Reactions:

Chlorine atoms were generated by the photolysis of Cl_2 in zero N_2 or artificial air at wavelengths 350-450 nm



Chlorine atoms generated via reaction (15) react with the substrate and reference compounds in an analogous manner to hydroxyl radical reactions, ie.



Reactions were carried out at room temperature (298 ± 2 K) and atmospheric pressure (730-750 torr). Assuming that the loss of substrate and reference compounds occur solely via reaction with chlorine atoms,

$$\ln \frac{[\text{substrate}]_0}{[\text{substrate}]_t} = \frac{k_{16}}{k_{17}} \ln \frac{[\text{reference compound}]_0}{[\text{reference compound}]_t} \quad (\text{VII})$$

A least-squares plot of $\ln\{[\text{substrate}]_0/[\text{substrate}]_t\}$ against $\ln\{[\text{reference compound}]_0/[\text{reference compound}]_t\}$ gave a straight line of zero intercept and slope k_{16}/k_{17} , Figures 19-23.

Table 9 lists the Cl reference rate constants used in this work.

Table 9

Cl reference rate constants used in this work.

k in $\text{cm}^3 \text{ molecule}^{-1} \text{ s}^{-1}$ at 298 K and 1 atm.

Reference compound	$k_{17} \times 10^{11}$
C_2H_6	6.17 ^a
i- C_4H_{10}	13.7 ^b
n- C_6H_{14}	30.3 ^b
c- C_6H_{12}	31.1 ^b
$(\text{CH}_3)_4$	11.0 ^b
$\text{C}_6\text{H}_5\text{CH}_3$	5.8 ^b
$(\text{CH}_3)_3\text{CCl}$	1.54 ^c
$(\text{CH}_3)_3\text{SiH}$	22.6 ^c
$(\text{CH}_3)_3\text{SiF}$	1.53 ^b

a, Atkinson et al.⁶¹

b, Atkinson et al.²¹

c, This work

Table 10 lists the reactant concentrations (ppm) and slope, k_{16}/k_{17} , for the various, Substrate / Reference Compound / Cl / N_2 (Air), mixtures, where 1 ppm = 2.40×10^{13} molecules cm^{-3} at 296 K and 735-torr total pressure.

TABLE 10

Reactant concentrations and slope, k_{16}/k_{17} , for the reaction of Cl atoms with substituted silanes at room temperature and atmospheric pressure.

Substrate	Concentration (ppm)	Reference	Concentration (ppm)	Cl Concentration (ppm)	Diluent Gas	$\frac{k_{16}}{k_{17}}$
SiH ₄	30-50	n-C ₆ H ₁₄	5	20	Air	1.18±0.44
	30-50	i-C ₄ H ₁₀	3-5	20-50	Air	2.92±0.37
SiD ₄	30-50	i-C ₄ H ₁₀	10	10	N ₂	3.05±0.16
	30-50	(CH ₃) ₃ SiH	15	10	N ₂	1.78
(CH ₃) ₃ SiH	5-50	i-C ₄ H ₁₀	5-10	10-20	N ₂	1.66±0.05
	5-10		5-10	10	Air	1.67±0.06
(CH ₃) ₃ SiD	20-30	i-C ₄ H ₁₀	5	10	N ₂	1.72±0.08
(C ₂ H ₅) ₃ SiH	5-20	c-C ₆ H ₁₂	5-20	10-20	N ₂	1.51±0.07
	5		5	10	Air	1.28±0.02
(C ₂ H ₅) ₂ SiH ₂	10	n-C ₆ H ₁₄	5	10	N ₂	1.33±0.04
	5-10		10	5-10	Air	1.39±0.02
C ₂ H ₅ SiH ₃	20-30	(CH ₃) ₄ C	10	10	Air	4.67±0.12
	20-30		5	10	N ₂	4.67±0.36
(CH ₃) ₂ SiH ₂	30-40	n-C ₆ H ₁₄	10-20	10-20	N ₂	1.09±0.03

Table 10/contd.

CH_3SiH_3	10-20	$i\text{-C}_4\text{H}_{10}$	10	10	Air	2.59 ± 0.13
	10-20		10	20	N_2	2.74 ± 0.08
$(\text{CH}_3)_2\text{SiHCl}$	20	$c\text{-C}_6\text{H}_{12}$	3	20	N_2	0.42 ± 0.05
	20	$\text{C}_6\text{H}_5\text{CH}_3$	10	20	N_2	2.15 ± 0.05
$\text{CH}_3\text{SiHCl}_2$	30-50	$i\text{-C}_4\text{H}_{10}$	5	20	N_2	0.61 ± 0.02
SiHCl_3	15-40	C_2H_6	10	20	Air	0.48 ± 0.03
$(\text{C}_2\text{H}_5)_4\text{Si}$	5-10	$c\text{-C}_6\text{H}_{12}$	3-10	10	N_2	1.27 ± 0.05
$(\text{CH}_3)_4\text{Si}$	10	$i\text{-C}_4\text{H}_{10}$	5	10	N_2	1.01 ± 0.13
	10		5	10	Air	0.98 ± 0.04
$(\text{CH}_3)_3\text{SiF}$	10	C_2H_6	5	10	Air	0.24 ± 0.03
	10	$i\text{-C}_4\text{H}_{10}$	6-10	6-10	Air	0.09 ± 0.02
$(\text{CH}_3)_2\text{SiF}_2$	10	$(\text{CH}_3)_3\text{SiF}$	10	20	Air	0.31 ± 0.02

Figures 19 - 23 show the data plotted in the form of equation VII.

FIGURE 19

Plots in the form of equation VII from which k_{16}/k_{17} was obtained

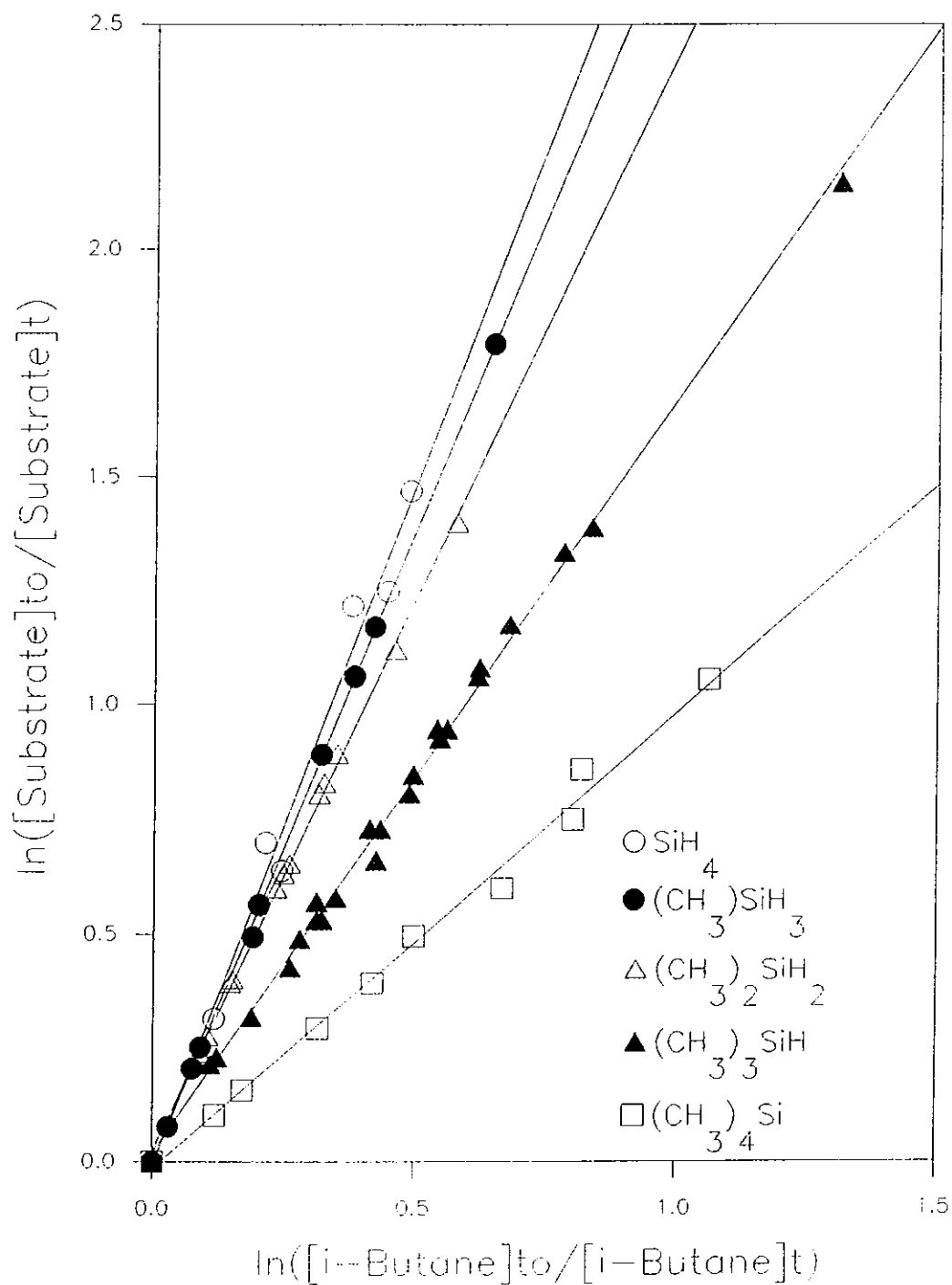
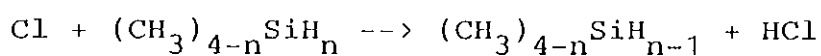
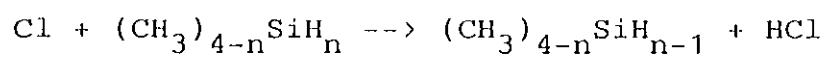


FIGURE 20

Plots in the form of equation VII from which k_{16}/k_{17} was obtained



showing isotope effects.

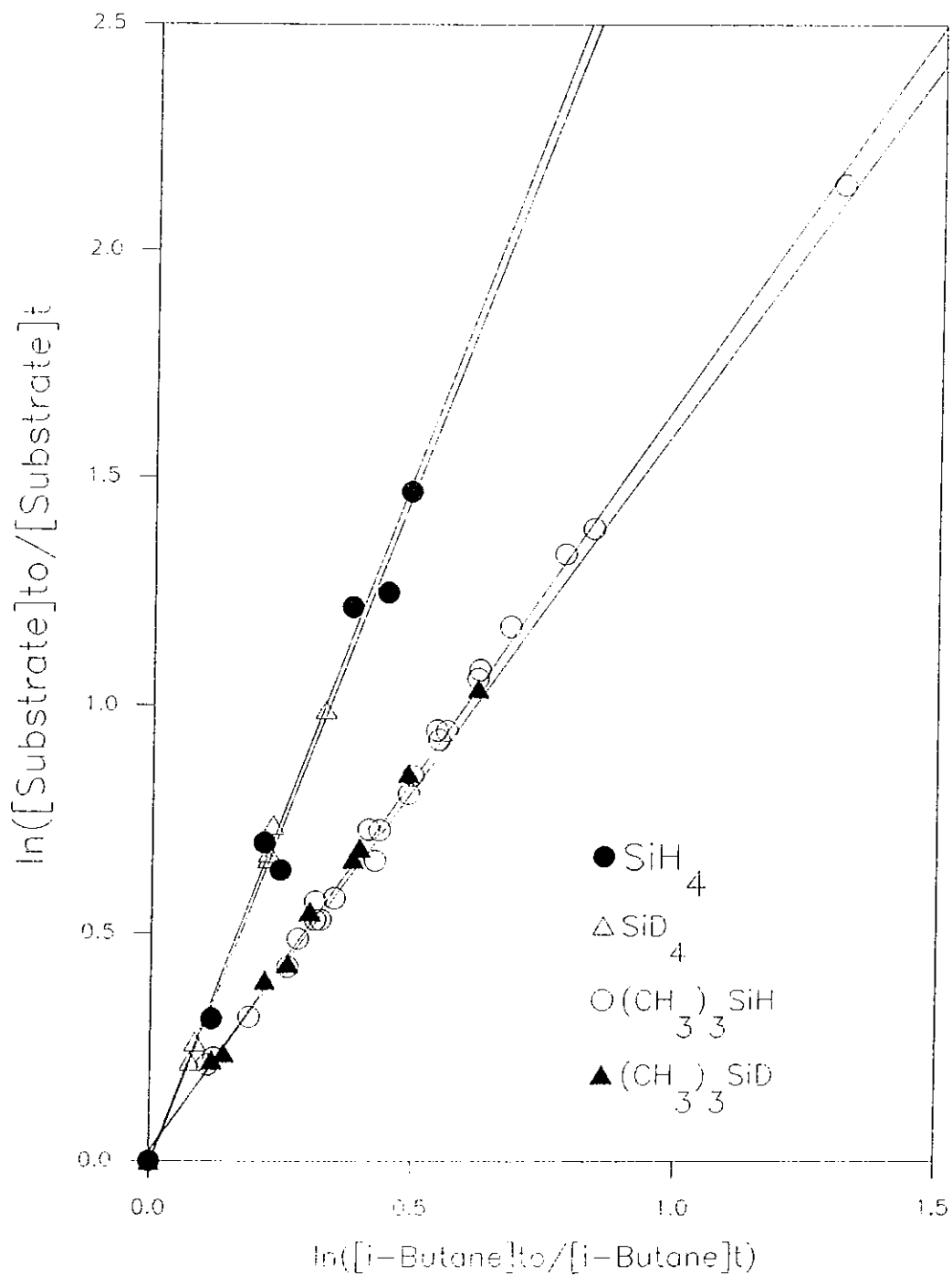


FIGURE 21

Plots in the form of equation VII from which k_{16}/k_{17} was obtained

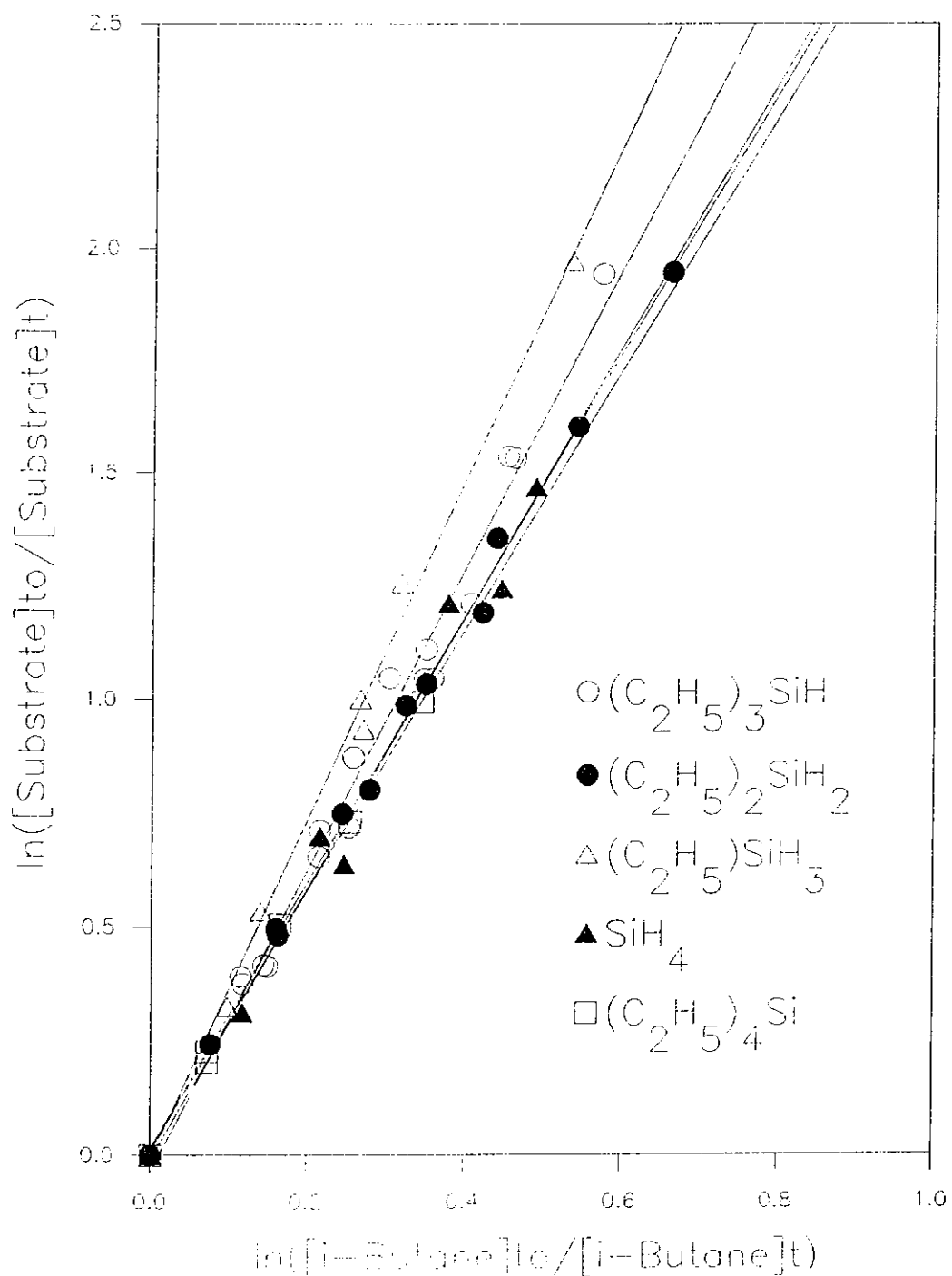
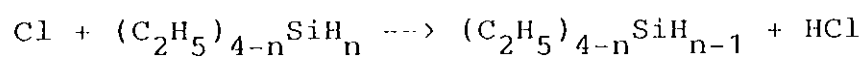


FIGURE 22

Plots in the form of equation VII from which k_{16}/k_{17} was obtained

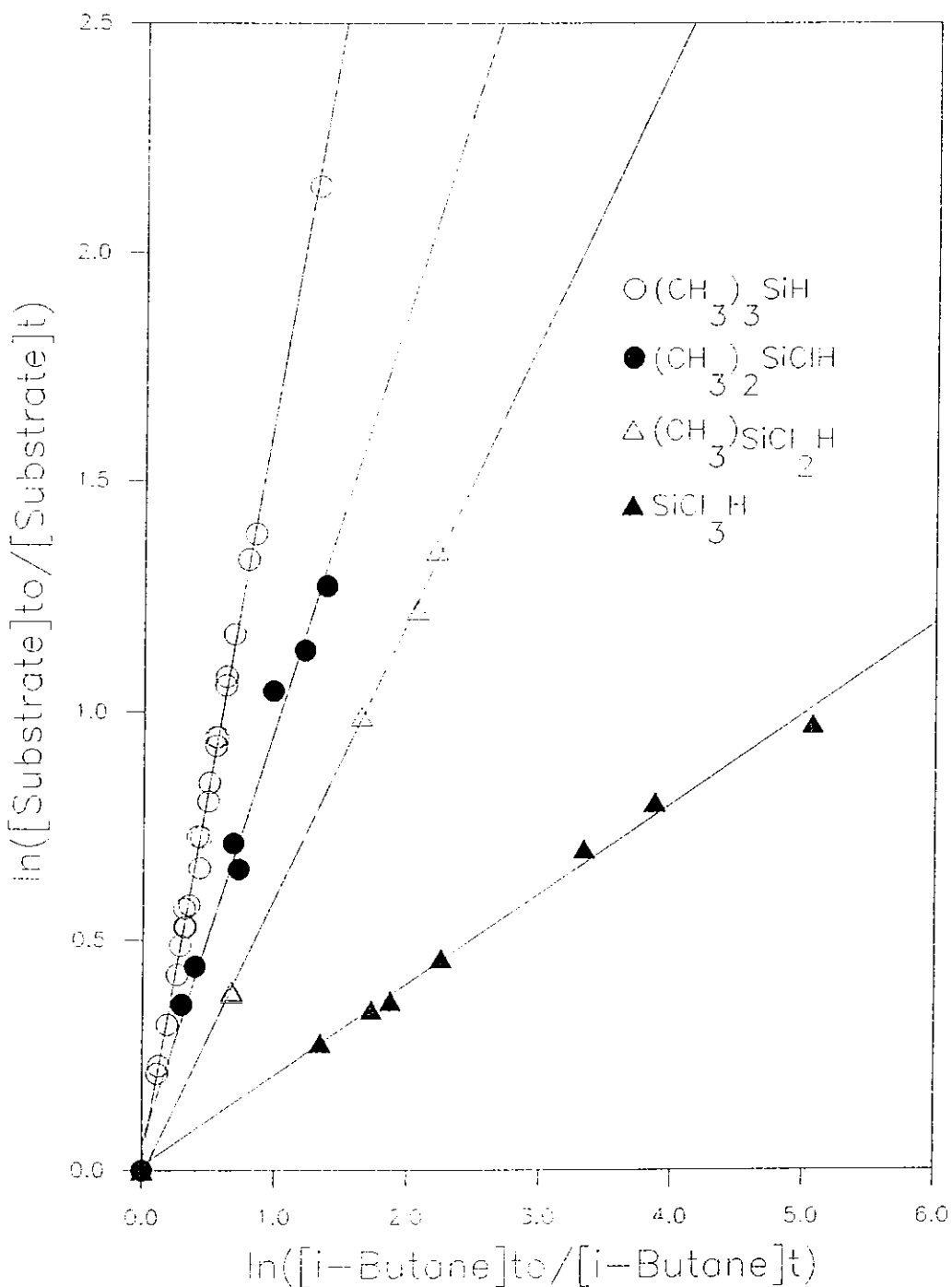
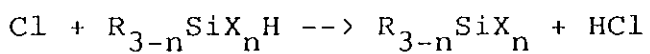
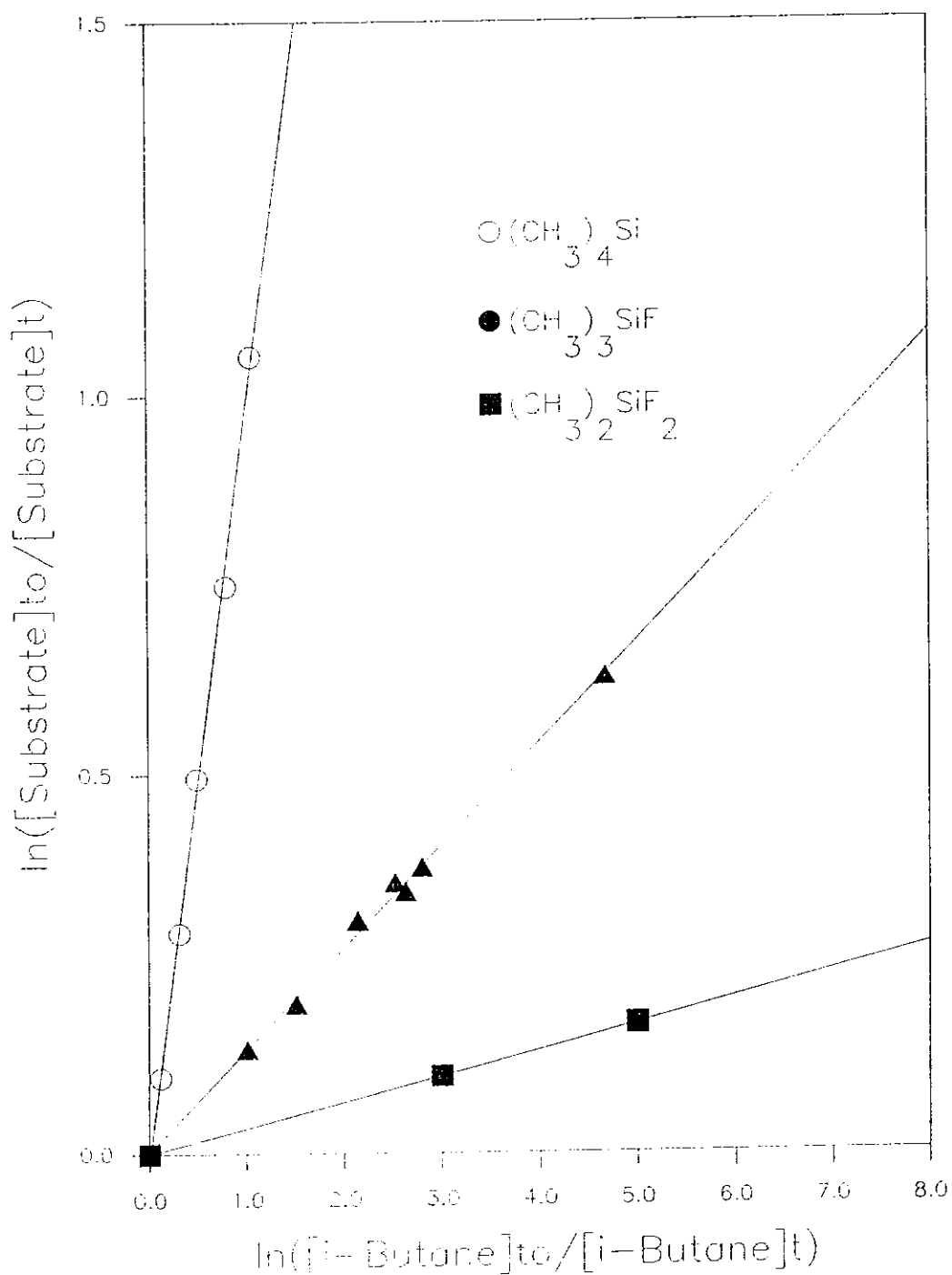
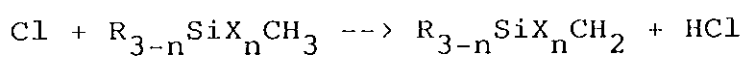


FIGURE 23

Plots in the form of equation VII from which k_{16}/k_{17} was obtained



B: The Absolute Rate Method

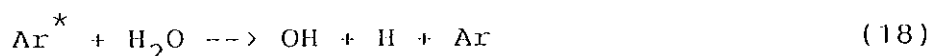
Pulse radiolysis may be defined as irradiation by a short pulse of ionizing radiation, combined with some kind of transient detection method.⁶² Electron beam pulses are preferred over x-rays because of the relatively high energy loss of electrons per unit of length traversed in condensed matter.⁶³

The dose rates employed in pulse radiolysis are high, and this can lead to the building up of high concentrations of radical species, thus giving rise to radical-radical reactions. The advantage of using a pulse forming network discharge accelerator, Febetron 705B, is that it has a pulse duration of 30 ns, the primary effect being the formation of secondary electrons, positive ions and excited atoms or molecules. Other species are formed on a longer timescale and hence do not interfere with the kinetics.⁶⁴ The Febetron 705B, used in a normal experimental situation produces free radicals in concentrations of about 6×10^{14} molecules cm^{-3} , sufficient for detection by a kinetic absorption system.⁶² Other advantages of the Febetron are a homogenous energy disposition and radical production throughout the gas sample, small temperature changes (1-

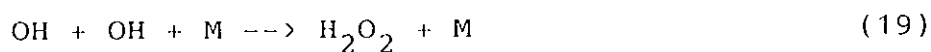
2 °C), and lack of errors due to wall effects.⁶²

2.3c Hydroxyl Radical Reactions:

Hydroxyl radicals were generated by excited Ar atoms, Ar^{*}, formed initially by a single pulse (30 ns duration) of 2 MeV electrons from a Febetron 705B field emission accelerator, which irradiated mixtures of 15 torr H₂O and Ar to 760 torr; OH being produced through the reaction



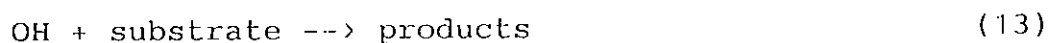
Formation of OH is extremely rapid relative to the time scale of the OH decay. In the absence of added compounds in the system, the decay of OH is governed by the reactions



where M is a third body, here Ar and H₂O. The OH decay is described to a good approximation by the differential equation

$$-d[\text{OH}]/dt = 2k_{19}[\text{OH}]^2[\text{M}] + k_{20}[\text{OH}][\text{H}][\text{M}] \quad (\text{VIII})$$

On introduction of a substrate compound, S,



$$-d[\text{OH}]/dt = k_{19}[\text{OH}]^2[\text{M}] + k_{20}[\text{OH}][\text{H}][\text{M}] + k_{13}[\text{OH}][\text{S}] \quad (\text{IX})$$

at sufficiently large concentrations of substrate, S,

such that

$$k_{13}[S] \gg 2k_{19}[\text{OH}][\text{M}] + k_{20}[\text{H}][\text{M}] \quad (\text{X})$$

then,

$$\begin{aligned} -d[\text{OH}]/dt &= k_{13}[\text{OH}][\text{S}] & (\text{XI}) \\ &= k'_{13}[\text{S}] \end{aligned}$$

where

$$k'_{13} = k_{13}[\text{S}] \quad (\text{XII})$$

A plot of the logarithm of the absorbance versus time allows a clear distinction between first- and second-order kinetics. Such a plot is linear in the pseudo-first-order approximation. Plotting slopes of these log plots, k'_{13} , versus $[\text{S}]$ gives a near linear plot with slope equal to k_{13} ,³² Figures 24-26.

Table 11 lists the reactant pressure ranges (torr) and the slope, k_{13} , for the various Substrate / H₂O / Ar, mixtures, where
Concentration (mol dm⁻³) = Pressure (torr)/760xRT
R = 8.2057 x 10⁻² dm³ atm mol⁻¹ K⁻¹
T = 298 K

TABLE 11

Reactant concentrations and rate constant, k_{13} ,
for the reaction of OH radicals with substituted
silanes at room temperature and atmospheric pressure.
The type and volume of the mixing chamber is included.

Substrate	Concentration range (torr)	Mixing chamber	Volume (cm^3)	$k_{13} \times 10^{12}$ ($\text{cm}^3 \text{ molecule}^{-1} \text{ s}^{-1}$)
$(\text{C}_2\text{H}_5)_3\text{SiH}$	0.05 - 0.095	Teflon bag	60,000	39.8 \pm 8.5
$(\text{CH}_3)_3\text{SiH}$	0.025- 0.28	Teflon bag	60,000	37.2 \pm 5.6
$(\text{C}_2\text{H}_5)_4\text{Si}$	0.10 - 1.00	Reaction Cell	1,000	7.92 \pm 0.54
$(\text{CH}_3)_4\text{Si}$	1.00 -10.00	Reaction Cell	1,000	1.12 \pm 0.18
$(\text{CH}_3)_3\text{SiF}$	0.56 - 3.75	Teflon bag	60,000	0.35 \pm 0.05
$(\text{CH}_3)_2\text{SiF}_2$	1.58 - 3.10	Teflon bag	60,000	0.09 \pm 0.04

FIGURE 24

Plot of k'_{13} versus substrate concentration from which k_{13} was obtained for

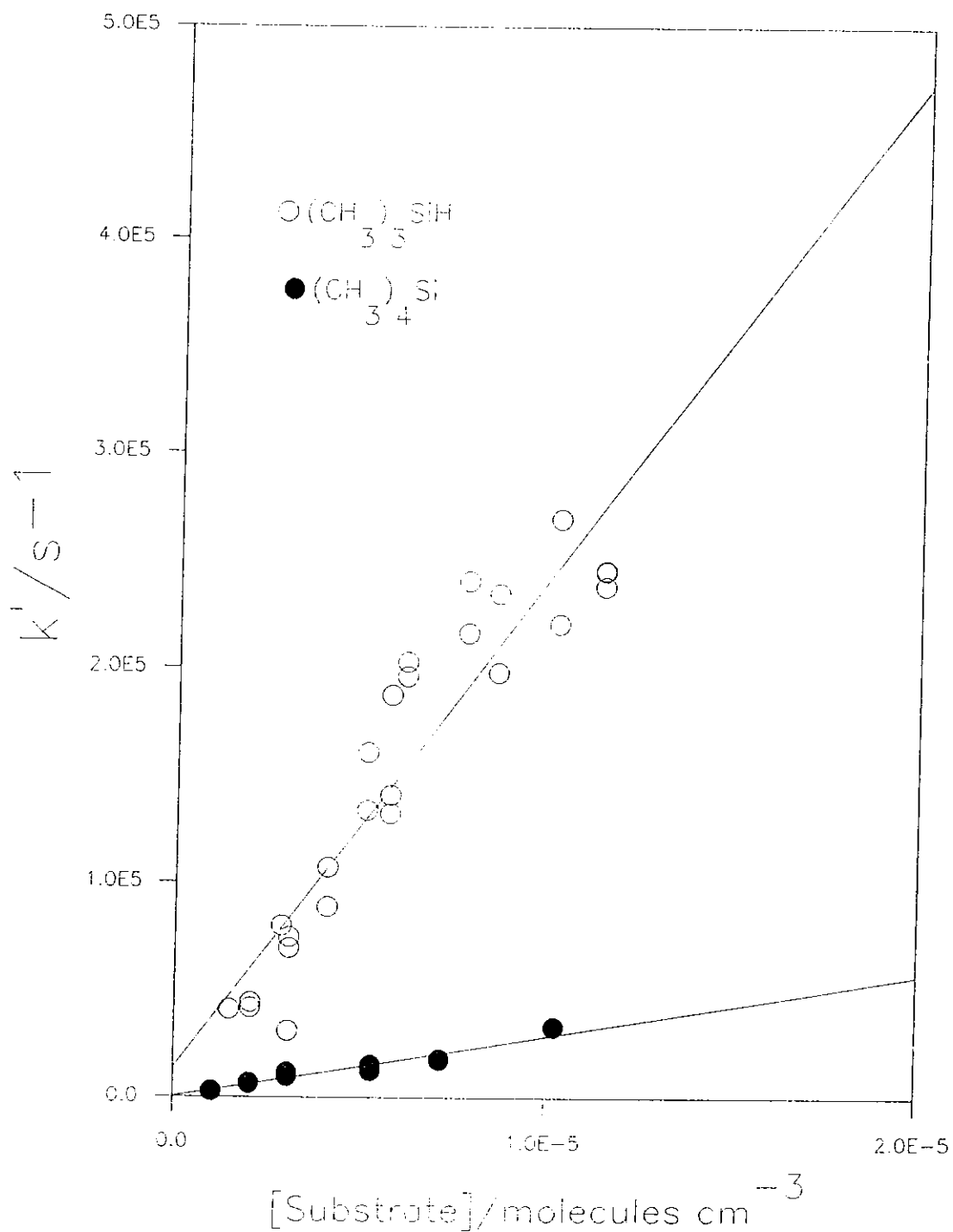
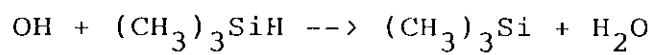


FIGURE 25

Plot of k'_{13} versus substrate concentration from which k_{13} was obtained for

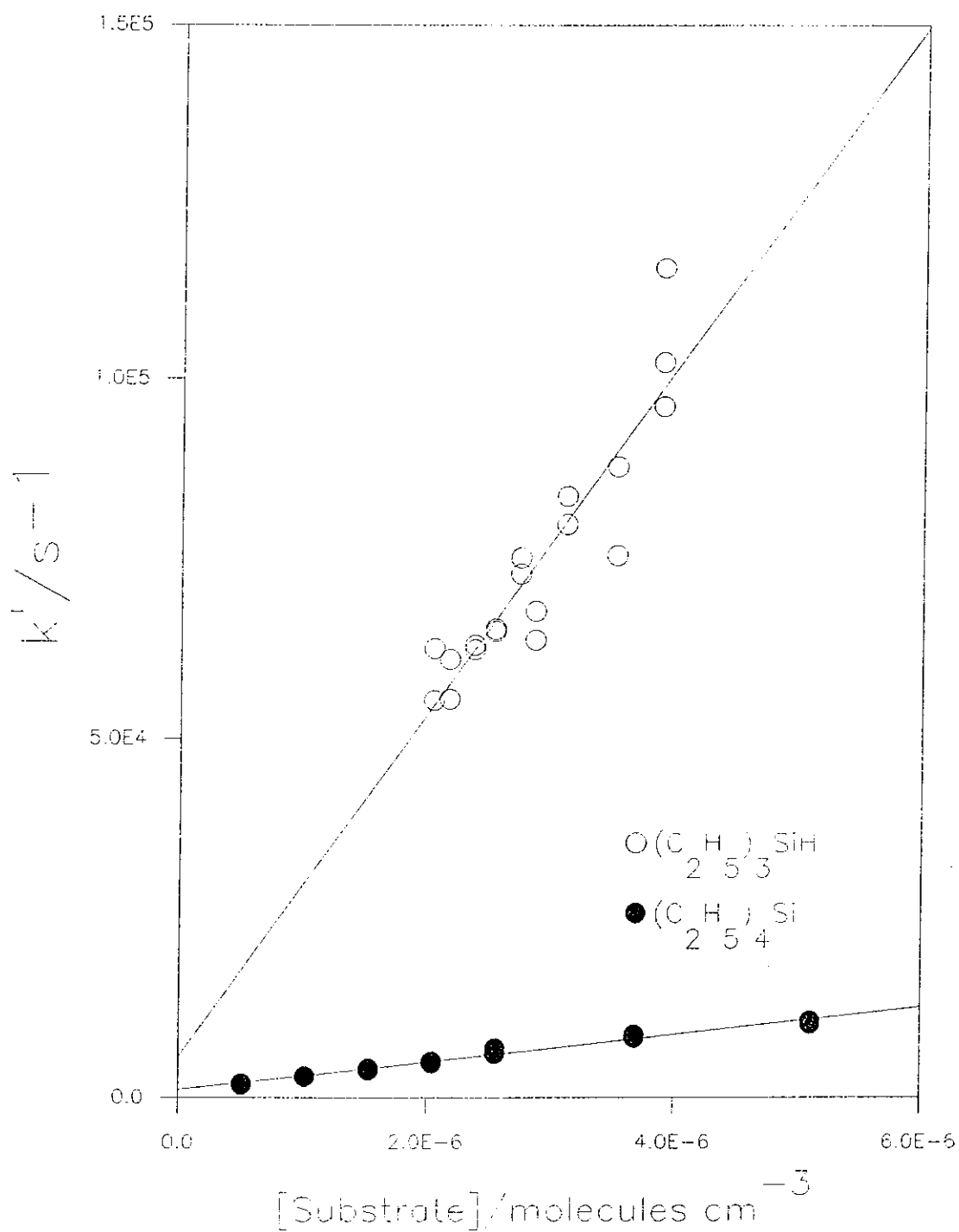
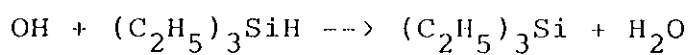
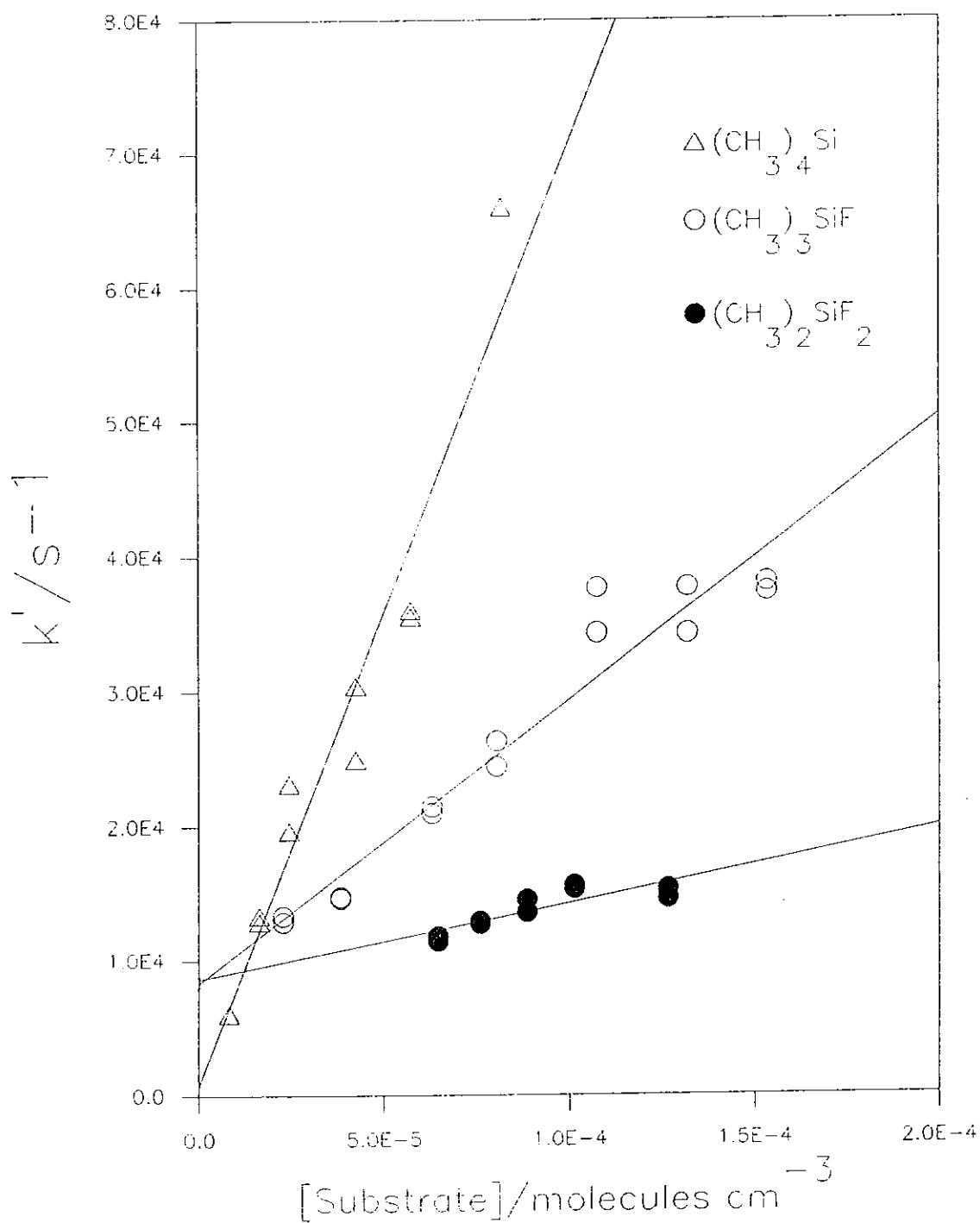
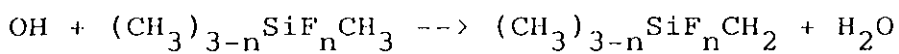


FIGURE 26

Plot of k'_{13} versus substrate concentration from which k_{13} was obtained for



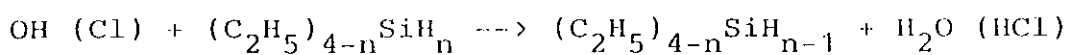
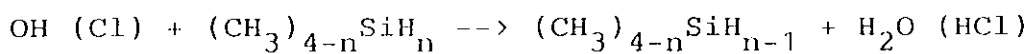
2.4 DISCUSSION

Previous studies²⁵ have shown that the pre-exponential factors for hydrogen atom abstraction from aliphatic hydrocarbons by atomic and radical species vary only slightly with the type of H-atom being abstracted, ie. 1^0 , 2^0 , 3^0 , with A factors for abstraction falling within the range $10^{-11 \pm 0.5} \text{ cm}^3 \text{ molecule}^{-1} \text{ s}^{-1}$ for atomic species, $10^{-13 \pm 0.5} \text{ cm}^3 \text{ molecule}^{-1} \text{ s}^{-1}$ for diatomic radicals and $10^{-14 \pm 0.5} \text{ cm}^3 \text{ molecule}^{-1} \text{ s}^{-1}$ for abstraction by polyatomic radicals. Similarly it has been shown²⁵ that the A factors for H-atom abstraction from silicon compounds also lie within these relatively narrow ranges. It is therefore not unreasonable to suppose that the A factors for OH radical and Cl atom induced H-atom abstraction reactions from silicon compounds play only a minor role in determining relative reactivities. Hence, variations in reaction rates arise mainly from differences in the activation energies, which, it may be assumed are largely determined by two factors, (i) the overall enthalpy change for the reaction and (ii) polar effects in the transition state between the attacking radical and the substrate.

Rate constant data are reported in this work,

Table 12, for the reaction of OH radicals with silane, deuteriosilane and a series of methyl and ethyl substituted silanes. Both relative and absolute rate constant data are reported for tetramethyl- and tetraethylsilane and for trimethyl- and triethylsilane. The quoted error limits for the rate data obtained from the relative rate measurements do not include any contribution from errors in the reference rate constants. Typically this would add about 20% to the quoted errors.

Table 12



Substrate	$k_{\text{OH}} \times 10^{12}$	$k_{\text{Cl}} \times 10^{11}$	D(Si-H)
SiH_4	15.6 ± 2.1^a	40.9 ± 4.7^a	377.8^g
	12.4 ± 1.9^c	41.7 ± 4.8^e	
		9.2 ± 2.0^f	
SiD_4	4.5 ± 2.6^a	41.6 ± 2.0^a	
CH_3SiH_3	33.8 ± 2.7^a	38.0 ± 0.5^a	374.9^h
$(\text{CH}_3)_2\text{SiH}_2$	40.9 ± 1.9^a	33.1 ± 0.8^a	374.1^h
$(\text{CH}_3)_3\text{SiH}$	36.4 ± 1.2^a	22.6 ± 0.5^a	377.8^i
	37.2 ± 5.6^b		
	40.0 ± 20^d		
$(\text{CH}_3)_3\text{SiD}$	26.6 ± 1.9^a	23.5 ± 1.8^a	
$(\text{C}_2\text{H}_5)\text{SiH}_3$		51.2 ± 3.2^a	

Table 12/contd.

$(C_2H_5)_2SiH_2$	44.8 ± 1.4^a	40.1 ± 1.2^a	
$(C_2H_5)_3SiH$	41.6 ± 3.9^a	45.6 ± 2.9^a	
	39.8 ± 8.5^b		
$(CH_3)_4Si$	1.05 ± 0.08^a	13.7 ± 0.8^a	415.1^j
	1.12 ± 0.18^b		
$(C_2H_5)_4Si$	8.24 ± 1.17^a	39.3 ± 1.6^a	
	7.92 ± 0.54^b		

k in $cm^3 \text{ molecule}^{-1} s^{-1}$ at 298±2K

D(Si-H) in $kJ \text{ mol}^{-1}$

Error limits are twice the standard deviation of the slope.

a, This work; relative rate

b, This work; pulse radiolysis, kinetic spectroscopy

c, Atkinson et al.⁴³ g, Doncaster et al.²⁸

d, Hoffmeyer et al.⁴⁸ h, Walsh²⁷

e, Niki et al.⁴⁵ i, Doncaster et al.³¹

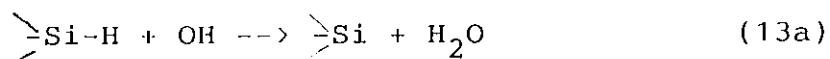
f, Schyler et al.⁴⁷ j, Doncaster et al.³³

Both the relative and absolute rate constant data reported in this work for OH radical reactions agree

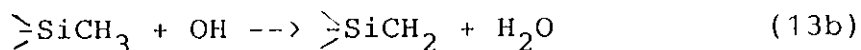
within experimental error. Such agreement gives confidence to the results obtained as both techniques differ greatly. The relative rate data measurements assume that substrate and reference compounds are removed only via OH radical reactions, whereas, in the pulse radiolysis experiments it is assumed that the only loss process for OH radicals is via reaction with the substrate. In addition, the rate constant data determined in this work are in good agreement with those reported in the literature.^{43,48} The room temperature relative rate constant for the reaction of OH + SiH₄ measured in this work is in good agreement with that reported by Atkinson et al.⁴³ using a flash photolysis technique. Hoffmeyer et al.⁴⁸ using a discharge flow technique, estimated the room temperature rate constant for the reaction of OH + (CH₃)₃SiH from experiments primarily designed to study the reaction of O(³P) with (CH₃)₃SiH. The estimated value of the rate constant is consistent with values obtained in this work using both relative and absolute rate techniques. The rate constants for methyl, dimethyl and trimethyl substituted silanes are similar and about twice that for silane, Table 12.

Three possible reaction pathways may be considered for the reaction of OH radicals with silane and the

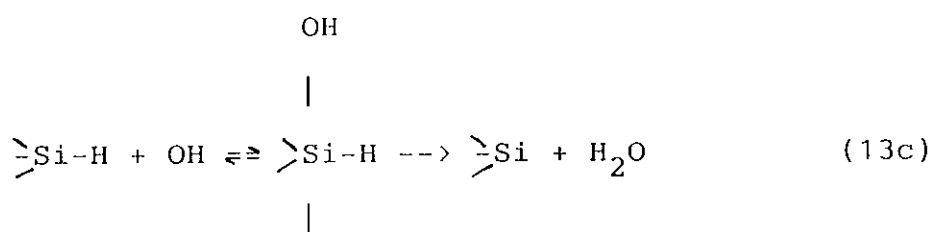
methyl substituted silanes. Direct hydrogen atom abstraction may involve either a hydrogen atom bonded to silicon



or a hydrogen atom from a methyl group



It is also possible that, due to the accessibility of the silicon 3d orbitals, the reaction of OH radicals with the silanes can occur via the formation of an addition complex. Subsequent decomposition of the complex would give the same reaction products as proposed for the direct abstraction of a hydrogen atom directly bonded to silicon, reaction (13a),



Tetramethylsilane is comparatively unreactive to the silanes containing an Si-H bond. Hence hydrogen atom abstraction from a methyl group, reaction (13b), cannot be an important reaction channel for the reaction of OH radicals with CH_3SiH_3 , $(\text{CH}_3)_2\text{SiH}_2$ and $(\text{CH}_3)_3\text{SiH}$. Thus the increase in reactivity of the methylated silanes relative to SiH_4 cannot be due to hydrogen abstraction from the methyl group.

A possible explanation for the reactivity trend is that formation of the addition complex is the dominant channel at least for the methylsilanes. However, it is difficult to justify such an argument on a number of grounds. Firstly, the rate constant for $\text{OH} + \text{SiH}_4$ shows no dependence on the reaction pressure. Atkinson's⁴³ room temperature rate constant for $\text{OH} + \text{SiH}_4$ was measured from 25-50 torr and is in excellent agreement with the corresponding rate constant reported in this work at 760 torr. The rate constant measured at low pressure might be expected to be lower since decomposition of the addition adduct back to reactants would become more likely at lower pressures. Secondly, rate constants for the $\text{OH} + \text{SiH}_4$ and $\text{OH} + (\text{CH}_3)_3\text{SiH}$ reactions show significant isotope effects on deuteration. The kinetic isotope ratio for k_{SiH_4} and k_{SiD_4} may be calculated using a simple model which assumes that, on passing from reactants to activated complex, the zero-point energy associated with the stretching frequency of the bond being attacked is lost,⁴⁴ ie,

$$k_{\text{H}}/k_{\text{D}} = \exp(\Delta \text{zpe})/RT \quad (\text{XIII})$$

where Δzpe is the difference in zero-point energies of the Si-H and Si-D bonds. The zero point energy difference calculated for a single Si-H stretching vibration is 3.6 kJ mol^{-1} ($\bar{\nu}(\text{Si-H}) = 2190 \text{ cm}^{-1}$ and

$\bar{\nu}(\text{Si-D}) = 1589 \text{ cm}^{-1}$), which from equation (XIII), gives $k_{\text{H}}/k_{\text{D}} = 4.3$ at 298 K. This is close to the experimental ratio of $k_{\text{H}}/k_{\text{D}} = 3.5$ at 298 K, Table 12, indicating that the addition pathway cannot be the major reaction channel for the OH + SiH₄ reaction. An isotope effect is also observed for the reaction of OH with trimethylsilane, $k_{\text{H}}/k_{\text{D}} = 1.4$ at 298 K, Table 12. Although this is somewhat below the calculated value of 3.5 at 298 K using a zero point energy difference estimated for a single Si-H stretching vibration of 3.1 kJ mol⁻¹ ($\bar{\nu}(\text{Si-H}) = 2105 \text{ cm}^{-1}$ and $\bar{\nu}(\text{Si-D}) = 1555 \text{ cm}^{-1}$), it may reflect an early transition state for the reaction. Both the SiD₄ and (CH₃)₃SiD isotope effects are relatively strong, implying that energies associated with the bending and stretching vibrations of the Si-H bond undergo significant change in going from reactants to the transition state. Thus, it may be inferred that the Si-H bond is being broken in the rate-controlling step of the reaction. Finally addition to substituted silanes must be less favoured on steric grounds. Hence the available evidence suggests that abstraction of a hydrogen atom bonded to silicon, reaction (13a), is the major reaction channel for the reaction of OH radicals with the methylsilanes.

The Si-H bond dissociation energies in the

silanes are almost equal,²⁷ and presuming that the reaction involves a simple hydrogen atom abstraction process, reaction (13a), one would expect the rate constant for the reaction of OH + SiH₄ to be higher than that for OH + (CH₃)₃SiH on a statistical basis alone. Indeed one might expect to see a steady increase in the reactivity for these reactions in the order - (CH₃)₃SiH < (CH₃)₂SiH₂ < (CH₃)₃SiH₃ < SiH₄, which was not observed experimentally.

The possibility of the alkyl group effecting the rate of abstraction of hydrogen atoms directly bonded to silicon was examined. Rate constant data for a series of methyl and ethyl substituted silanes were determined, Table 12, and the values of the rate constants are reported per Si-H bond in Table 13. The reaction of OH radicals with (C₂H₅)₄Si is significantly more facile than the corresponding reaction with (CH₃)₄Si. Hence, the contribution to the measured rate constant of H-atom abstraction from the ethyl group in the ethylsilanes is non-negligible. In order to estimate the rate constant for hydrogen abstraction per Si-H bond in these compounds the contribution from H-atom abstraction from the C₂H₅ groups, based on the rate constant for OH + (C₂H₅)Si, was subtracted from the measured rate constant.

Table 13

Rate constants per Si-H bond

Substrate	k_{OH} $\times 10^{12}$	$k_{\text{O(3P)}}$ $\times 10^{13}$	k_{Cl} $\times 10^{11}$	k_{CF_3} $\times 10^{15}$	k_{H} $\times 10^{13}$	k_{CH_3} $\times 10^{17}$
SiH_4	3.9 ^a 3.1 ^c	1.2 ^c 0.5 ^d	10.2 ^a 10.4 ^f 2.3 ^g	0.63 ^e	6.43 ^h 1.44 ⁱ	5.0 ^e
SiD_4	1.1 ^a	0.2 ^d	10.4 ^a	0.2 ^e	0.51 ⁱ	1.3 ^e
CH_3SiH_3	11.3 ^a		11.5 ^a		3.83 ^h 2.71 ⁱ	3.8 ^e
$(\text{CH}_3)_2\text{SiH}_2$	20.5 ^a		13.1 ^a		2.09 ^h 4.36 ⁱ	2.9 ^e
$(\text{CH}_3)_3\text{SiH}$	36.4 ^a 37.2 ^b 40.0 ^c	26.0 ^c	12.4 ^a	2.95 ^e	3.72 ^h 7.59 ⁱ	2.4 ^e
$(\text{CH}_3)_3\text{SiD}$	26.6 ^a		13.3 ^a			
$\text{C}_2\text{H}_5\text{SiH}_3$			13.8 ^a		3.33 ⁱ	

Table 13/contd.

$(C_2H_5)_2SiH_2$	20.3 ^a	10.2 ^a	8.30 ⁱ
$(C_2H_5)_3SiH$	35.2 ^a	16.1 ^a	13.50 ⁱ
	33.5 ^b		

k in $cm^3 \text{ molecule}^{-1} s^{-1}$ at $298 \pm 2K$ except for k_{CH_3} and k_{CF_3} which are at 400K

a, This work; relative rate

b, This work; pulse radiolysis, kinetic spectroscopy

c, Atkinson et al.⁴³

d, Hoffmeyer et al.⁴⁶

e, Arthur et al.⁴⁴

f, Niki et al.⁴⁵

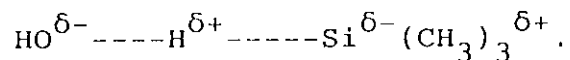
g, Schyler et al.⁴⁷

h, Cowfer et al.⁶⁵

i, Austin et al.⁶⁶

The data in Table 13 indicates that the rate constants per Si-H bond for H atom abstraction by OH radicals from the silanes increases with increasing methyl or ethyl substitution. This can be explained by the inductive effect of the methyl or ethyl group

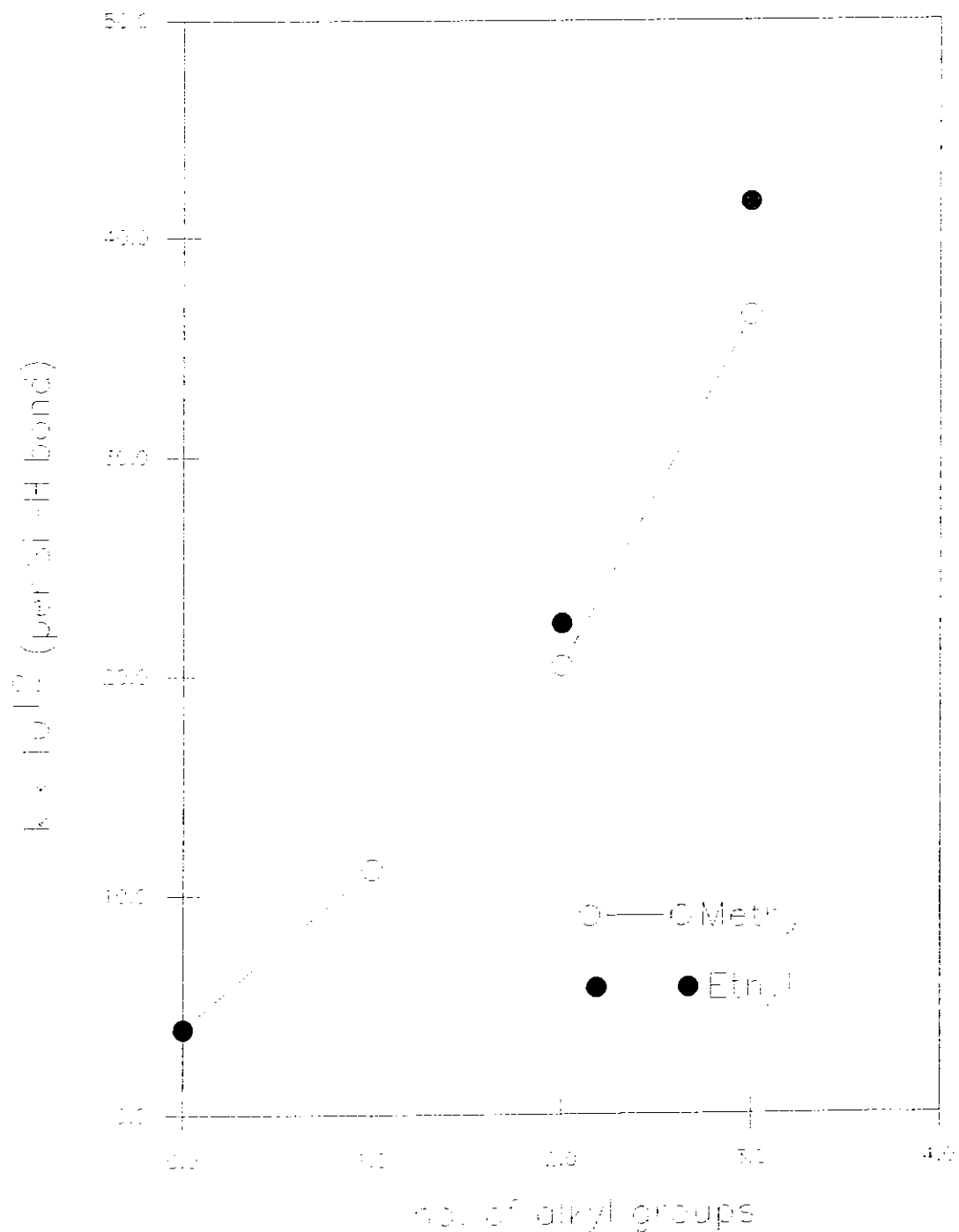
increasing the electron density on the abstracted H atom, resulting in an increased polar attraction in the transition state for the reaction of the electrophilic OH radical with methyl or ethyl silanes,



It is apparent from the data that the inductive effect of methyl and ethyl groups are approximately equal. The rate constants per Si-H bond are plotted against the numbers of substituent alkyl groups in the silane in Figure 27. The data show rather convincingly that the rate constant for abstraction increases almost linearly with the number of alkyl groups present, Figure 27.

FIGURE 27

Plot of $k_{OH} \times 10^{12}$ ($\text{cm}^3 \text{ molecule}^{-1} \text{ s}^{-1}$) per Si-H bond versus the number of substituent alkyl groups for a series of methyl and ethyl substituted silanes.

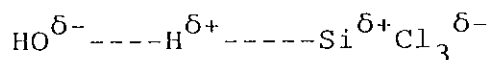


The reactions of electrophilic chlorine atoms with the silanes are expected to show similar trends to those for the analogous hydroxyl radical reactions. The value reported in this work for the reaction, $\text{Cl} + \text{SiH}_4$, Table 12, is in good agreement with that previously reported by Niki et al.⁴⁵ who sighted evidence, based on the stoichiometry of the reaction, for a direct H-atom abstraction mechanism. The rate constant data presented in this work, Table 12, show a constant decrease down the series from SiH_4 to $(\text{CH}_3)_3\text{SiH}$. However, when the relatively large contribution of H-atom abstraction from the methyl group, based on the value for $\text{Cl} + (\text{CH}_3)_4\text{Si}$, is subtracted and the rate constants recalculated per Si-H, it becomes apparent that the reaction rate constants per Si-H bond are approximately equal, Table 13. Similarly, the rate of H-atom abstraction from the ethylsilanes by Cl atoms is about equal to that in the methylsilanes, Table 13. The reactions do, however, as pointed out by Niki et al.⁴⁹ approach a collision rate with virtually zero activation energy. The lack of any isotope effect is thus explained by a very slight weakening of the Si-H bond being sufficient to bring the silane to the transition state. In such a case any increase in the rate constant due to a polar effect is likely to be negligible.

The enhanced rate constant, observed for OH radical atom abstraction of H-atoms from methyl substituted silanes should also prevail with CF_3 radicals and $\text{O}(^3\text{P})$ atoms since both species are also electrophilic. Results previously reported by Arthur et al.⁴⁴ and Hoffmeyer et al.⁴⁶ do indeed show this trend, with a $\text{SiH}_4:(\text{CH}_3)_3\text{SiH}$ rate constant ratio of at least 1:20 at 298 K for $\text{O}(^3\text{P})$ atoms and 1:5 at 400 K for CF_3 radical reactions, Table 13. The smaller ratio for the corresponding OH radical reactions of 1:9 need not imply a lesser effect to $\text{O}(^3\text{P})$, as the reactions are significantly faster. Hydroxyl radicals are less selective and any enhancement would therefore appear less pronounced. Reaction with H-atoms would not be expected to show a polar effect since the H-atom cannot be described as being electrophilic or nucleophilic. There is some disagreement in the literature^{65,66} about the rates of H-atom abstraction from the silanes by H-atoms, however, there is no obvious trend in the rate constants per Si-H bond which show little variation when compared with the analogous $\text{O}(^3\text{P})$ atom reactions, Table 13. Nucleophilic CH_3 radicals should effect the rate constant in the opposite direction to electrophilic atoms or radicals. Again, evidence of this effect is obtained from the rate constant data for the reaction of CH_3 radicals with a series of substituted silanes,⁴⁴

Table 13. where the rate constant ratio of $\text{SiH}_4:(\text{CH}_3)_3\text{SiH}$ is 1:0.48.

The importance of polar effects in these reactions was further investigated by measuring the rate constants for H-atom abstraction by OH radicals and Cl atoms from a series of halogen substituted silanes. The strongly electron withdrawing halogens are expected to cause an inductive effect in the opposite direction to that of the alkyl groups, thus inhibiting the abstraction process. Substitution of methyl in $(\text{CH}_3)_3\text{SiH}$ by chlorine atoms reduces the electron density on the hydrogen atom which is abstracted. Thus, there is an increase in the polar repulsion between the electrophilic hydroxyl radical and the substrate



and as a consequence chlorination leads to an increase in the activation energy for abstraction.

The data presented in this work, Table 14, shows a continuous decrease in the rate constant per Si-H as the methyl groups on silicon are successively replaced by Cl atoms. The data for OH radical reactions show a decrease in the rate constant with the rate constant ratio for $(\text{CH}_3)_3\text{SiH} : \text{SiCl}_3\text{H}$ being of the order of 15 : 1. Enthalpy effects may be considered to play only a

minor role in the relative reaction rates since the Si-H bond strengths are similar throughout the series, $D[(\text{CH}_3)_3\text{Si-H}] = 377.8 \text{ kJ mol}^{-1}$ and $D[\text{Cl}_3\text{Si-H}] = 382.0 \text{ kJ mol}^{-1}$.²⁷ Thus it may be inferred that the major factor contributing to the activation energies is a polar effect.

Table 14

Rate constants for H atom abstraction from methyl- and chloro- substituted silanes.

Substrate	k_{OH} $\times 10^{12}$	k_{Cl} $\times 10^{11}$	k_{CF_3} $\times 10^{15}$	k_{CCl_3} $\times 10^{17}$	k_{CH_3} $\times 10^{17}$
$(\text{CH}_3)_3\text{SiH}$	$36.4 \pm 1.2^{\text{a}}$ $37.2 \pm 5.6^{\text{b}}$ $40.0 \pm 20^{\text{c}}$	$22.6 \pm 0.5^{\text{a}}$	3.0^{e}	6.6^{f} 1.7^{g}	2.4^{e}
$(\text{CH}_3)_2\text{SiClH}$	$15.9 \pm 1.4^{\text{a}}$	$12.5 \pm 1.3^{\text{a}}$		1.7^{f}	
$\text{CH}_3\text{SiCl}_2\text{H}$	$5.2 \pm 0.2^{\text{a}}$	$8.3 \pm 0.2^{\text{a}}$		1.0^{f}	10.7^{e}
SiCl_3H	$2.4 \pm 0.3^{\text{a}}$	$2.7 \pm 0.2^{\text{a}}$ $2.9 \pm 0.3^{\text{d}}$	0.44^{e}	0.66^{f} 0.66^{h}	49.0^{e}

Table 14/contd.

Error limits are twice the standard deviation of the slope.

k in $\text{cm}^3 \text{ molecule}^{-1} \text{ s}^{-1}$ at $298 \pm 2 \text{ K}$ for a-d

k in $\text{cm}^3 \text{ molecule}^{-1} \text{ s}^{-1}$ at 400 K for e-h

a, This work; relative rate

b, This work; pulse radiolysis, kinetic spectroscopy

c, Hoffmeyer et al.⁴⁸

d, Niki et al.⁴⁹

e, Arthur et al.⁴⁴

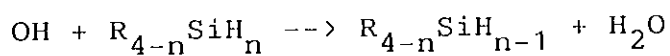
f, Rice et al.³⁷

g, Baruch et al.⁶⁷

h, Ormson et al.⁶⁸

It can be seen from Figure 28 and Table 15 that substitution of SiH_4 by methyl-groups or halogen-atoms leads to opposing polar effects when reacted with OH radicals.

Table 15



Substrate	k x10 ¹²	k x10 ¹¹	D(Si-H)
SiH_4	3.9 ^a	10.2 ^a	377.8 ^b
$(\text{CH}_3)_3\text{SiH}$	36.4 ^a	12.3 ^a	377.8 ^c
SiCl_3H	2.4 ^a	2.7 ^a	382.0 ^d

Table 15/contd.

k in $\text{cm}^3 \text{ molecule}^{-1} \text{ s}^{-1}$ at $298 \pm 2\text{K}$ and 1 atm.

$D(\text{Si-H})$ in kJ mol^{-1}

Error limits are twice the standard deviation of the slope.

a, This work; relative rate

b, Doncaster et al.²⁸

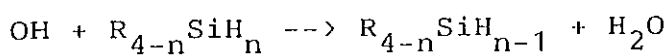
c, Doncaster et al.³³

d, Walsh et al.³²

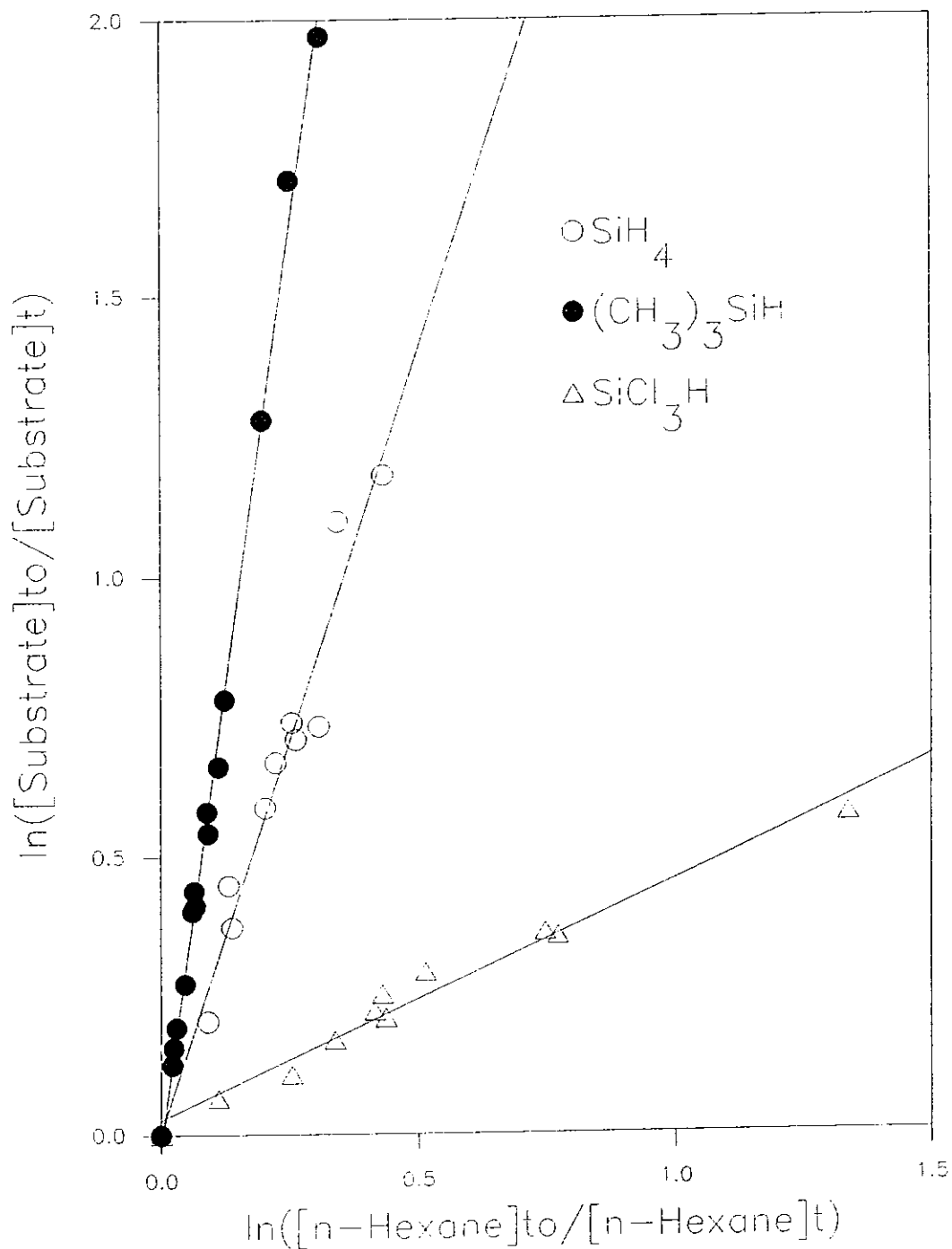
Similar effects have also been observed for the electrophilic CF_3 radical while an analogous but opposite effect is evident for methyl radicals, Table 14. Bell and Zucker⁶⁹ have suggested that the inductive effect of chlorine atoms bonded to silicon is offset to a certain extent by $\text{dn}\pi\text{-p}\pi$ electron transfer in the Si-Cl bond. Gowenlock and Thomas⁷⁰ proposed that this back-coordination reaches a maximum when three chlorine atoms are attached to silicon. On this basis, the inductive effect may well be about the same for mono-, di- and trichloro substitution leading to a similar electron density on the hydrogen atom and thus a fairly constant polar effect.

FIGURE 28

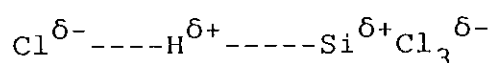
Plots in the form of equation VI for



showing polar effects.



Similar polar effects are suggested for the corresponding reactions of Cl atoms with the chloro-substituted silanes, Table 14. The Cl atoms attached to silicon reduce the electron density on the H-atom which is abstracted, increasing the polar repulsion between the electrophilic Cl atom and the substrate thereby increasing the activation energy for abstraction.



Electron withdrawing substituents attached to silicon also effect the rate of H-atom abstraction from alkyl groups. Rate constant data for OH radical reactions with mono- and difluoro substituted methylsilanes are reported in Table 16. In contrast to the effect of halogen substitution of a methyl group on the Si-H rate constant, the effect of halogen substitution on the $\text{>SiCH}_2\text{-H}$ rate constant was examined.

Table 16

Rate data for H atom abstraction from fluoro- substituted methylsilanes.

Substrate	k_{OH} $\times 10^{12}$	k_{Cl} $\times 10^{11}$	k_{CF_3} $\times 10^{16}$	k_{CCl_3} $\times 10^{19}$
$(\text{CH}_3)_4\text{Si}$	$1.05 \pm 0.08^{\text{a}}$ $1.12 \pm 0.18^{\text{b}}$	$13.65 \pm 0.80^{\text{a}}$	1.4^{c}	5.5^{d}
$(\text{CH}_3)_3\text{SiF}$	$0.28 \pm 0.03^{\text{a}}$ $0.35 \pm 0.05^{\text{b}}$	$1.53 \pm 0.60^{\text{a}}$	0.28^{c}	
$(\text{CH}_3)_2\text{SiF}_2$	$< 0.10^{\text{a}}$ $0.09 \pm 0.04^{\text{b}}$	$< 0.47^{\text{a}}$	0.05^{c}	0.70^{d}

k in $\text{cm}^3 \text{ molecule}^{-1} \text{ s}^{-1}$ at 298 ± 2 K, except for CF_3 at 400 K and CCl_3 at 250 K.

Error limits are twice the standard deviation of the slope

a, This work; relative rate

b, This work; pulse radiolysis, kinetic spectroscopy

c, Arthur et al.⁴⁴

d, Rice et al.³⁷

The data reported in Table 16 shows that replacement of a methyl group in $(\text{CH}_3)_4\text{Si}$ by a F atom changes the rate constant significantly for reaction with a variety of radical species. This may be explained by the inductive effect of the F atom decreasing the electron density on the methyl-hydrogen atoms and therefore increasing the polar repulsion in the transition state. The effect is enhanced by substitution by a second F atom. Similar effects have been observed for the electrophilic CF_3 and CCl_3 radicals.

The corresponding Cl atom reactions with these substrates show similar effects, Table 16. Substitution of a methyl group by a F atom results in a large decrease in the rate of reaction, which is further decreased by substitution of a second F atom. The value reported for $(\text{CH}_3)_2\text{SiF}_2$ is, however, an upper limit as experimental difficulties prevented a more accurate measurement from being obtained.

REACTION OF HYDROXYL RADICALS AND CHLORINE ATOMS
WITH TETRAALKYL COMPOUNDS OF GROUP IV ELEMENTS

3.1 INTRODUCTION

Organolead compounds have been added to gasoline to prevent pre-ignition or "knocking" since 1923 when tetraethyllead was first added to gasoline in the United States. Within a couple of years its use had been briefly suspended due to several deaths occurring in the production and handling of $(C_2H_5)_4Pb$. From 1960, mixtures of $(CH_3)_4Pb$ and $(C_2H_5)_4Pb$ were marketed, with $(CH_3)_4Pb$ soon gaining a greater share of the market as a lead additive to gasoline.⁷¹ By 1977, 3.4×10^4 tons of lead compounds were being used as gasoline additives in the western world.⁷² The effective concentration of $(C_2H_5)_4Pb$ added to prevent knock is normally 1-3g/gal of fuel.⁷² Environmental concern has led to a decrease in overall lead consumption in recent years, particularly in Europe, Japan, the US and USSR where lead free petrol is encouraged. However, its usage in some other countries is still extensive.⁷²

As the body burden of organolead compounds in

urban populations is thought to be primarily caused by the uptake of R_4Pb from the air, sources of air pollution are of particular interest.⁷¹ Much of the R_4Pb in urban air, 7000 tons,⁷¹ still comes from lead additives to gasoline. About 75% of alkyllead additive in fuel is emitted from the exhaust as a complex mixture of inorganic lead salts, about 1% is emitted unchanged in the exhaust, while perhaps another 1% comes from evaporation and spillage.⁷²

For over a decade the use of organolead compounds has given rise to concern. Traces of organolead compounds found in human brain tissue, particularly in inner city areas, has led to legislation to reduce or eliminate organolead additives to gasoline. Organolead compounds are readily absorbed through the respiratory and gastrointestinal tracts and through the skin. They are metabolized into trialkyllead compounds which are responsible for the toxic effects. These include insomnia, anorexia, nausea, tremor, restlessness, cramps, delirium and coma.⁷¹ The brain being the organ most sensitive to intoxication, means that children with a developing nervous system are particularly at risk.⁷¹

The main atmospheric removal pathway for tetraalkyllead compounds appear to be the reaction with

the OH radical. Removal by photolysis or by reaction with O_3 and $O(^3P)$ are less important^{62,74}. The estimation of atmospheric lifetimes based on the reaction with OH radicals and the fate of the products of such reactions therefore becomes important.

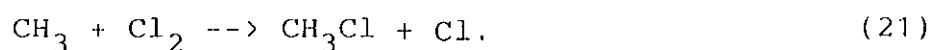
To-date, two room temperature studies of the reaction of OH radicals with $(CH_3)_4Pb$ have been reported.^{74,75} Harrison et al.⁷⁴ using a relative method determined a rate constant for $k(OH + (CH_3)_4Pb)$ of $(9.4 \pm 1.7) \times 10^{-12} \text{ cm}^3 \text{ molecule}^{-1} \text{ s}^{-1}$. Nielsen et al.⁷⁵ using a pulsed radiolysis technique measured a value of $(6.3 \pm 1.3) \times 10^{-12} \text{ cm}^3 \text{ molecule}^{-1} \text{ s}^{-1}$ for this reaction. Although these values are in reasonably good agreement, the same papers report widely differing values for the analogous reactions of OH radicals with $(C_2H_5)_4Pb$, Harrison et al.⁷⁴ reporting a value of $(83.1 \pm 12.0) \times 10^{-12} \text{ cm}^3 \text{ molecule}^{-1} \text{ s}^{-1}$, while Nielsen et al.⁷⁵ determined a value of $(11.6 \pm 1.7) \times 10^{-12} \text{ cm}^3 \text{ molecule}^{-1} \text{ s}^{-1}$. Harrison et al.⁷² subsequently re-determined their value, placing it on an absolute basis based on the previous $(CH_3)_4Pb$ values reported.^{74,75} Their new value of $(30.5 \pm 3.0) \times 10^{-12} \text{ cm}^3 \text{ molecule}^{-1} \text{ s}^{-1}$, does little to resolve the discrepancy.

Published OH radical rate constant data^{74,75} for

$(\text{CH}_3)_4\text{Pb}$ show it to be considerably more reactive than its carbon analogue, neo-pentane, which has a well-defined room temperature rate constant with OH radicals of $0.85 \times 10^{-12} \text{ cm}^3 \text{ molecule}^{-1} \text{ s}^{-1}$.⁴ No value for the analogous reaction of OH radicals with $(\text{C}_2\text{H}_5)_4\text{C}$ has been reported. An estimate of the room temperature rate constant for this reaction of about $5 \times 10^{-12} \text{ cm}^3 \text{ molecule}^{-1} \text{ s}^{-1}$, can be derived from Atkinson's²⁰ recommended "group rate constants" for OH radical attack on organic compounds. Clearly, the reported values of the rate constant for the reaction of OH with $(\text{C}_2\text{H}_5)_4\text{Pb}$ also demonstrate an enhanced reactivity over its carbon analogue.

The increase in reactivity for the reaction of tetraalkyllead compounds with Cl atoms over their carbon analogues is also evident. Kikuchi et al.⁷⁶ have determined a room temperature rate constant for the reaction of Cl atoms with $(\text{CH}_3)_4\text{Pb}$ of $(16.0 \pm 3.5) \times 10^{-11} \text{ cm}^3 \text{ molecule}^{-1} \text{ s}^{-1}$. They later⁸³ recalculated their data and obtained a value of $(41.0 \pm 5.0) \times 10^{-11} \text{ cm}^3 \text{ molecule}^{-1} \text{ s}^{-1}$. The analogous reaction of Cl atoms with neo-pentane has a rate constant of $(11.0 \pm 0.3) \times 10^{-11} \text{ cm}^3 \text{ molecule}^{-1} \text{ s}^{-1}$.¹⁶ Kikuchi et al.⁷⁶ did not give a value for the reaction of Cl atoms with $(\text{C}_2\text{H}_5)_4\text{Pb}$. However, they noted that the rate appears to

be faster than that for Cl atoms with $(\text{CH}_3)_4\text{Pb}$. The authors have shown that about 18% of the Cl atoms react with $(\text{CH}_3)_4\text{Pb}$ to give CH_3Cl , and assumed that the remainder of the reaction involves H atom abstraction. Their study of Cl atom reactions with $(\text{C}_2\text{H}_5)_4\text{Pb}$ has shown a yield of $\text{C}_2\text{H}_5\text{Cl}$ of approximately $7 \pm 2\%$, with almost 90% of the reaction presumably being H-atom abstraction. The authors did not discuss a possible mechanism, however, the absence of an effect on the CH_3Cl yield with added O_2 clearly shows that CH_3Cl is not formed via the reaction



since O_2 would rapidly scavenge CH_3 radicals.²⁴

The aim of this work was to determine room temperature rate constants for the reactions of OH radicals and Cl atoms with tetraalkyl compounds of Group IV elements. It was hoped that the results would resolve the discrepancy in the reported rate constants for the reactions of OH radicals with $(\text{C}_2\text{H}_5)_4\text{Pb}$. Also, it was hoped that the data determined in this work would, by establishing reactivity trends, provide an explanation for the enhanced reactivity of the tetraalkyllead compounds over their carbon analogues.

3.2 EXPERIMENTAL

3.2a Materials:

The materials used and their suppliers are listed below.

3,3-Diethylpentane (>99%), tetraethylsilane (99%), tetramethylsilane (99.9%), tetraethylgermanium (>98%), tetramethylgermanium (99.5%), tetraethyltin (97%), tetramethyltin (99%), n-heptane (99%), n-nonane (99%) were all obtained from the Aldrich Chemical Company Ltd.

Neo-pentane (>99%), n-butane (99%), i-butane (>99%), sodium nitrite (96%), sulphuric acid (98%), methanol (99%), nitric oxide (99.6%), hydrogen peroxide (60% w/v), chlorine (99.9%) were all obtained from BDH Chemicals Ltd.

n-Hexane (>99.96%) was obtained from Fluka AG.

Propene (99%) was obtained from Messer Griesheim GmbH.

c-Hexane (99.95%) was obtained from May and Baker Ltd.

Artificial air (HP grade), zero nitrogen (OFN grade), gas

chromatography gases; air, hydrogen and nitrogen were obtained from BOC Ltd.

Argon (99.9%) was obtained from AGA Denmark.

Water was triply distilled.

Tetraethyllead and tetramethyllead were gifts from Risø National Laboratory, Denmark.

All investigated materials were degassed and trap to trap distilled, discarding the upper and lower fractions and retaining the middle fifth before use.

3.2b Preparation of materials.

The preparation of materials is described in section 2.2b.

A: The Relative Rate Study

3.2c Apparatus:

The apparatus used is described in section 2.2c.

3.2d Procedure:

The procedure is described in section 2.2d.

3.2e Analysis:

The analytical method used was gas chromatography and has been described in section 2.2e. Tables 17 and 18 list the analytical conditions used for the reaction of OH radicals with tetramethyl compounds and tetraethyl compounds of Group IV elements respectively. Tables 19 and 20 list the analytical conditions used in the corresponding Cl atom reactions.

TABLE 17

Analytical conditions for OH radical reactions with tetramethyl compounds of Group IV elements.

Substrate	Reference	Column Type	Support	Mesh Size	Length and O.D.	Oven Temperature (°C)	Flow Rate (cm ³ min ⁻¹)
(CH ₃) ₄ C	n-C ₄ H ₁₀	Poropak Q		80/100	4'x1/8"	100	30
(CH ₃) ₄ Si	i-C ₄ H ₁₀	20% DC200	Chromosorb-WHP	80/100	12'x1/8"	40	10
	n-C ₆ H ₁₄	15% Squalane	Chromosorb-P	80/100	6'x1/8"	40	10
(CH ₃) ₄ Ge	i-C ₄ H ₁₀	20% DC200	Chromosorb-WHP	80/100	6'x1/4"	40	35
(CH ₃) ₄ Sn	(CH ₃) ₄ C	20% DC200	Chromosorb-WHP	80/100	4'x1/8"	25	15
(CH ₃) ₄ Pb	n-C ₆ H ₁₄	20% DC200	Chromosorb-WHP	80/100	4'x1/8"	60	30
	c-C ₆ H ₁₂	20% DC200	Chromosorb-WHP	80/100	4'x1/8"	60	30

TABLE 18

Analytical conditions for the reaction of OH radicals with tetraethyl compounds of Group IV elements.

Substrate	Reference	Column	Support	Mesh	Length	Oven	Flow
		Type		Size	and O.D.	Temperature	Rate
						(°C)	(cm ³ min ⁻¹)
(C ₂ H ₅) ₄ C	c-C ₆ H ₁₂	20% DC200	Chromosorb-WHP	80/100	2'x1/4"	35	25
(C ₂ H ₅) ₄ Si	c-C ₆ H ₁₂	20% DC200	Chromosorb-WHP	80/100	4'x1/8"	95	20
(C ₂ H ₅) ₄ Ge	c-C ₆ H ₁₂	20% DC200	Chromosorb-WHP	80/100	4'x1/8"	40	35
	n-C ₇ H ₁₆	20% DC200	Chromosorb-WHP	80/100	4'x1/8"	40	35
	n-C ₉ H ₂₀	20% DC200	Chromosorb-WHP	80/100	4'x1/8"	40	35
(C ₂ H ₅) ₄ Sn	c-C ₆ H ₁₂	20% DC200	Chromosorb-WHP	80/100	4'x1/8"	100	35
(C ₂ H ₅) ₄ Pb	n-C ₉ H ₂₀	20% DC200	Chromosorb-WHP	80/100	2'x1/8"	110	35
	C ₃ H ₆	Poropak Q		80/100	2'x1/8"	60	40

TABLE 19

Analytical conditions for the reaction of Cl atoms with tetramethyl compounds of Group IV elements.

Substrate	Reference	Column Type	Support	Mesh Size	Length and O.D.	Oven Temperature (°C)	Flow Rate (cm ³ min ⁻¹)
(CH ₃) ₄ C	i-C ₄ H ₁₀	Poropak Q		80/100	4'x1/8"	60	30
(CH ₃) ₄ Si	i-C ₄ H ₁₀	20% DC200	Chromosorb-WHP	80/100	4'x1/8"	40	5
	n-C ₆ H ₁₄	15% Squalane	Chromosorb-P	80/100	6'x1/8"	30	15
(CH ₃) ₄ Ge	i-C ₄ H ₁₀	20% DC200	Chromosorb-WHP	80/100	6'x1/4"	40	35
(CH ₃) ₄ Sn	(CH ₃) ₄ C	20% DC200	Chromosorb-WHP	80/100	4'x1/8"	25	15
	(CH ₃) ₄ Si	20% DC200	Chromosorb-WHP	80/100	4'x1/8"	25	15
(CH ₃) ₄ Pb	c-C ₆ H ₁₂	20% DC200	Chromosorb-WHP	80/100	4'x1/8"	60	30

TABLE 20

Analytical conditions for the reaction of Cl atoms with tetraethyl compounds of Group IV elements.

Substrate	Reference	Column Type	Support	Mesh Size	Length and O.D.	Oven Temperature (°C)	Flow Rate (cm ³ min ⁻¹)
(C ₂ H ₅) ₄ C	c-C ₆ H ₁₂	20% DC200	Chromosorb-WHP	80/100	2'x1/4"	35	25
	n-C ₆ H ₁₄	20% DC200	Chromosorb-WHP	80/100	2'x1/8"	35	25
(C ₂ H ₅) ₄ Si	c-C ₆ H ₁₂	20% DC200	Chromosorb-WHP	80/100	4'x1/8"	90	20
(C ₂ H ₅) ₄ Ge	n-C ₆ H ₁₄	20% DC200	Chromosorb-WHP	80/100	2'x1/8"	55	35
(C ₂ H ₅) ₄ Sn	c-C ₆ H ₁₂	20% DC200	Chromosorb-WHP	80/100	4'x1/8"	100	35
	(C ₂ H ₅) ₄ Ge	20% DC200	Chromosorb-WHP	80/100	4'x1/8"	100	35
(C ₂ H ₅) ₄ Pb	c-C ₆ H ₁₂	20% DC200	Chromosorb-WHP	80/100	2'x1/8"	110	35
	n-C ₇ H ₁₆	20% DC200	Chromosorb-WHP	80/100	2'x1/8"	110	35

B. The Absolute Rate Study

3.2f Apparatus:

The apparatus used is described in section 2.2f.

3.2g Procedure:

The procedure used is described in section 2.2g.

3.2h Analysis:

The analysis of the reactions is described in section 2.2h.

3.3 RESULTS

A: The Relative Rate Method

3.3a Hydroxyl Radical Reactions:

The reactions of OH radicals are discussed in detail in section 2.3.

The OH radical reference rate constants used in this work are listed in Table 21.

Table 21

OH reference rate constants used in this work.

k in $\text{cm}^3 \text{ molecule}^{-1} \text{ s}^{-1}$ at 298K and 1 atm.

Reference compound	$k_{14} \times 10^{12}$
n-C ₄ H ₁₀	2.53 ^a
i-C ₄ H ₁₀	2.37 ^a
n-C ₆ H ₁₄	5.58 ^a
c-C ₆ H ₁₂	7.38 ^a
n-C ₇ H ₁₆	7.2 ^a
n-C ₉ H ₂₀	10.0 ^a
(CH ₃) ₄	0.85 ^a
C ₃ H ₆	26.3 ^a
(CH ₃) ₄ Si	1.05 ^b

a, Atkinson⁴ b, This work

Table 22 lists the reactant concentrations (ppm) and slope, k_{13}/k_{14} for the reaction of OH radicals with tetramethyl compounds of Group IV elements, where 1 ppm = $2.40 \times 10^{13} \text{ molecule cm}^{-3}$ at 296 K and 735-torr total pressure.

Table 22

Reactant Concentrations and slope, k_{13}/k_{14} , for the reaction of OH radicals with tetramethyl compounds of Group IV elements at room temperature and atmospheric pressure.

Substrate	Reference	CH ₃ ONO	NO	$\frac{k_{13}}{k_{14}}$
Concentration (ppm)	Concentration (ppm)	Concentration (ppm)	Concentration (ppm)	
(CH ₃) ₄ C	n-C ₄ H ₁₀	20-40	0-10	0.33±0.04
(CH ₃) ₄ Si	i-C ₄ H ₁₀	20	0-5	0.44±0.04
	n-C ₆ H ₁₄	20	0-5	0.17±0.01
(CH ₃) ₄ Ge	i-C ₄ H ₁₀	20	0-10	0.54±0.04
(CH ₃) ₄ Sn	(CH ₃) ₄ C	20	0-10	2.02±0.03
	(CH ₃) ₄ Si	20	10	1.74±0.04
(CH ₃) ₄ Pb	n-C ₆ H ₁₄	15	0-10	0.71±0.05
	c-C ₆ H ₁₂	15	0-10	0.51±0.05

FIGURE 29

Plots in the form of equation VI from which k_{13}/k_{14} was obtained.

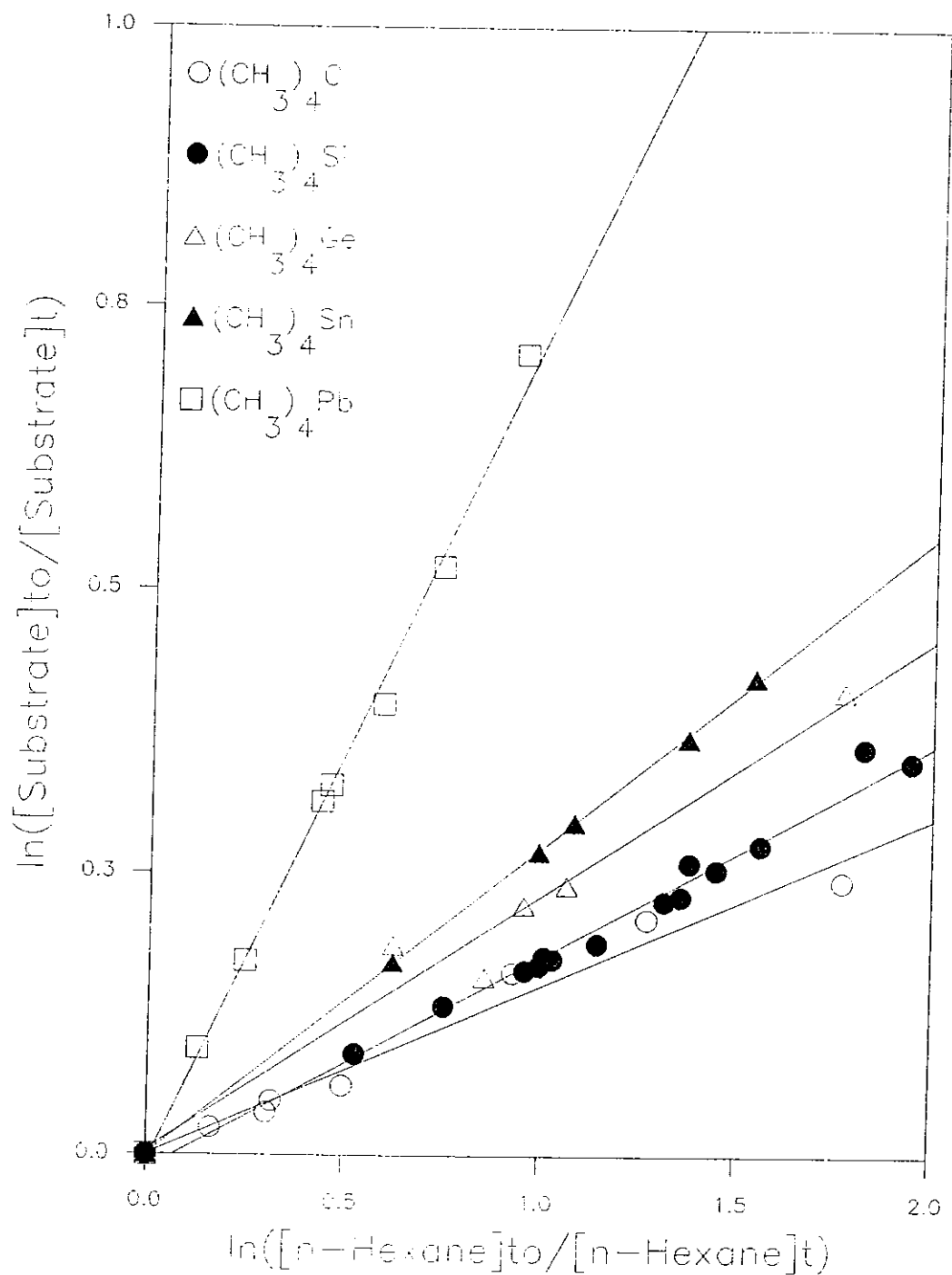
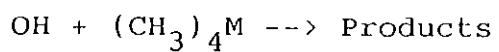


Table 23 lists the reactant concentrations (ppm) and slope, k_{13}/k_{14} for the reaction of OH radicals with tetraethyl compounds of Group IV elements, where 1 ppm = 2.40×10^{13} molecule cm^{-3} at 296 K and 735-torr total pressure.

Table 23

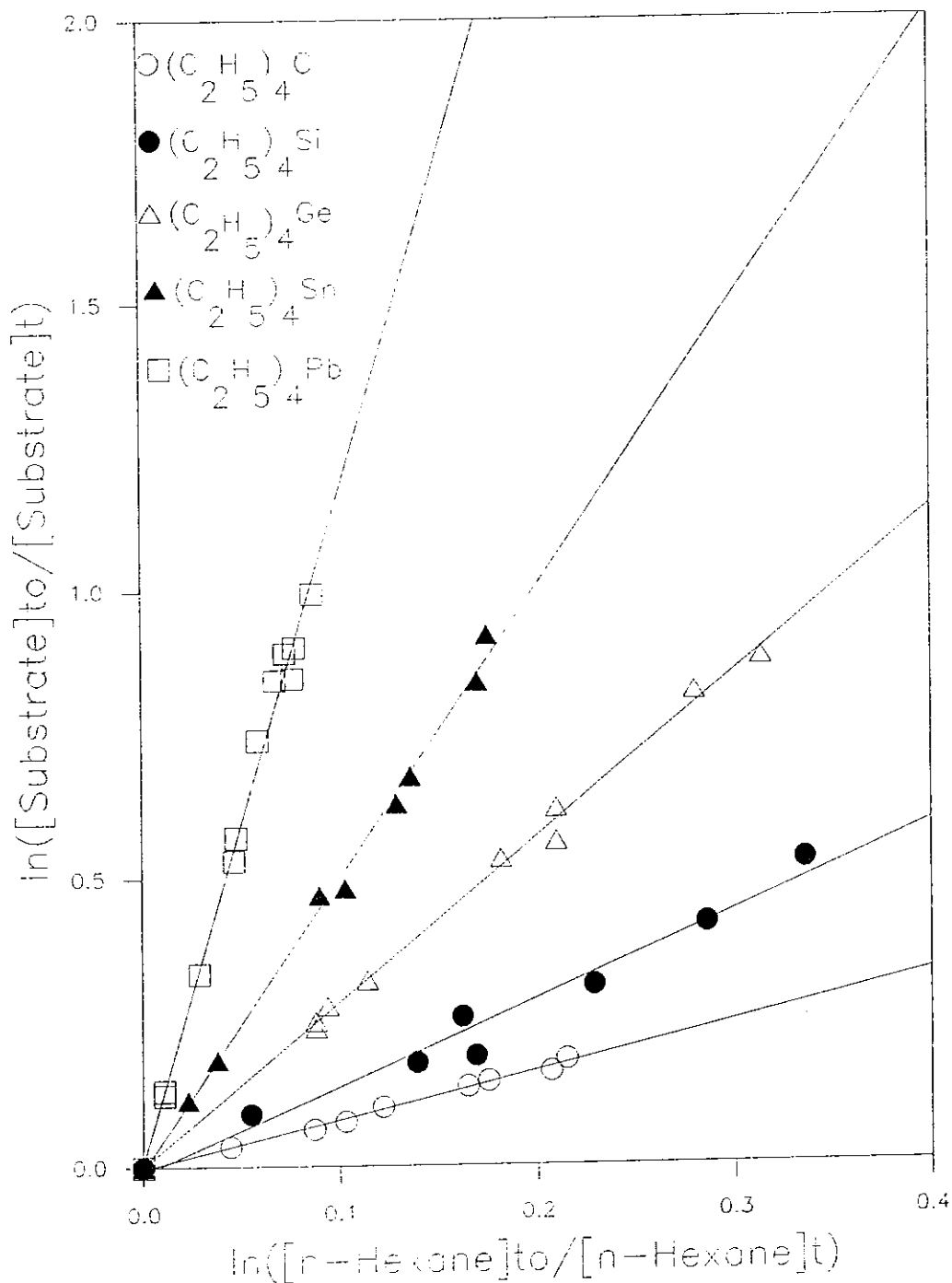
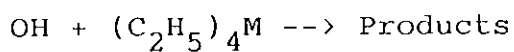
Reactant Concentrations and slope, k_{13}/k_{14} , for the reaction of OH radicals with tetraethyl compounds of Group IV elements at room temperature and atmospheric pressure.

Substrate	Reference	CH ₃ ONO	NO	$\frac{k_{13}}{k_{14}}$		
Concentration (ppm)	Concentration (ppm)	Concentration (ppm)	Concentration (ppm)			
(C ₂ H ₅) ₄ C	5-15	c-C ₆ H ₁₂	5-15	10-20	0-20	0.64±0.04
(C ₂ H ₅) ₄ Si	5-10	c-C ₆ H ₁₂	5-10	10-15	0-5	1.15±0.16
(C ₂ H ₅) ₄ Ge	6-10	c-C ₆ H ₁₂	5	10-15	0-5	2.12±0.12
	5	n-C ₇ H ₁₆	10	15	0-10	2.33±0.01
	5	n-C ₉ H ₂₀	10	15	0-10	1.53
(C ₂ H ₅) ₄ Sn	5	c-C ₆ H ₁₂	3-10	10-15	0-10	3.81±0.20
(C ₂ H ₅) ₄ Pb	4	n-C ₉ H ₂₀	5-10	10-15	0-10	5.28±1.4
	4	C ₃ H ₆	10	10	0-10	2.52±0.04

FIGURE 30

Plots in the form of equation VI from

which k_{13}/k_{14} was obtained.



3.3b Chlorine Atom Reactions:

The reactions of Cl atoms are described in detail in section 2.3.

The Cl atom reference rate constants used in this work are listed in Table 24.

Table 24

Cl reference rate constants used in this work.

k in $\text{cm}^3 \text{ molecule}^{-1} \text{ s}^{-1}$ at 296K and 1 atm.

Reference Compound	$k_{17} \times 10^{11}$
n-C ₄ H ₁₀	19.7 ^a
i-C ₄ H ₁₀	13.7 ^a
n-C ₆ H ₁₄	30.3 ^a
c-C ₆ H ₁₂	31.1 ^a
C ₆ H ₅ CH ₃	34.1 ^a
(CH ₃) ₄ C	11.0 ^a
(CH ₃) ₄ Si	13.7 ^b
(C ₂ H ₅) ₄ Ge	53.3 ^b

a, Atkinson et al.²¹

b, This work

Table 25 lists the reactant concentrations (ppm) and slope, k_{16}/k_{17} for the reaction of Cl atoms with tetramethyl compounds of Group IV elements.

Table 25

Reactant Concentrations and slope, k_{16}/k_{17} , for the reaction of Cl atoms with tetramethyl compounds of Group IV elements at room temperature and atmospheric pressure.

Substrate	Reference	Cl	Diluent	$\frac{k_{16}}{k_{17}}$		
Concentration (ppm)	Concentration (ppm)	Concentration (ppm)	Gas			
$(\text{CH}_3)_4\text{C}$	n- C_4H_{10}	5-10	10	N_2	0.51 ± 0.08	
		5	10	Air	0.52 ± 0.02	
$(\text{CH}_3)_4\text{Si}$	i- C_4H_{10}	10	5	N_2	1.01 ± 0.13	
		10	5	Air	0.98 ± 0.04	
$(\text{CH}_3)_4\text{Ge}$	i- C_4H_{10}	5-10	10	N_2	1.40 ± 0.10	
$(\text{CH}_3)_4\text{Sn}$	$(\text{CH}_3)_4\text{C}$	5-35	6-35	10-20	N_2	2.03 ± 0.07
	$(\text{CH}_3)_4\text{Si}$	4	4	5	Air	1.53 ± 0.10
	n- C_6H_{14}	10	10	10	Air	0.67 ± 0.01
$(\text{CH}_3)_4\text{Pb}$	c- C_6H_{12}	5	3	5-10	N_2	0.95 ± 0.01

FIGURE 31

Plots in the form of equation VII from
 which k_{16}/k_{17} was obtained.

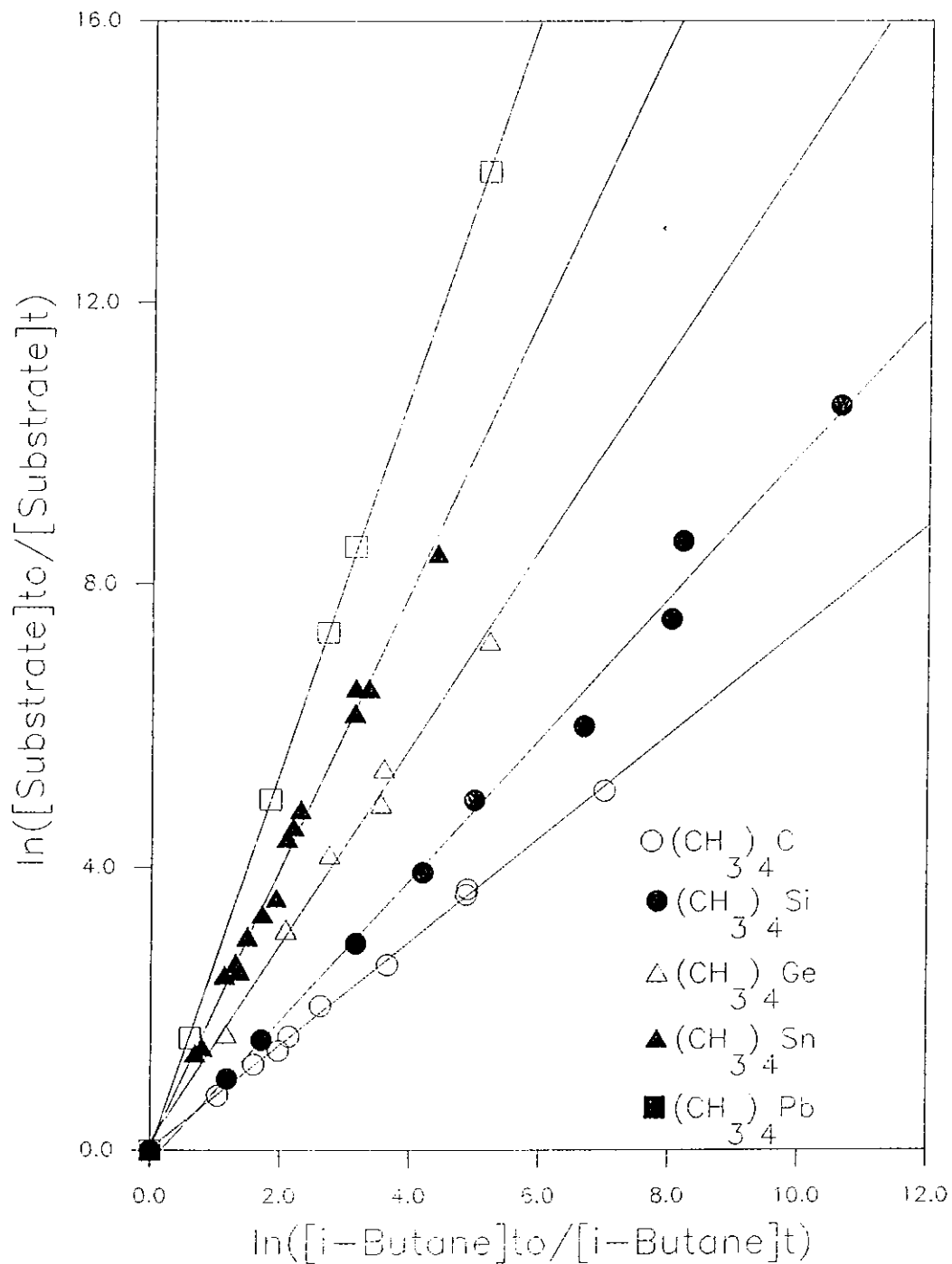
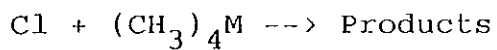


Table 26 lists the reactant concentrations (ppm) and slope, k_{16}/k_{17} for the reaction of Cl atoms with tetraethyl compounds of Group IV elements.

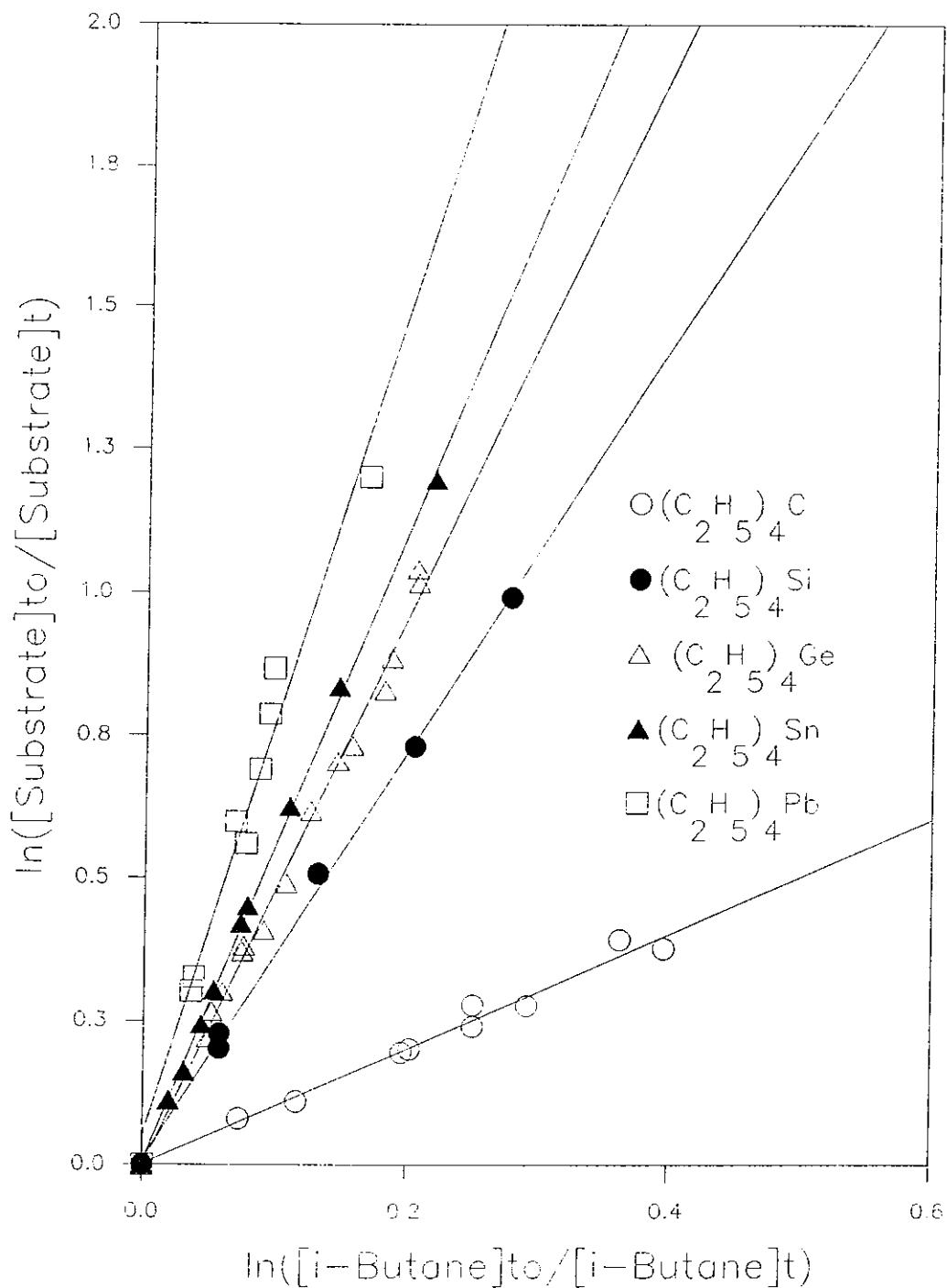
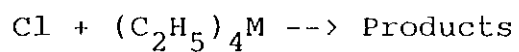
Table 26

Reactant Concentrations and slope, k_{16}/k_{17} , for the reaction of Cl atoms with tetraethyl compounds of Group IV elements at room temperature and atmospheric pressure.

Substrate	Reference	Cl	Diluent	$\frac{k_{16}}{k_{17}}$	
Concentration (ppm)	Concentration (ppm)	Concentration (ppm)	Gas		
$(C_2H_5)_4C$	6	c-C ₆ H ₁₂ 3	10	Air	0.92±0.09
	10-15	n-C ₆ H ₁₄ 5-10	10-20	N ₂	0.98±0.10
$(C_2H_5)_4Si$	5-10	c-C ₆ H ₁₂ 5-10	7-10	N ₂	1.27±0.05
$(C_2H_5)_4Ge$	6	n-C ₆ H ₁₄ 5-10	7-10	N ₂	1.72±0.08
	5	5	7	Air	1.82±0.10
$(C_2H_5)_4Sn$	5	c-C ₆ H ₁₂ 5-10	5-10	N ₂	2.03±0.05
	5	3	10	Air	1.93±0.05
	5	$(C_2H_5)_4Ge$ 5	10	Air	1.21±0.01
$(C_2H_5)_4Pb$	4	n-C ₆ H ₁₂ 3-10	10	N ₂	2.53±0.31
	4	n-C ₇ H ₁₆ 10	10	N ₂	2.69±0.72

FIGURE 32

Plots in the form of equation VI from
 which k_{16}/k_{17} was obtained.



B: The Absolute Rate Method

Table 27 lists the reactant pressure ranges (torr), and the rate constant, k_{13} , for the various, Substrate / H_2O / Ar, mixtures.

TABLE 27

Reactant pressures (torr) and rate constant, k_{13} , for the reaction of OH radicals with tetraalkyl compounds of Group IV elements at room temperature and atmospheric pressure. The type and volume of the mixing chamber is included.

Substrate	Pressure range (torr)	Mixing chamber	Volume (cm^3)	$k_{13} \times 10^{12}$ ($cm^3 \text{ molecule}^{-1} s^{-1}$)
$(CH_3)_4C$	1.0 - 3.52	Reaction cell	1,000	0.79±0.10
$(CH_3)_4Si$	1.00 - 10.0	Reaction Cell	1,000	1.12±0.18
$(CH_3)_4Ge$	0.25 - 3.0	Reaction cell	1,000	1.36±0.17
$(C_2H_5)_4Si$	0.10 - 1.00	Reaction Cell	1,000	7.92±0.54
$(C_2H_5)_4Ge$	0.022- 0.125	Glass bulb	60	15.0 ±2.1
$(C_2H_5)_4Sn$	0.008- 0.020	Glass bulb	60	40.8 ±8.1
$(C_2H_5)_4Pb$	0.006- 0.015	Glass bulb	60	66.6 ±24.1

FIGURE 33

Plot of k_{13}' versus substrate concentration from which k_{13} was obtained for
 $\text{OH} + (\text{CH}_3)_4\text{M} \rightarrow \text{Products}$

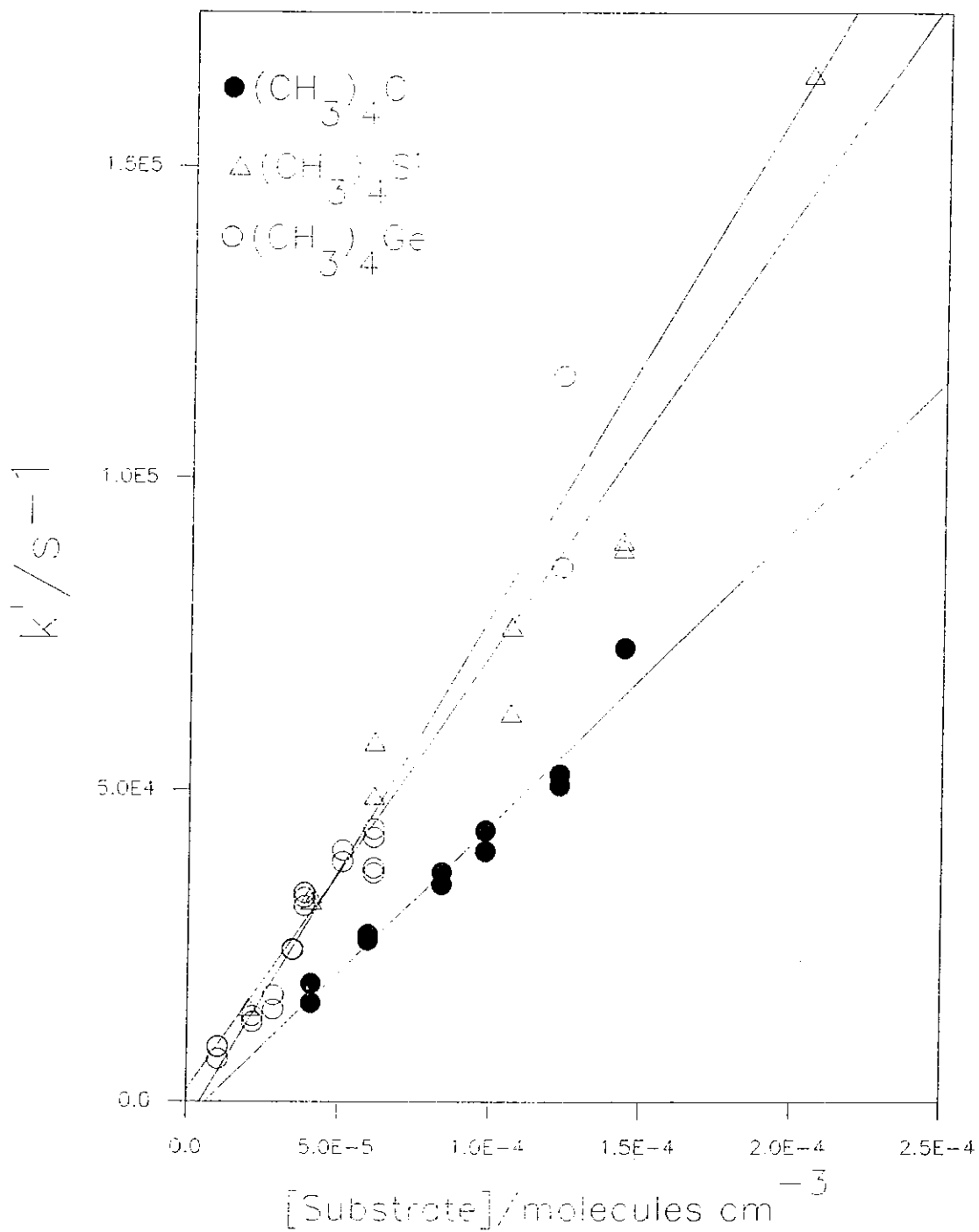
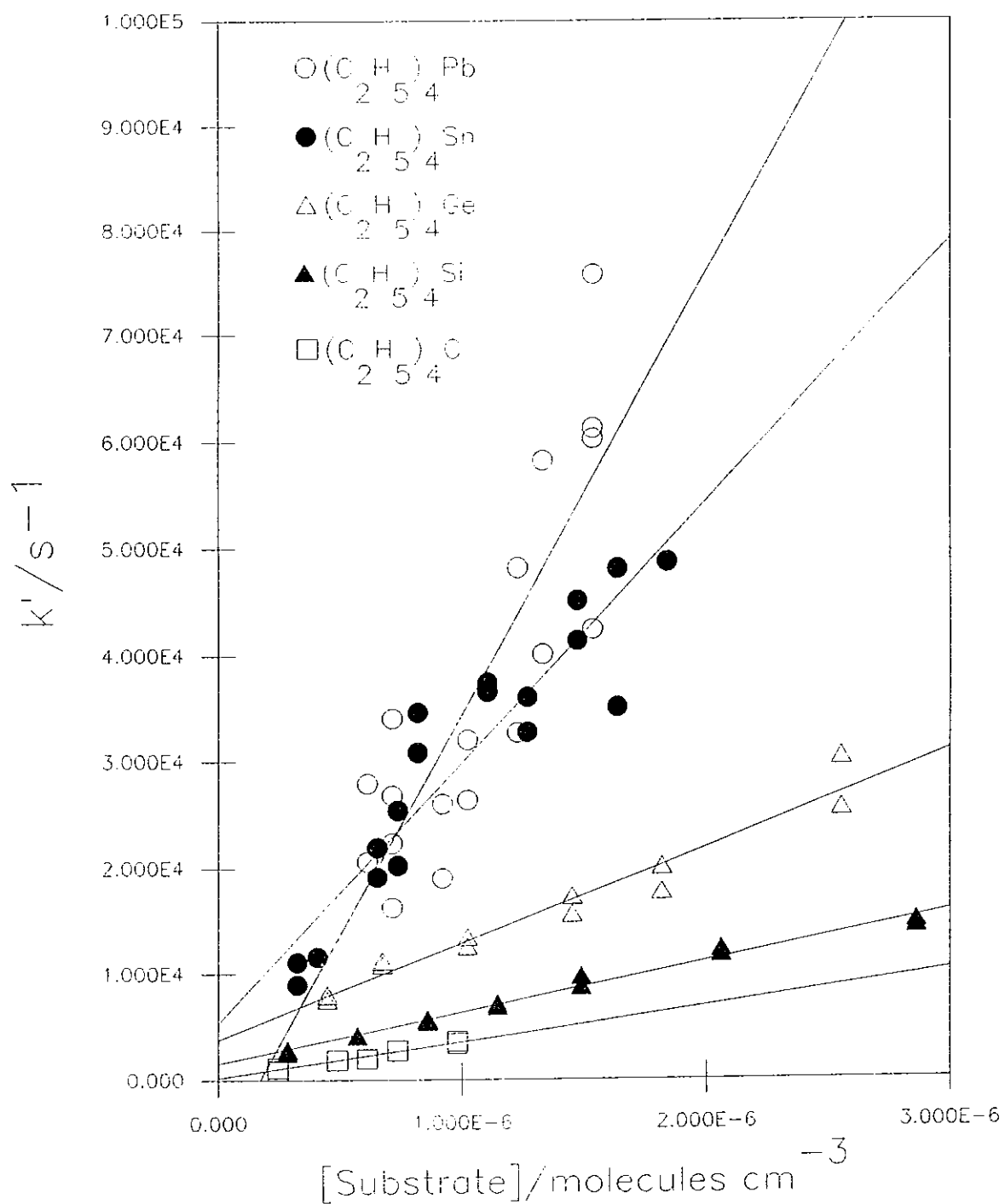


FIGURE 34

Plot of k_{13}' versus substrate concentration from which k_{13} was obtained for
 $\text{OH} + (\text{C}_2\text{H}_5)_4\text{M} \rightarrow \text{Products}$



3.4 DISCUSSION

Generally good agreement was obtained between the room temperature rate constant data determined from both the relative technique and the absolute technique, Table 28. However, the measured rate constant for the reaction of OH radicals with $(C_2H_5)_4Sn$ obtained by the pulse radiolysis technique was about 30% higher than that obtained using the relative rate technique. It is not clear as to the reason for this relatively large difference, however, it is felt that the most likely explanation is that some reactive impurity was present in the sample of $(C_2H_5)_4Sn$ employed. The presence of such an impurity would not affect the results from the relative rate experiments but would provide a high value for the determined rate constant in the pulse radiolysis study.

Table 28

OH + (CH₃)₄M --> ProductsOH + (C₂H₅)₄M --> Products

Substrate	k _{OH} × 10 ¹²	\bar{v}_{CH} ^g	D(M-C)
(CH ₃) ₄ C	0.84 ± 0.11 ^a	2934	343.5 ^h
	0.79 ± 0.10 ^b		351.5 ⁱ
	0.85 ^c		367.0 ^j
(CH ₃) ₄ Si	1.05 ± 0.08 ^a	2939	386.6 ^h
	1.12 ± 0.18 ^b		374.1 ⁱ
			316.3 ^j
(CH ₃) ₄ Ge	1.22 ± 0.08 ^a	2954	250.6 ^h
	1.36 ± 0.17 ^b		347.3 ⁱ
(CH ₃) ₄ Sn	1.52 ± 0.03 ^a	2960	201.3 ^h
			297.1 ⁱ
			226.0 ^j
(CH ₃) ₄ Pb	4.10 ± 0.22 ^a	2978	137.7 ^h
	9.4 ± 1.7 ^e		238.5 ⁱ
	6.3 ± 1.3 ^f		157.7 ^j

Table 28/contd.

$(C_2H_5)_4C$	4.69 ± 0.28^a	343.1^h
	5.11 ± 0.75^b	330.6^i
	5.07^c	
$(C_2H_5)_4Si$	8.42 ± 1.17^a	259.4^h
	7.92 ± 0.54^b	
$(C_2H_5)_4Ge$	15.9 ± 0.7^a	237.2^h
	15.0 ± 2.1^b	
$(C_2H_5)_4Sn$	28.1 ± 3.1^a	193.3^h
	40.8 ± 8.1^b	263.6^i
$(C_2H_5)_4Pb$	65.1 ± 3.6^a	128.9^h
	66.6 ± 24.1^b	230.1^i
	83.1 ± 12.0^e	
	11.6 ± 1.7^f	
	30.5 ± 3.0^k	

k in $cm^3 \text{ molecule}^{-1} s^{-1}$ at $298 \pm 2K$

$D(M-C)$ in $kJ \text{ mol}^{-1}$, $\bar{\nu}_{CH}$ in cm^{-1} .

Errors are twice the standard deviation of the slope

Table 28/contd.

- a, This work; relative rate
- b. This work; pulse radiolysis, kinetic spectroscopy
- c, Atkinson⁴
- d, Estimate²⁰
- e, Harrison et al.⁷⁴
- f, Nielsen et al.⁷⁵
- g, McKean et al.⁷⁷
- h, Lappert et al.⁷⁸
- i, McMillen et al.⁷⁹
- j, Steel⁸⁰
- k, Hewitt et al.⁷²

The room temperature rate constant determined in this work for the reaction of OH radicals with $(\text{CH}_3)_4\text{Pb}$ is slightly lower, though in reasonable agreement, with that measured by Harrison et al.⁷⁴ and by Nielsen et al.⁷⁵ Table 28. The value reported by Nielsen et al. is an absolute measurement, determined by pulse radiolysis, whereas the value given by Harrison et al. was determined from a relative study under smog-chamber-like conditions. Although reaction with ozone is a possibility in a smog-chamber study, it is unlikely to effect the result to any great extent since the $(\text{O}_3 + (\text{CH}_3)_4\text{Pb})$ reaction is relatively slow.^{74,81} However, reaction of the substrate with an additional reactive

species in the smog-chamber can lead to erroneously high results, hence one is drawn in favour of the lower estimate. The values reported in this work for the reaction of OH radicals with $(\text{CH}_3)_4\text{C}$ are in good agreement with the value recommended by Atkinson,²⁰ Table 28. The first kinetic data on H-atom abstraction from 3,3-diethylpentane (tetraethylcarbon), is reported in this work. The room temperature rate constant obtained for the OH radical reaction agrees well with a value calculated using Atkinson's²⁰ recommended "group rate constants" for OH radical attack on organic compounds.

The room temperature rate constant data available in the literature^{72,74,75} for the reaction of OH radicals with $(\text{C}_2\text{H}_5)_4\text{Pb}$ are in considerable disagreement, Table 28. The first reported value was a smog chamber study by Harrison et al.⁷⁴ who found $(\text{C}_2\text{H}_5)_4\text{Pb}$ to be nine times more reactive towards OH radicals than $(\text{CH}_3)_4\text{Pb}$. This result was contested by Nielsen et al.⁷⁵ using a pulse radiolysis technique, who found a corresponding variance in reactivity of less than a factor of two. Later, Harrison et al.⁷² remeasured their value of the rate constant for the OH radical reaction with $(\text{C}_2\text{H}_5)_4\text{Pb}$, again using a relative rate technique and a complex mixture of

reactants. Although they obtained a lower estimate for the rate constant, there is still a considerable discrepancy between their value and that of Nielsen et al. The rate constant obtained in this work using the relative rate method supports an answer considerably higher than that of Nielsen et al. and is in reasonable agreement with that first reported by Harrison et al. Table 28. The possibility of ozone influencing the reaction to any significant extent is unlikely as its reaction with $(C_2H_5)_4Pb$ is known to be relatively slow.^{74,81} The presence of NO in the reaction mixture used in the present study would also have inhibited ozone formation.¹⁶ Other reactive species could of course still be responsible for the high rate constant, but it seemed logical to re-examine the absolute rate data originally reported by Nielsen et al.⁷⁵

Initial room temperature experiments using the pulse radiolysis technique of Nielsen et al., performed during the course of this study, reproduced their original value for the reaction of OH radicals with $(C_2H_5)_4Pb$ of ca. $12 \times 10^{-12} \text{ cm}^3 \text{ molecule}^{-1} \text{ s}^{-1}$. However, the possibility of some wall loss due to the "sticky" nature of $(C_2H_5)_4Pb$ exists and since the technique requires an absolute concentration of substrate to be known, any such wall loss would thus lead to a lower rate constant

being calculated. Careful pre-mixing of the lead

Table 29

Cl + (CH₃)₄M --> Products

Cl + (C₂H₅)₄M --> Products

Substrate	k _{Cl} × 10 ¹¹	\bar{v}_{CH} ^e	D(M-C)
(CH ₃) ₄ C	10.0 ± 0.3 ^a	2934	343.5 ^f
	11.0 ± 0.3 ^b		351.5 ^g
			367.0 ^h
(CH ₃) ₄ Si	13.7 ± 0.8 ^a	2939	286.6 ^f
			374.1 ^g
			316.3 ^h
(CH ₃) ₄ Ge	15.4 ± 1.1 ^a	2954	250.6 ^f
			347.3 ^g
(CH ₃) ₄ Sn	21.6 ± 1.0 ^a	2960	201.3 ^f
			297.1 ^g
			226.0 ^h
(CH ₃) ₄ Pb	29.6 ± 0.3 ^a	2978	137.7 ^f
	16.0 ± 3.5 ^c		238.5 ^g
	41.0 ± 5.0 ^d		157.7 ^h

Table 29/contd.

$(\text{C}_2\text{H}_5)_4\text{C}$	$30.4 \pm 2.8^{\text{a}}$	343.1^{f} 330.6^{g}
$(\text{C}_2\text{H}_5)_4\text{Si}$	$39.3 \pm 1.6^{\text{a}}$	259.4^{f}
$(\text{C}_2\text{H}_5)_4\text{Ge}$	$53.3 \pm 2.4^{\text{a}}$	237.2^{f}
$(\text{C}_2\text{H}_5)_3\text{Sn}$	$61.1 \pm 1.2^{\text{a}}$	193.3^{f} 263.6^{g}
$(\text{C}_2\text{H}_5)_4\text{Pb}$	$80.5 \pm 10.3^{\text{a}}$	128.9^{f} 230.1^{g}
	100^{c}	

k in $\text{cm}^3 \text{ molecule}^{-1} \text{ s}^{-1}$ at $298 \pm 2 \text{ K}$

$D(\text{M-C})$ in kJ mol^{-1} , $\bar{\nu}_{\text{CH}}$ in cm^{-1} .

Errors are twice the standard deviation of the slope

a, This work; relative rate

b, Atkinson et al.²¹

c, Kikuchi et al.⁷⁶

d, Iyer et al.⁸²

e, McKean et al.⁷⁷

f, Lappert et al.⁷⁸

g, McMillen et al.⁷⁹

h, Steel⁸⁰

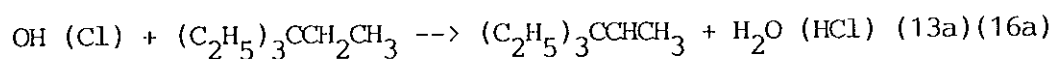
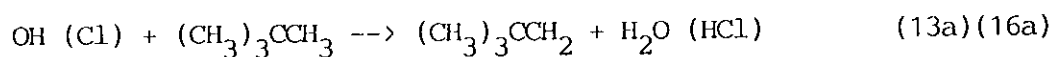
substrate in a vessel where wall loss could be minimized would alleviate the problem. Such experiments were performed using the method described in section 3.2, and the results reported, Table 28, indicated the low answer of Nielsen et al.⁷⁵ to be in error.

The corresponding reactions of Cl atoms have also been investigated, Table 29. There is good agreement between the room temperature value for $k(\text{Cl} + (\text{CH}_3)_4\text{C})$ obtained in this work and that reported by Atkinson et al.²¹ This value also agrees with that calculated using the "group rate" data reported by Atkinson et al.²¹ for Cl atom attack on organic compounds. Similarly, the data reported for the reaction of Cl atoms with $(\text{C}_2\text{H}_5)_4\text{C}$ is in good agreement with the value calculated from "group rate" data recommended by Atkinson et al.²¹

There is, however some discrepancy between the rate data determined in this work for the reaction of Cl atoms with $(\text{CH}_3)_4\text{Pb}$ and that reported by Kikuchi et al.^{76,83} The original estimate of the rate constant was determined relative to the rate constant for the reaction of Cl atoms with C_2H_4 . The value of the rate constant was later re-evaluated based on a more recent estimate for $k(\text{Cl} + \text{C}_2\text{H}_4)$ ⁸³, Table 29. However, this could still lead to error as the reaction of Cl atoms

with C_2H_4 has been shown to be pressure dependent.⁸³ Kikuchi et al.⁷⁶ also showed that the overall reactivity of $(C_2H_5)_4Pb$ towards Cl atoms was about eight times that of $(CH_3)_4Pb$, thus, an approximate room temperature rate constant for the reaction of Cl atoms with $(C_2H_5)_4Pb$ is about $1 \times 10^{-10} \text{ cm}^3 \text{ molecule}^{-1} \text{ s}^{-1}$. This is in reasonable agreement with the corresponding room temperature rate constant obtained in this work.

A number of possible mechanisms may be postulated for the reaction of OH radicals or Cl atoms with the tetraalkyl compounds of Group IV elements. At first sight the most likely primary step would appear to be abstraction of a hydrogen atom from the alkyl group by the OH radical or Cl atom, ie.



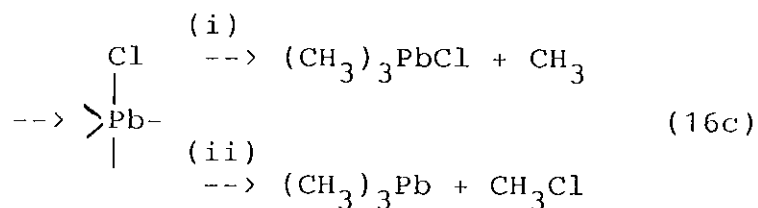
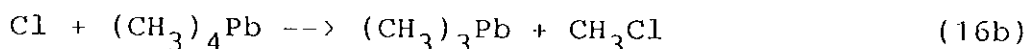
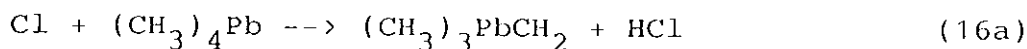
Good agreement between the rate constant data reported in this work for the reaction of OH radicals and Cl atoms with $(CH_3)_4C$ and $(C_2H_5)_4C$ and those calculated using Atkinsons "group rate" data^{20,21}, Tables 28 and 29, suggest the above primary steps to be correct at least for the carbon compounds. The difference in rate constants between $(CH_3)_4C$ and $(C_2H_5)_4C$ is likely to be due to the presence of secondary hydrogen atoms in $(C_2H_5)_4C$. Abstraction of a secondary hydrogen atom is

more rapid than of a primary hydrogen atom.^{20,21}

Similar C-H stretching frequencies⁸⁰ for all the tetramethyl compounds of Group IV elements, suggest similar C-H bond dissociation energies, in these compounds. This implies that the observed increase in the values of the rate constants going from neo-pentane to tetramethyllead is unlikely to be due to differences in the rate of H atom abstraction. In this work the data reported for OH radical and Cl atom reactions with both the tetramethyl and the tetraethyl compounds show a increase in reactivity in the order, C < Si < Ge < Sn < Pb, Tables 27,28. Similarly nuclear magnetic resonance data obtained in this work for $(\text{CH}_3)_4\text{Ge}$, $(\text{CH}_3)_4\text{Sn}$, $(\text{C}_2\text{H}_5)_4\text{C}$, $(\text{C}_2\text{H}_5)_4\text{Si}$, $(\text{C}_2\text{H}_5)_4\text{Ge}$, $(\text{C}_2\text{H}_5)_4\text{Sn}$ and $(\text{C}_2\text{H}_5)_4\text{Pb}$ relative to $(\text{CH}_3)_4\text{Si}$ show no significant difference in the chemical shifts of the CH_3 groups or of the C_2H_5 groups. This suggests that the electron density on the C-H bonds varies little down the group and hence is unlikely to contribute significantly to the increase in rate constants down the group.

An additional reaction channel might provide an explanation for the increase in the observed Cl atom rate constants going from tetraalkylcarbon to tetraalkyllead. Kikuchi et al.⁷⁶ observed CH_3Cl and

C_2H_5Cl in the reactions of Cl atoms with $(CH_3)_4Pb$ and $(C_2H_5)_4Pb$ respectively which they proposed to come from a bimolecular substitution reaction. However, they did not discuss a specific reaction mechanism. A weakening of the M-C bond down the series,^{77,78,79} Tables 28,29, indicates that a reaction pathway involving attack at the M-C bond could be of increasing importance in going from carbon to lead. A number of reaction channels are possible,



Route (16a) involves direct bimolecular abstraction of CH_3 by the Cl atom whereas route (16c) involves formation of an addition complex followed by either (i) loss of a CH_3 radical or (ii) elimination of CH_3Cl . Kikuchi et al.⁷⁶ found that approximately $18 \pm 2\%$ of the Cl atoms reacted with $(CH_3)_4Pb$ to form CH_3Cl . They assumed that the remainder of the Cl atoms form HCl by H-atom abstraction in reaction (16a). Similarly, they observed about $7 \pm 2\%$ of the Cl atoms reacted with

$(C_2H_5)_4Pb$ to form C_2H_5Cl , the remainder again forming HCl by H-atom abstraction.

The results determined in this work confirm the observations of Kikuchi et al. The yield of CH_3Cl from the reaction of Cl atoms with $(CH_3)_4Pb$ was about 25% of the $(CH_3)_4Pb$ consumed, Figure 35. An estimate for C_2H_5Cl formed from the corresponding reaction of Cl atoms with $(C_2H_5)_4Pb$ was below 10% of the $(C_2H_5)_4Pb$ consumed. No effect on the yield of CH_3Cl was observed when O_2 was added to the system. This clearly shows that CH_3Cl is not formed via the reaction



since O_2 would very rapidly scavenge CH_3 radicals.²⁴

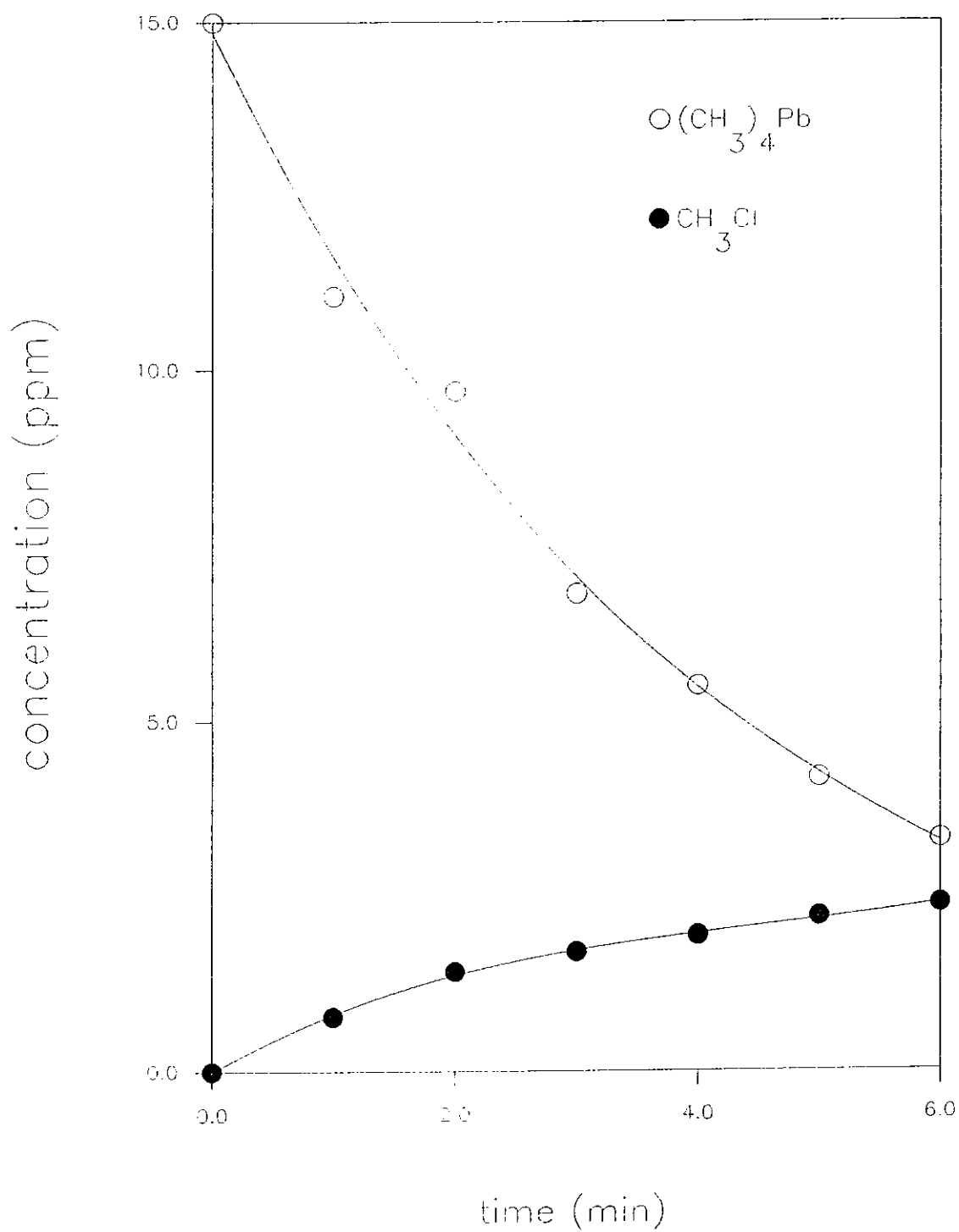
Thus reaction (16ci) cannot be important.

Kikuchi et al.⁸³ have also shown that $(CH_3)_4Sn$ reacts with F atoms to form CH_3F , with a yield of approximately 8%. In this work a CH_3Cl yield of about 2% from the reaction of Cl atoms with $(CH_3)_4Sn$ was observed. This, of course cannot account for the enhanced reactivity of $(CH_3)_4Sn$ relative to $(CH_3)_4C$. Methyl chloride was not detected in the reactions of Cl atoms with $(CH_3)_4Ge$, $(CH_3)_4Si$ and $(CH_3)_4C$. Similarly, C_2H_5Cl was not detected in the reaction of Cl atoms with $(C_2H_5)_4Sn$. Secondary reactions of CH_3Cl and C_2H_5Cl with

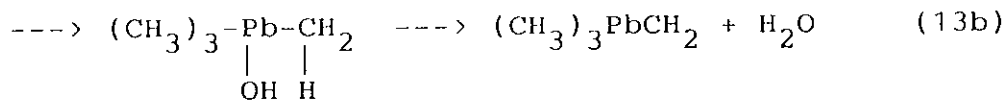
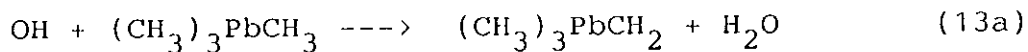
Cl atoms are unlikely under present experimental conditions as the reactions of Cl atoms with CH_3Cl and $\text{C}_2\text{H}_5\text{Cl}$ are relatively slow compared to the reaction of Cl atoms with the tetraalkyl compounds.^{84,85} The room temperature rate constants for reaction of Cl atoms with CH_3Cl and $\text{C}_2\text{H}_5\text{Cl}$ are $(5.10 \pm 0.14) \times 10^{-13} \text{ cm}^3 \text{ molecule}^{-1} \text{ s}^{-1}$ and $8.3 \times 10^{-12} \text{ cm}^3 \text{ molecule}^{-1} \text{ s}^{-1}$, respectively.

FIGURE 35

Concentration versus time profile of $(\text{CH}_3)_4\text{Pb}$ decay and CH_3Cl formation



Evidence for an alternative reaction channel to H-atom abstraction exists at least for the reaction of Cl atoms with $(\text{CH}_3)_4\text{Pb}$ and $(\text{C}_2\text{H}_5)_4\text{Pb}$. However, the relatively low yields of CH_3Cl and $\text{C}_2\text{H}_5\text{Cl}$ indicate that alkyl chloride production cannot provide the explanation for the large increase in reactivity down the group. The corresponding reaction of OH radicals with $(\text{CH}_3)_4\text{Pb}$ and $(\text{C}_2\text{H}_5)_4\text{Pb}$ might be expected to produce CH_3OH and $\text{C}_2\text{H}_5\text{OH}$ respectively, if the Pb-C bond was being broken in the reaction. No such products have been detected for these reactions, or in the reactions of any of the other tetraalkyl compounds studied in this work. However, an addition pathway may still be possible and may correlate with increasing d-character down the group. In addition to a direct hydrogen atom abstraction reaction (13a), an addition complex may form, reaction (13b), which subsequently decomposes to give the same reaction products as in the direct H-atom abstraction process, ie.



Additional experiments would have to be carried out to demonstrate the likelihood or otherwise of such a

reaction pathway. Pressure studies and the effect of isotopic substitution would help in the elucidation of such a reaction channel.

It is evident from both the reactions of OH radicals and Cl atoms with tetraalkyl compounds of Group IV elements reported in this work that a correlation exists between the rate constant for the reaction and the bond strength of the M-C bond, although there are inconsistencies in the bond strength data reported.^{78,79,80} The most recent bond strength data for tetramethyl compounds is reported by Steele,⁸⁰ and a plot of the OH and Cl rate constants obtained in this work against the corresponding M-C bond dissociation energies $D(M-C)$ shows a direct correlation in the order $Pb > Sn > Si > C$, Figures 36, 37.

The size of the central metal atom and the rate constant for reaction of OH radicals and Cl atoms with the tetraalkyl compounds of Group IV elements appears also to be related. Both properties decrease in the order $C < Si < Ge < Sn < Pb$. This may provide an explanation, at least in part, for the reactivity trends in these reactions. It is suggested that the methyl or ethyl groups on the smaller central atoms restrict the approach of the attacking radical due to a higher degree

of crowding. Thus the increase in reactivity, with respect to the addition channel, in going from carbon to lead may be a consequence of decreasing steric hinderance, together with increasing availability of d orbitals down the group.

FIGURE 36

Plot of $\log_{10} k_{\text{OH}}$ versus $D(\text{M-C})^{.80} k$ in cm^3
molecule $^{-1} \text{ s}^{-1}$, $D(\text{M-C})$ in kJ mol^{-1} .

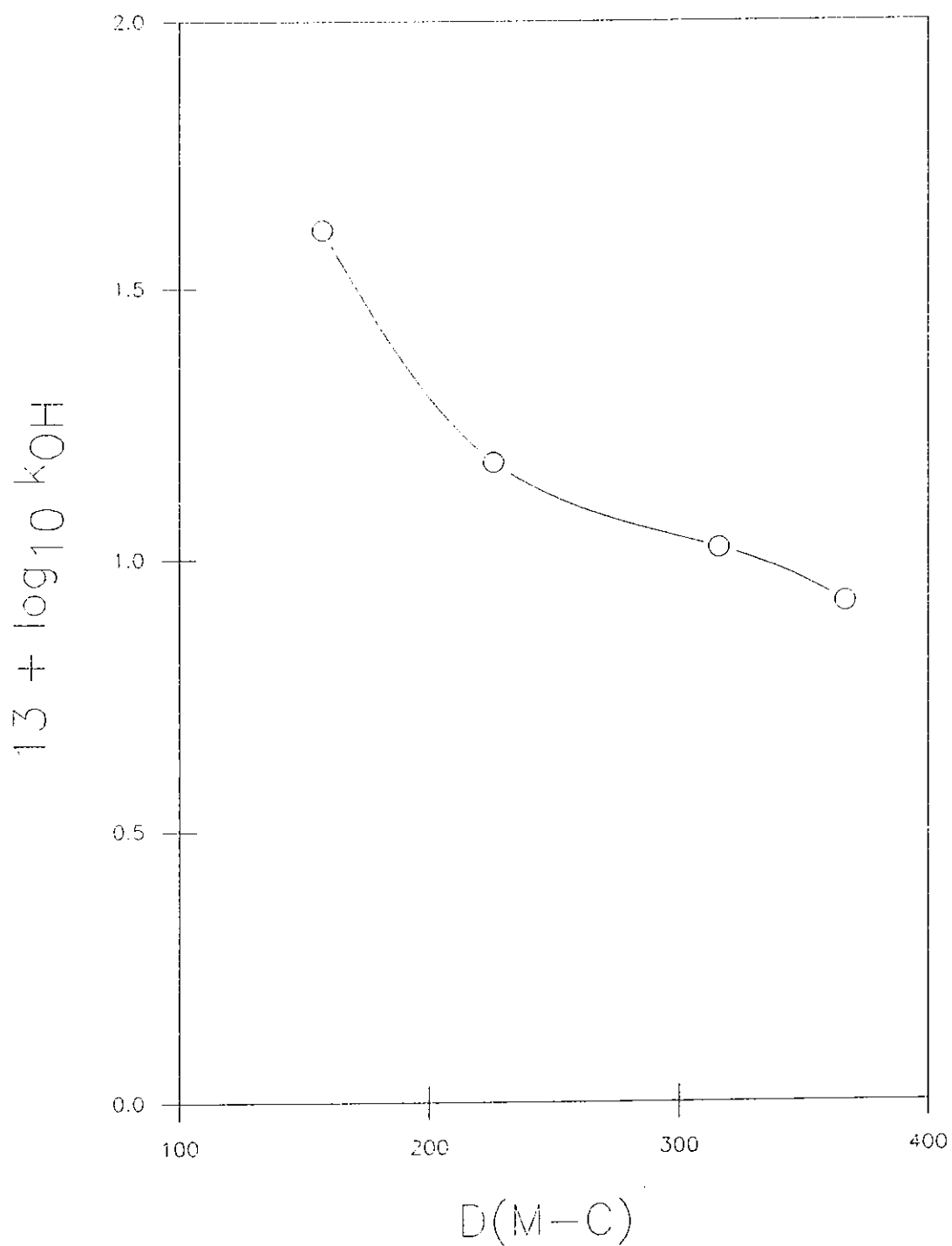


FIGURE 37

Plot of $\log_{10} k_{Cl}$ versus $D(M-C)$. k in cm^3
 $\text{molecule}^{-1} \text{s}^{-1}$, $D(M-C)$ in kJ mol^{-1} .

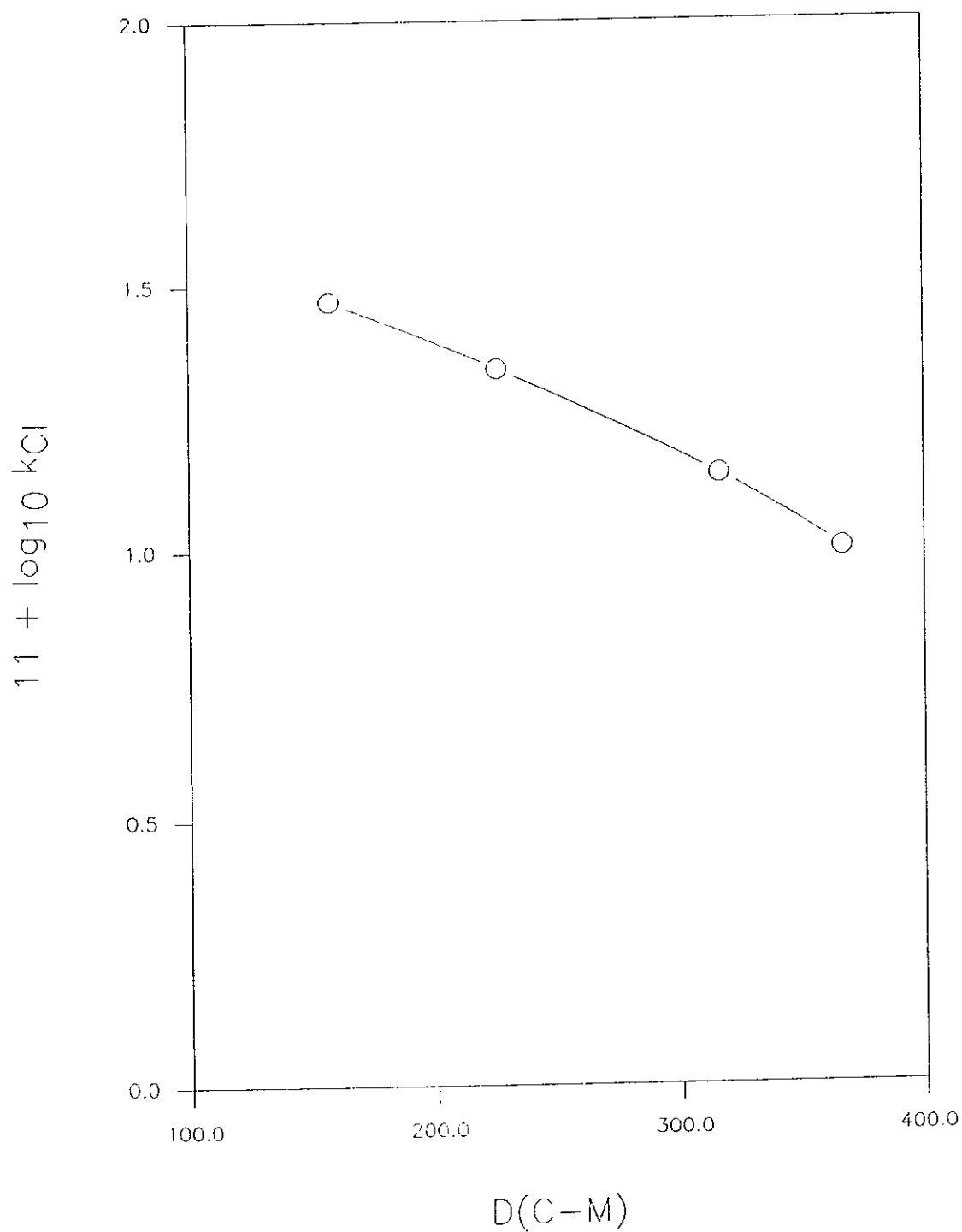


TABLE 30

Arrhenius parameters for the reactions of CH_3 , CD_3 and CF_3 with a series of tetraalkyl compounds of Group IV elements.

Substrate	CH_3^a			CD_3^b			CF_3^b		
	$A \times 10^{13}$	E	$k \times 10^{18}$	$A \times 10^{13}$	E	$k \times 10^{19}$	$A \times 10^{13}$	E	$k \times 10^{17}$
$(\text{CH}_3)_4\text{C}$				33.1	50.2	9.2	16.6	35.1	4.3
$(\text{CH}_3)_4\text{Si}$	66.1	45.9	11.2	16.6	45.1	20.9	13.2	30.5	13.6
$(\text{CH}_3)_4\text{Ge}$	10.5	40.1	8.0	4.2	42.2	12.7	8.3	30.9	7.5
$(\text{CH}_3)_4\text{Sn}$	2.1	36.0	5.3	26.3	47.2	17.7	8.3	30.5	8.6
$(\text{CH}_3)_4\text{Pb}$	0.3	30.9	3.0						

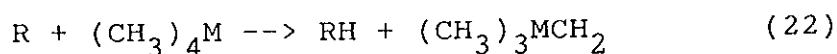
A in $\text{cm}^3 \text{ molecule}^{-1} \text{ s}^{-1}$. E in kJ mol^{-1} . k in $\text{cm}^3 \text{ molecule}^{-1} \text{ s}^{-1}$ at 400 K.

a, Chaudhry et al.⁸⁷

b, Bell et al.⁸⁶

Although trends in the reactivity of the series of tetramethyl compounds of Group IV elements towards CH_3 , CD_3 and CF_3 radicals have been reported

previously,^{87,86} Table 30, the results of Bell et al.⁸⁶ for CD₃ and CF₃ radicals are somewhat at variance with those of Chaudhry and Gowenlock⁸⁷ for CH₃ radicals. The rate constants for both these studies were determined using a competitive method in which the rate of hydrogen atom abstraction



was measured relative to that of the corresponding radical recombination



Chaudhry et al.⁸⁷ found an increase in reactivity for abstraction by nucleophilic CH₃ radicals in the order Si > Ge > Sn > Pb. The large variation in the pre-exponential factors for the reactions indicates that the mechanisms are more complex than originally assumed. Azomethane was used as the radical source in these studies, however, subsequent work by Bell et al.⁸⁶ have shown that data obtained from the photolysis of hexadeuteroazomethane in the presence of the higher members of the Group IV alkyls did not give the simple kinetic order expected for a H-atom abstraction process, despite the observation of linear Arrhenius plots. They suggested the presence of some additional complicating molecular reaction which occurs at a sufficiently fast rate to interfere with the kinetic analysis applied to the formation of methane. Thus, the

available evidence suggests the kinetic data reported for reaction of CH_3 radicals with the tetramethyl compounds of higher members of Group IV are in error. Bell et al.⁸⁶ studied the analogous reactions with CD_3 and CF_3 radicals using the corresponding ketones as the radical sources. The A factors were all in the range expected for hydrogen atom abstraction processes and the differences in reactivity of the methyl alkyls towards abstraction by both CD_3 and CF_3 radicals showed little variation along the series for each radical. Such differences as exist showed a reactivity sequence $\text{Si} > \text{Sn} > \text{Ge} > \text{C}$ which follows the Allred Rochow electronegativity values⁸⁸ for the central atoms and also correlates with the proton chemical shift. No such relationship was found in this work for either the OH radical or Cl atom reactions, suggesting that the relatively large increase in the rate constants observed down the group is not a consequence of enhanced H-atom abstraction but of the involvement of a new reaction channel.

LITERATURE CITED

1. R.P. Wayne, Chemistry of Atmospheres, Clarendon Press, Oxford (1985)
2. B.J. Finlayson-Pitts and J.N. Pitts, Jr., Atmospheric Chemistry, Wiley, New York, (1986)
3. C.N. Hewitt and R.M. Harrison, Atmos. Environ., 19, No.4 (1985)
4. R. Atkinson, Chem. Rev., 85, 69-201 (1985)
5. K.R. Darnall, A.C. Lloyd, A.M. Winer and J.N. Pitts Jr., Environ. Sci Technol., 10, No.7 (1976)
6. F.P. Tully, M.L. Koszykowski and J.S. Binkley, Twentieth Symposium (International) on Combustion, ISSN 00820784, pp 715 (1984)
7. W.W. Watson, Astrophysics J., 60, 145 (1924)

8. K.F. Bonhoeffer and H. Reichardt, *Z. Physik, Chem.*, 139, 75 (1928)
9. O. Oldenberg, *J. Chem. Phys.*, 3, 266 (1935)
10. D.R. Bates and A.E. Witherspoon, *Man. Nat. Astron. Soc.* 112, 101 (1952)
11. P.A. Leighton, "Photochemistry of Air Pollution", Academic Press, N.Y. (1961)
12. W.L. Chamedies and D.D. Davis, *Chem. Eng. News*, 60, 38 (1982)
13. M.S. Matheson and L.M. Dorfman, *J. Chem. Phys.* 32, 1870 (1960)
14. M.C. Sauer Jr. and L.M. Dorfman, *J. Am. Chem. Soc.*, 86, 4218 (1964)
15. J.H. Baxendale and M.A. Rodgers, *Chem. Soc. Revs.*, 7, 235 (1978)
16. R. Atkinson, S.M. Aschmann, A.M. Winer, and J.N. Pitts Jr., *Int. J. Chem. Kinet.*, 14, 507 (1982)

17. T.J. Wallington, L.M. Skewes, W.O. Siegl, C. Wu and S.M. Japar, *Int. J. Chem. Kinet.*, 20, 867 (1988)
18. W.S. Nip, D.L. Singleton, R. Overend, G. Paraskevopoulos, *J. Phys. Chem.* 83, 2440 (1979)
19. J.P. Martin and G. Paraskevopoulos, *Can. J. Chem.* 61, 861 (1983)
20. R. Atkinson, *Int. J. Chem. Kinet.*, 19, 799 (1987)
21. R. Atkinson and S.M. Aschmann, *Int. J. Chem. Kinet.*, 17, 33 (1985)
22. H. Niki, P.D. Maker, C.M. Savage, L.P. Breithenbach, *Int. J. Chem. Kinet.*, 12, 915 (1980)
23. R.S. Timonen and D. Gutman, *J. Phys. Chem.* 90, 2987 (1986)
24. D. O'Farrell, J. Treacy and H. Sidebottom, Commission of the European Communities, Air Pollution Research Report 9, Eur 11440 (1987) 24.

25. J. Rice, MSc. Thesis, University College, Dublin, Ireland (1983)
26. I.M.T. Davidson, The Chem. Soc. Quaterly Revs, 25, 111 (1971)
27. R. Walsh, Acc. Chem. Res., 14, 246 (1981)
28. A.M. Doncaster and R. Walsh, Int. J. Chem. Kinet., 13, 503 (1981)
29. M.H. Baghal-Vayjooee, A.J. Colussi and S.W. Benson, J. Am. Chem. Soc., 101, 3214 (1978)
30. D.M. Golden and S.W. Benson, Chem. Rev., 69, 125 (1969)
31. A.M. Doncaster and R. Walsh, J. Chem. Soc., Faraday Trans. 1, 75, 1126 (1979)
32. R. Walsh and J.M. Wells, J. Chem. Soc., Faraday Trans. 1, 72, 1212 (1976)
33. A.M. Doncaster and R. Walsh, J. Chem. Soc., Faraday Trans. 1, 72, 2908 (1976)

34. J.A. Kerr, Strength of Chemical Bonds, C.R.C. Handbook of Chemistry and Physics, pp F-222 (1981)
35. R.E. Berkley, I. Safarik, H.E. Gunning and O.P. Strausz, J. Phys. Chem., 77, 1734 (1973)
36. E.R. Morris and J.C.J. Thynne, Trans. Faraday Soc., 66, 183 (1970)
37. J.A. Rice, J.J. Treacy and H.W. Sidebottom, Int. J. Chem. Kinet., 16, 1505 (1984)
38. J.A. Kerr, A. Stephens and J. Young, Int. J. Chem. Kinet., 1, 371 (1969)
39. T.N. Bell and U.F. Zucker, J. Phys. Chem., 74, 979 (1970)
40. T.N. Bell, T. Yokota and A.G. Sherwood, Can. J. Chem., 54, 2359 (1976)
41. W.J. Cheng and M. Szwarc, J. Phys. Chem., 72, 494 (1968)

42. T.N. Bell and U.F. Zucker, *Can. J. Chem.*, 48, 1209 (1970)
43. R. Atkinson and J.N. Pitts Jr., *Int. J. Chem. Kinet.*, 10, 1151 (1978)
44. N.L. Arthur and T.N. Bell, *Rev. of Chem. Intermediates*, 2, 37 (1978)
45. H.Niki, P.D. Maker, C.M. Savage and L.P. Breithenbach, *J. Phys. Chem.*, 89, 1752 (1985)
46. H. Hoffmeyer, O. Horie, P. Potzinger and B. Reinmann, 9th International Symposium on Gas Kinetics, Bordeaux, France (1986)
47. D.J. Schyler, A.P. Wolf, and P.P. Gasper, *J. Phys. Chem.*, 82, 2633 (1978)
48. H. Hoffmeyer, O. Horie, P. Potzinger and B. Reinmann, *J. Phys. Chem.*, 89, 2901 (1985)

49. H. Niki, R.D. Maker, C.M. Savage L.P.
Breithenbach and M.D. Hurley, *J. Phys. Chem.*, 89,
3725 (1985)
50. R. Walsh, *J. Chem. Soc. Faraday Trans. 1* 79,
2233 (1983)
51. A.E. Finholt, A.C. Bond Jr., K.E. Wilzbach and
H.I. Schlesinger, *Am. Soc.*, 69, 2692 (1947)
52. S. Kaye and S. Tannenbaum, *J. Org. Chem.*, 18,
1750 (1953)
53. H. Westermark, *Acta Chemica Scand.*, 9, 947 (1955)
54. E.A.V. Ebsworth, M. Onyszchilk and N. Sheppard,
J. Chem. Soc., 1453 (1958)
55. J. Hawkins Meal and M. Kent Wilson, *J. Chem.*
Phys., 24, 385 (1956)
56. W.D. Taylor, T.D. Allston, M.J. Moscato, G.B.
Fazekas, R. Kozlowski and G.A. Takacs, *Int. J.*
Chem. Kinet., 12, 231 (1980)
57. P. Tarte, *J. Chem. Phys.*, 20, 1570 (1952)

58. J.U. White, J. Opt. Soc. Am. 32, 285 (1942)
59. S.S Gordon, W. Mulac, P. Nangia, J. Phys. Chem., 75, 2087 (1971)
60. A.B. Caller and W.J. Tyerman, Trans. Faraday Soc., 62, 371 (1966)
61. R. Atkinson and S.M. Aschmann, Int. J. Chem. Kinet., 19, 1097 (1987)
62. O.J. Nielsen, Risoe-R-480, Risoe National Laboratory, Roskilde, Denmark (1984)
63. L.H. Luthjens, Deft University Press (1986)
64. M.C. Sauer Jr., Adv. Rad. Chem., 5, 97 (1976)
65. J.A. Cowfer, K.P. Lynch and J.V. Michael, J. Phys. Chem., 79, 1139 (1975)
66. E.R. Austin and F.W. Lampe. J. Phys. Chem., 81, 1134 (1977)
67. G. Baruch and A. Horowitz, J. Phys. Chem., 84, 2535 (1980)

68. B.N. Ormson, W.D. Perrymore and M.L. White, *Int. J. Chem. Kinet.*, 9, 663 (1977)
69. T.N. Bell and V.F. Zucker, *Can. J. Chem.*, 48, 1209 (1970)
70. B.G. Gowenlock and K.E. Thomas, *J. Chem. Soc.*, 5068 (1965)
71. P. Grandjean and T. Nielsen. Organolead compounds, Environmental health aspects. Springer - Verlag, New York Inc. 97 (1979)
72. C.N. Hewitt and R.M. Harrison, *Environ. Sci. Technol.*, 20, 797 (1986)
73. S.W. Benson, *J. Phys. Chem.*, 92, 1531 (1988)
74. R.M. Harrison and D.P.H. Laxen, *Environ. Sci. Technol.*, 12, 1384 (1978)

75. O.J. Nielsen, T. Nielsen and P. Pasberg, Risoe-R-463, Risoe National Laboratory, Roskilde, Denmark (1982)
76. M. Kikuchi, F.S.C. Lee and F.S. Rowland, J. Phys. Chem., 85, 84 (1981)
77. D.C. McKean, J.L. Duncan and L. Batt, Spectrochimica Acta, 29A, 1037 (1973)
78. M.F. Lappert, J.B. Pedley, J. Simpson and T.R. Spalding, J. Organometal. Chem., 29, 195 (1971)
79. D.F. McMillen and D.M. Golden, Ann. Rev. Phys. Chem., 33, 493 (1982)
80. W.V. Steele, J. Chem. Thermodyn. 15, 595 (1983)
81. J.C. Patel, D. Strawley and P. Webster, Unpublished Data, cited in reference 74.
82. R.S. Iyer, P.J. Rogers and F.S. Rowland, J. Phys. Chem., 87, 3799 (1983)

83. M. Kikuchi, J.A. Cramer, R. Iyer, J.P. Frank and F.S. Rowland, J. Phys. Chem., 86, 2677 (1982)
84. R.G. Manning and M.J. Kurylo, J. Phys. Chem., 81, 291 (1977)
85. P.H. Wine and D.H. Semmes, J. Phys. Chem., 87, 3572 (1983)
86. T.N. Bell, P. Slade and A.G. Sherwood, Can. J. Chem., 52, 1662 (1974)
87. A.U. Chaudhry and B.G. Gowenlock, J. Organometal. Chem., 16, 221 (1969)
88. A.L. Allred and E.G. Rochow, J. Inorg. Nucl. Chem., 5, 269 (1958)